This is the authors' accepted manuscript. The published version, subject to editorial changes, will appear in Algebraic & Geometric Topology.

ASYMPTOTIC CONES OF SNOWFLAKE GROUPS AND THE STRONG SHORTCUT PROPERTY

CHRISTOPHER H. CASHEN, NIMA HODA, AND DANIEL J. WOODHOUSE

Abstract. We exhibit an infinite family of snowflake groups all of whose asymptotic cones are simply connected. Our groups have neither polynomial growth nor quadratic Dehn function, the two usual sources of this phenomenon. We further show that each of our groups has an asymptotic cone containing an isometrically embedded circle or, equivalently, has a Cayley graph that is not strongly shortcut. These are the first examples of groups whose asymptotic cones contain 'metrically nontrivial' loops but no topologically nontrivial ones.

Contents

1. Introduction

The strong shortcut property was introduced by the second named author in order to explore commonalities between the many theories of nonpositively curved groups which have been developed in recent decades [25]. A graph Γ is *strongly shortcut* if, for some $K > 1$, there is a bound on the lengths of the K-biLipschitz cycles of Γ. This property has a natural generalization to rough geodesic metric spaces [23]. A group G is *strongly shortcut* if it satisfies one of the following three equivalent conditions [23]:

(1) G has a strongly shortcut Cayley graph.
(2) G acts properly and cocompactly on a strongly shorcut graph.
(3) G acts metrically properly and coboundedly on a strongly shortcut rough geodesic metric space.

2020 *Mathematics Subject Classification.* 20F65, 20F69, 51F30.

Key words and phrases. snowflake group, asymptotic cone, shortcut group, strongly shortcut group.

Strongly shortcut groups are finitely presented and have polynomial isoperimetric functions [25].

The class of strongly shortcut spaces is vast. It includes:

- Asymptotically CAT(0) spaces [28, 23], in particular: CAT(0) spaces [18, 12], Gromov-hyperbolic spaces [18] and $\mathrm{SL}(2,\mathbb{R})$ with the Sasaki metric [28].
- 1-skeletons of systolic [40, 15, 22, 27], quadric [3, 24] and finite dimensional CAT(0) cubical [2, 32, 18] complexes [25].
- Standard Cayley graphs of Coxeter groups [25, 33].
- Coarsely injective spaces of uniformly bounded geometry [21], in particular: Helly graphs [14] of bounded degree.
- Heisenberg groups of all dimensions [26].

In particular, all Thurston geometries except Sol are strongly shortcut. The class of strongly shortcut groups is correspondingly vast, including: CAT(0) groups, hyperbolic groups, Helly groups, systolic groups, quadric groups, the discrete Heisenberg groups and hierarchically hyperbolic groups [5, 4, 21]. In particular, finitely presented small cancellation groups [42, 35, 24, 14] and mapping class groups [31, 30] of surfaces are strongly shortcut.

There is a characterization of strongly shortcut spaces in terms of asymptotic cones [23] (see Section 2.3 for definitions): a space is strongly shortcut if and only if none of its asymptotic cones contains an isometrically embedded copy of a unit length circle with its length metric. One might wonder whether, for Cayley graphs of groups, this condition is equivalent to all asymptotic cones being simply connected. We provide the first counterexamples.

We consider an infinite family of *snowflake groups*:

$$G_L := \langle a, x, y, s, t \mid sas^{-1} = x, tat^{-1} = y, a^L = xy, [a, x] = [x, y] = [y, a] = 1\rangle$$

where $L \geq 6$ is an even integer. These are special cases[1] of the groups introduced by Brady and Bridson [9], who show that the Dehn function for such a group is $n^{2\alpha}$ for $\alpha := \log_2 L$.

Our main results are:

Theorem (Theorem 9.0.1)**.** *For all even $L \geq 6$, every asymptotic cone of G_L is simply connected.*

Theorem (Corollary 4.0.3)**.** *For all even $L \geq 6$, some asymptotic cone of G_L contains an isometrically embedded circle.*

We find an isometrically embedded circle in an asymptotic cone of the Cayley graph of G_L corresponding to the generating set $\{a, s, t\}$. This means that this particular Cayley graph is not a shortcut graph. We do not know if G_L is a strongly shortcut group—it is possible that it admits an action on some other graph that is strongly shortcut. If G_L is a strongly shortcut group then this is the first example of a group for which the strong shortcut property depends on the choice of generating set. If G_L is not a strongly

[1] Specifically, $G_{p,1}$ of Brady and Bridson is G_{2p} in our notation, which is why the parameter L is even. The restriction to $L \geq 6$ is explained in Remark 3.1.2.

shortcut group then this is the first example of a group for which every asymptotic cone being simply connected does not imply the strong shortcut property.

The structures of asymptotic cones of snowflake groups are interesting independent of the strong shortcut property. An application of having all cones simply connected is due to Riley [38, Theorem C]: the isodiametric and filling length functions of G_L are both linear. It is also interesting just to have more diverse examples of groups with all cones simply connected. As far as we are aware, the only existing examples are groups of polynomial growth, groups with at most quadratic Dehn function, and certain combinations of these, see Section 2.3. Our examples are not in any of these classes. We also do not know any other examples of groups having all of their asymptotic cones simply connected, but with at least some of them containing isometrically embedded circles. Conjecturally there are no such groups of polynomial growth. It is an open question whether there exist such groups with quadratic Dehn function.

The idea of the proof that asymptotic cones are simply connected. There is a criterion, the "Loop Subdivision Property", which we recall in Theorem 2.3.2, for a group to have all of its asymptotic cones simply connected. This says that every asymptotic cone is simply connected if and only if every word in the generators representing the trivial element of the group can be filled by a van Kampen diagram of uniformly bounded area, subject to the constraint that the boundary lengths of 2–cells of the diagram are bounded above by a fixed fraction of the length of the word to be filled.

To construct such diagrams, we establish a fat/thin dichotomy. The "fat" words are those such that the corresponding loop in the Cayley graph is a K–biLipschitz loop for K close to 1. Thin words we cut into a bounded number of small pieces and at most one fat one using the "Circle Tightening Lemma" of [23]. This reduces the problem to constructing diagrams for K–biLipschitz loops for K arbitrarily close to 1. This reduction step occurs in Section 6.

For $K = 1$, i.e., geodesic loops, there are some natural example words to consider: the "snowflake words" that give the groups their names. We describe how to fill loops made from snowflake words in Section 5.1.

In the general case our thesis is that, for K sufficiently close to 1, all K–biLipschitz loops "ought to look like" a snowflake loop, and admit a filling diagram using a similar construction. In retrospect, this is more a declaration of naïveté than adroitness. It turns out to be true, but it was much harder than we had initially expected to make rigorous.

Why is it hard? Consider these two facts:

Fact 1.0.1 (Reverse Hölder inequality)**.** For any $\alpha > 1$ and any $r_1, r_2, \ldots, r_n \geq 0$, the following inequalities hold.

$$\left(\frac{1}{n}\right)^{1-1/\alpha}(r_1^{1/\alpha} + \cdots + r_n^{1/\alpha}) \leq (r_1 + \cdots + r_n)^{1/\alpha} \leq r_1^{1/\alpha} + \cdots + r_n^{1/\alpha}$$

Fact 1.0.2 (Power-law distortion, cf [9] or Theorem 3.2.9)**.** Given even $L \geq 6$ and setting $\alpha := \log_2 L$, there exist C_{lo} and C_{hi} such that for $g \in \{a, x, y\}$ and all $|m| > 0$ we have:

$$C_{lo} \leq \frac{|g^m|}{|m|^{1/\alpha}} < C_{hi}$$

We will show in Section 3.2 that Fact 1.0.2 is about as good as can be expected; the relationship between $|m|$ and $|g^m|$ is not monotone.

Taken together, these two facts suggest that to travel between two points of a distorted subgroup like $\langle a\rangle$, it is more efficient to make one long hop rather than several short ones; the distortion is non-linear, so the long hop can achieve proportionally more savings. For example, consider, for $m, n > 0$ a path between 1 and a^{m+n} consisting of a geodesic from 1 to a^m, followed by a geodesic from a^m to a^{m+n}. We expect:

$$\frac{|a^m| + |a^n|}{|a^{m+n}|} \sim \frac{m^{1/\alpha} + n^{1/\alpha}}{(m+n)^{1/\alpha}} = \frac{1 + (n/m)^{1/\alpha}}{(1 + n/m)^{1/\alpha}}$$

This ratio goes to 1 as n/m goes to 0 or infinity, but equals $2^{1-1/\alpha}$ when $m = n$. So the expectation should be that the path is very efficient, in the sense that the ratio of its length to the distance between its endpoints is very close to 1, if and only if one of the two subpaths dominates the other, in the sense that n/m is either very large or very small. If this were true it would give us good control over biLipschitz paths when the biLipschitz constant is close to 1; they would, more or less, have to be dominated by a long segment that makes good use of the distortion, possibly with some relatively very short additional segments at the beginning and end.

However, Fact 1.0.2 is too rough an estimate to confirm this intuition. It can only tell us, for instance, that $\frac{|a^m|+|a^m|}{|a^{2m}|} > \frac{C_{lo}}{C_{hi}} \cdot 2^{1-1/\alpha}$, but $\frac{C_{lo}}{C_{hi}} \cdot 2^{1-1/\alpha}$ is less than 1 when $L \geq 10$ (see Proposition 3.2.10), so this bound is useless. The deviation of the distortion function from being a power-law on the nose overwhelms the efficiency estimates coming from reverse Hölder. We must make finer estimates. The bulk of the paper is a detailed analysis of biLipschitz paths in snowflake groups.

The plan of the paper. Section 2 is background material. In Section 3 we analyze geodesics between elements in the vertex group of the snowflake group. In Section 4 we show that snowflake loops are geodesic loops, and conclude that our Cayley graph is not strongly shortcut.

In Section 5 we describe how snowflake loops satisfy the loop subdivision property and give a more detailed explanation of how we will adapt this construction to the general case. The first step, in Section 6, is to reduce to the case of biLipschitz loops with biLipschitz constant sufficiently close to 1. We analyze such loops in Section 7, and construct fillings of them in Section 8. We tie things up and make some closing remarks in Section 9.

Acknowledgements. C. Cashen is supported by the Austrian Science Fund (FWF): P30487-N35 and P34214-N and visited the University of Arkansas during part of this work. N. Hoda is supported by the ERC grant GroIsRan.

2. Preliminaries

2.1. **Basics.** If S is a finite set, let $F(S)$ denote the free group generated by S.

If G is a group generated by a finite set S, then the *word metric* on G with respect to S is defined by taking $|g|_S$ to be the minimal length of a word $w \in F(S)$ such that $w =_G g$. The *Cayley graph* $\mathrm{Cay}(G, S)$ of G with respect to S is the labelled directed graph whose vertices are in bijection with G, and such that there is an edge from g to h labelled s when $h = gs$. We say that a word in $F(S)$ labels an edge path, or is read on an edge path, if it is the concatenation of labels of the edges, with the convention that an s edge traversed against its orientation contributes the letter s^{-1}. Given a word $w \in F(S)$ and a basepoint $g \in G$ there is a unique edge path starting from g labelled by w.

Paths in $\mathrm{Cay}(G, S)$ will always start and end at vertices and will always be parameterized by arclength. If γ is a path, $\bar{\gamma}$ is the path with opposite parameterization. We use $+$ to denote concatenation. We frequently conflate paths with their labels, but there will be only one reasonable interpretation. For example, if γ is a path in $\mathrm{Cay}(G, S)$ from g to h, with $g, h \in G$, δ is another path in $\mathrm{Cay}(G, S)$ whose endpoints differ by $k \in G$, and $s, t \in S$ then $s.\gamma + \bar{\delta} + st^{-1}$ is a path from sg to $shk^{-1}st^{-1}$ while $s + \gamma + \bar{\delta} + st^{-1}$ is a path from 1 to $sg^{-1}hk^{-1}st^{-1}$.

Let $\langle S \mid \mathcal{R} \rangle$ be a finite presentation of a group G. If $w =_G 1$ then w can be written in $F(S)$ as $w = \prod_{i=1}^{n} u_i r_i u_i^{-1}$ for some u_i and r_i such that either r_i or r_i^{-1} belongs to $\mathcal{R}$. Define $\mathrm{Area}(w)$ to be the minimal such n. The *Dehn function* or *isomperimetric function* of the presentation is the function $n \mapsto \max_{|w|_S \leq n,\, w =_G 1} \mathrm{Area}(w)$. While the precise function depends on the choice of presentation, it turns out that up to a certain notion of equivalence of functions all of the finite presentations yield equivalent functions, so we define the *Dehn function of the group* to be this equivalence class. The equivalence relation preserves, in particular, degrees of polynomial growth, so it makes sense to say that a group has a Dehn function of a particular polynomial degree.

2.2. van Kampen diagrams.

Definition 2.2.1. Let $\mathcal{A}$ be an alphabet. A *van Kampen diagram* for a word $w \in \mathcal{A}^*$ over a subset $\mathcal{R} \subset \mathcal{A}^*$ of cyclically reduced words is a compact, connected, simply connected 2-dimensional cell complex D embeded in the plane such that edges are directed and labelled by elements of $\mathcal{A}$ in such a way that starting from some base boundary vertex the word read around ∂D is w and the word read around the boundary of each 2–cell is freely and cyclically reduced and, up to cyclic permutation and inversion, belongs to $\mathcal{R}$.

A 2-cell of D is also called a *region*.

A van Kampen diagram is *reduced* if there does not exist a pair of 2-cells sharing an edge such that the boundary labels starting from a shared edge are inverses.

The *area* of a van Kampen diagram is the number of 2–cells.

A van Kampen diagram is *minimal* or has *minimal area* if it has the fewest number of 2-cells among all van Kampen diagrams for the given boundary word. Minimal diagrams are necessarily reduced.

A *disk diagram* is a van Kampen diagram that is topologically a disk.

An *arc* is a maximal segment in the 1–skeleton of D such that every interior vertex has valence 2. For the purpose of drawing pictures it is often convenient to replace each arc by a single directed edge labelled by the word in $\mathcal{A}^*$ read along the arc. In this case the length of the new edge is defined to be the length of its label, that is, the length of the original arc. This is called *forgetting the valence 2 vertices*.

The *mesh* of a diagram is the maximum length of the boundary of a 2–cell.

Given a specified base vertex in D, there is a unique label and orientation preserving map $D^{(1)} \to \mathrm{Cay}(G, \mathcal{A})$ sending the base vertex to 1, where $G = \langle \mathcal{A} \mid \mathcal{R} \rangle$. Thus, we sometimes say that D gives a *filling* for the word read around ∂D, which is a word $w \in F(\mathcal{A})$ such that $w =_G 1$.

The groups we are interested in are double HNN extensions over $\mathbb{Z}$; that is, groups G having a presentation of the form $\langle a_1, \dots, a_k, s, t \mid \mathcal{R}, sus^{-1}v^{-1}, twt^{-1}x^{-1}\rangle$, where $H := \langle a_1, \dots, a_k \mid \mathcal{R}\rangle$ is the *vertex group*, s and t are called *stable letters*, and u, v, w, and x are infinite order elements of H. It is a standard result of Bass-Serre theory that H is a subgroup of the resulting group G.

Let $\mathcal{R}' := \mathcal{R} \cup \{sus^{-1}v^{-1}, twt^{-1}x^{-1}\}$. Since each stable letter appears in only one relator, and appears as an inverse pair, we can say more about the structure of reduced diagrams over $\mathcal{R}'$. Suppose D is a reduced diagram and some region has an s–edge in its boundary. Either this edge belongs to ∂D, or there is an adjacent region that shares the s–edge. However, there are only two possible occurrences of $s^{\pm}$ in $\mathcal{R}$, and one of the possible choices would create an unreduced diagram, so there is a unique way that the boundary of the adjacent region can be labelled. That region has one more edge labelled with s or s^{-1}, which is either on ∂D or else is adjacent to another region whose boundary label is determined, etc. Define an equivalence relation on 1–cells of D labelled $s^{\pm}$ such that two such edges are equivalent if they belong to a common 2–cell. For each equivalence class of s–edge, define the *s–corridor* containing it to be the union of cells containing one of those edges in its closure. We define t–corridors similarly, and just say *corridor* if we do not care which of the stable letters the corridor corresponds to. It is immediate from the definitions that distinct corridors have disjoint interiors.

A priori there are three possible types of s–corridor: a single s–edge, a closed loop of 2-cells, or a string of 2-cells ending at distinct edges of ∂D. The first type cannot occur if D is a disk diagram. This is true in particular when ∂D embeds in X. The second type cannot occur in a minimal diagram because if it did the subdiagram inside the closed corridor would be a diagram filling a power of u, v, w, or x, but these were assumed to be infinite order elements. The same argument shows that not only does a corridor have distinct edges of ∂D, these two edges are disjoint.

Define an *HNN diagram* (with respect to the above presentation as a multiple HNN extension) as a minimal diagram over the set of relations:

$$\{g \in F(\{a_i\}_{i=1}^k) \mid g =_G 1\} \cup \{su^ns^{-1}v^{-n} \mid n \in \mathbb{N}\} \cup \{tw^nt^{-1}x^{-n} \mid n \in \mathbb{N}\}$$

Regions with boundary labelled by an element of the latter two sets correspond to corridors in a diagram over $\mathcal{R}$, and we again call them *corridors*. Regions labelled by element of the first set correspond to vertices in the tree dual to the corridors in a diagram over $\mathcal{R}$. We call such a region a *vertex region*.

2.3. Asymptotic cones.

We briefly recall the definition and some history of asymptotic cones. See [17, 38, 10] for more.

Definition 2.3.1. Let (X, d) be a metric space, ω a non-principal ultrafilter, $\mathbf{s} = (s_n) \to \infty$ a 'scaling sequence' of positive numbers, and $\mathbf{o} = (o_n)$ a sequence of 'observation points' in X.

Define a pseudometric on sequences $\mathbf{x} = (x_n)$ of points in X as follows.

$$d_{\omega,\mathbf{s}}(\mathbf{x}, \mathbf{y}) := \lim_{\omega} \frac{d(x_n, y_n)}{s_n}$$

Define the asymptotic cone $\mathrm{Cone}_\omega(X, \mathbf{o}, \mathbf{s})$ of X with respect to ω, $\mathbf{s}$, and $\mathbf{o}$ to be the quotient of the space of sequences $\mathbf{x}$ at finite $d_{\omega,\mathbf{s}}$–distance from $\mathbf{o}$ by identifying sequences at $d_{\omega,\mathbf{s}}$–distance 0 from one another.

It turns out that asymptotic cones are complete metric spaces.

We are interested in the case that X is the Cayley graph of a group, in which case X is homogeneous. In this case the choice of observation points does not matter, and we can take $\mathbf{o} = 1$ to be the constant sequence at the identity vertex.

Gromov [20] used a process of passing to a convergent subsequence of rescaled metric spaces in his proof of the Polynomial Growth Theorem. Outside of the polynomial growth case, convergence fails, but van den Dries and Wilkie [41] recognized that this could be fixed by the imposition of an ultrafilter.

Pansu [36] proved nilpotent groups have simply connected asymptotic cones. Gromov [19, $5F_1''$] showed that if every asymptotic cone of G is simply connected, then G is finitely presented and has polynomial Dehn function. Papasoglu [37] proved the converse for groups with quadratic Dehn function, but it is not true in general [11, 39, 34], even for groups with cubic Dehn function.

Drutu and Sapir characterized relatively hyperbolic groups as having asymptotic cones that are tree-graded with respect to the asymptotic cones of their peripheral subgroups [16] and used this notion to give quasi-isometric rigidity results. Behrstock [7] showed that the asymptotic cone of the mapping class group is tree graded, although it is not relatively hyperbolic. The tree graded structure of the asymptotic cones of the mapping class group were further studied by Behrstock-Minsky [8] and Behrstock-Kleiner-Minsky-Mosher [6] as part of proving quasi-isometric rigidity.

Kent [29] defines a *prairie group* to be one for which every asymptotic cone is simply connected. As far as we are aware, the only groups currently known to be prairie groups are either virtually nilpotent or have quadratic Dehn function or are built by combining such pieces: direct products of prairie groups are prairie groups, and groups that are hyperbolic relative to prairie groups are prairie groups [16].

Snowflake groups are not virtually nilpotent, have superquadratic Dehn functions, do not split as direct products, and are not hyperbolic relative to any collection of subgroups. We show that snowflake groups are prairie groups using a criterion suggested by Gromov and explained in detail by Papasoglu [37, Section 1]. As expressed by Riley [10] (cf [38]):

Theorem 2.3.2 (Loop Subdivision Property [10, Theorem II.4.3.1])**.** *Let G be a group with finite generating set S. Fix a non-principal ultrafilter ω. The following are equivalent.*

(1) *The asymptotic cone* $\mathrm{Cone}_\omega(\mathrm{Cay}(G, S), 1, \mathbf{s})$ *is simply connected for all scaling sequences* $\mathbf{s} \to \infty$.

(2) *Given $\lambda \in (0, 1)$ there exist $N, J \in \mathbb{N}$ such that for all null-homotopic words w there is an equality*

$$w = \prod_{i=1}^{N} u_i w_i u_i^{-1}$$

in the free group $F(S)$ for some words u_i and w_i such that the w_i are null homotopic and have length $\ell(w_i) \le \lambda \ell(w) + J$.

(3) *Given* $\lambda \in (0,1)$ *there exist* $A, M \in \mathbb{N}$ *such that for all words* $w \in F(S)$ *with* $w =_G 1$ *there is a van Kampen diagram for* w *over* $\mathcal{R} = \{g \in F(S) \mid g =_G 1\}$ *with area at most* A *and mesh at most* $\lambda|w| + M$*.*

Remark 2.3.3. Change of finite generating set gives a biLipschitz map between Cayley graphs, which in turn induces a biLipschitz homeomorphism between asymptotic cones for a common ultrafilter and scaling sequence, so if all asymptotic cones of $\mathrm{Cay}(G,S)$ are simply connected, then the same is true with respect to any finite generating set of G.

3. Snowflake groups

We consider the following family of groups for $L \geq 6$ and even:

$$G_L := \langle a, x, y, s, t \mid sas^{-1} = x, tat^{-1} = y, a^L = xy, [a,x] = [x,y] = [y,a] = 1\rangle \tag{3.0.1}$$

Such a group is isomorphic, via $x = a^p b$ and $y = a^p b^{-1}$, to the Brady-Bridson snowflake group [9] $G_{p,q}$ with $p = L/2$ and $q = 1$ defined by:

$$G_{p,q} := \langle a, b, s, t \mid [a,b] = 1, sa^q s^{-1} = a^p b, ta^q t^{-1} = a^p b^{-1}\rangle \tag{3.0.2}$$

The group $G = G_L$ is a double HNN extension over $\mathbb{Z}$ of the subgroup $H := \langle a, x, y\rangle \cong \mathbb{Z}^2$. Note that $\langle a\rangle$, $\langle x\rangle$, and $\langle y\rangle$ pairwise have trivial intersections since $H \cong \mathbb{Z}^2$, and that $H = \coprod_{i=0}^{L-1} a^i\langle x, y\rangle$. Let $X = X_L$ denote the Cayley graph of G_L with respect to the generating set $\{a, x, y, s, t\}$, with the following modification: we declare that the a, s and t edges have length 1 as usual, but assign length L to the x and y edges[2]. This follows the convention of [1] and leads to a simpler description of geodesics. This is not a significant deviation from the standard conventions, because the induced metric on vertices is still a word metric: it is the one corresponding to the generating set $\{a, s, t\}$. Metrically the x and y edges are extraneous. We include them to preserve the correspondence between the group structure as an HNN extension and the topological structure of the universal cover of the corresponding graph of spaces, which is a torus with two annuli glued on. In this correspondence we have, for instance, that cosets of $\langle a, x, y\rangle$ correspond to the planes that are the connected components of the preimage of the torus in the universal cover, so we would like to think of cosets of $\langle a, x, y\rangle$ as connected subsets of X, even if they are not convex.

Brady and Bridson introduced snowflake groups to furnish examples of groups with interesting power-law Dehn functions: the Dehn function of $G_{p,q}$ is $n^{2\alpha}$ where $\alpha := \log_2(2p/q)$.

For each $n \geq 1$ we inductively construct a pair of paths $\sigma_{n,s}$ and $\sigma_{n,t}$ from 1 to a^{L^n} by:

$$\begin{aligned}
\sigma_{1,s} &:= sas^{-1}tat^{-1}\\
\sigma_{1,t} &:= tat^{-1}sas^{-1}\\
\sigma_{n+1,s} &:= s + \sigma_{n,s} + s^{-1} + t + \sigma_{n,s} + t^{-1}\\
\sigma_{n+1,t} &:= t + \sigma_{n,t} + t^{-1} + s + \sigma_{n,t} + s^{-1}
\end{aligned}$$

[2]For the purposes of this paper one may choose any length at least 6 for the length of the x and y edges, since this is enough to guarantee that no 2–biLipschitz path contains such an edge. We choose L because it is the length induced by the maximally symmetric metric for this group as in [13].

We call $\sigma_{n,s}$ and $\sigma_{n,t}$ *snowflake paths* and call $\sigma_{n,s} + \bar{\sigma}_{n,t}$ a *snowflake loop.* The snowflake loops are precisely the loops that Brady and Bridson showed were hard to fill, witnessing the Dehn function. An HNN diagram for $\sigma_{7,s} + \bar{\sigma}_{7,t}$ is illustrated in Figure 1. (The central diamond and all triangular regions are vertex regions, and the trapezoidal regions are corridors.)

We will show in Theorem 4.0.1 that the snowflake loops are geodesic. In particular, we can then compute lengths:

$$|a^{L^n}| = 5 \cdot 2^n - 4 \text{ if } n > 0 \tag{3.0.3}$$

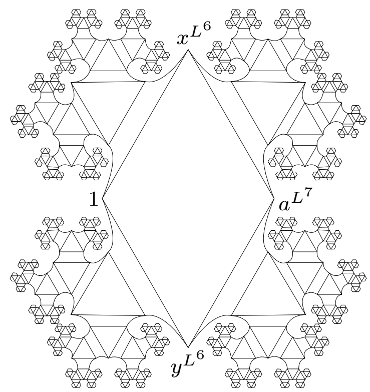

FIGURE 1. A snowflake for a^{L^7}.

3.1. **A first result about geodesics.** Recall that $H = \langle a, x, y\rangle \cong \mathbb{Z}^2$ is the vertex group of G. With respect to a fixed coset gH of H, an *escape* is a nontrivial path $\gamma\colon\ P \to X$ that intersects gH precisely at its endpoints. The difference between the endpoints of such a γ is a power of either a, x, or y, and we call γ an *a–escape*, an *x–escape* or a *y–escape*, respectively. Note that there are two types of a–escape: paths of the form $s^{-1} + \gamma + s$ or of the form $t^{-1} + \gamma + t$. On the other hand, every x–escape is of the form $s + \gamma + s^{-1}$, and every y–escape is of the form $t + \gamma + t^{-1}$.

A *toral path*, with respect to gH, is an edge path contained in gH. By our choice of metric on X, a toral path whose biLipschitz constant is less than 2 does not contain any x or y edges, so it is just an a–path.

If γ is a single escape, then its endpoints differ by g^n for some $g \in \{a, x, y\}$ and some $n \in \mathbb{Z}$. Define the *trace* of γ to be the toral path between the endpoints of γ consisting of n–many g–edges. Define the *exponent* of γ to be n.

Given a path γ with endpoints on gH we can decompose it into a concatenation $\gamma = \gamma_1 + \cdots + \gamma_n$ of escapes and toral subpaths. We then define the trace of γ (in gH) by replacing each escape by its trace.

Since H is Abelian, for any permutation σ of $\{1, \ldots, n\}$ there are translations $g_i \in H$ that give a new path $\gamma' = g_1.\gamma_{\sigma(1)} + \cdots + g_n.\gamma_{\sigma(n)}$ with the same length and the same endpoints as γ. *Consolidating toral subpaths, x–escapes, etc* means choosing the permutation σ so that in γ' all of the toral subpaths, x–escapes, etc are adjacent. Thus, by consolidating toral subpaths we may replace γ by a path γ' with the same endpoints that is a concatenation of escapes followed by a single toral subpath, for instance.

Notice that our presentation (3.0.1) for G has a symmetry that exchanges x and y and fixes $\langle a\rangle$. This induces an isometry on X, which we refer to as an *x/y–symmetry.*

Proposition 3.1.1. *For all $h \in H = \langle a, x, y\rangle$, every geodesic from 1 to h consists of a concatenation, in some order, of at most one x–escape, at most one y–escape, and some number of toral subpaths that are all of the form a^{ℓ_i}, where all of the ℓ_i have the same sign. If $L > 6$ or if $L = 6$ and $h \notin \{a^{-10}, a^{-9}, \dots, a^{10}\}$ then $|\sum_i \ell_i| < L$. If $L = 6$ and $1 \neq h \in \{a^{-10}, a^{-9}, \dots, a^{10}\}$ then the a–path from 1 to h is a geodesic but there also exists a geodesic consisting of at most one x–escape, at most one y–escape, and a toral path that is an a–path of exponent strictly less than L.*

Consequently, there is a geodesic from 1 to h of the form $\gamma_x+\gamma_y+\gamma_a$ (or any permutation of the order of these three paths) where γ_x is trivial or a geodesic x–escape, γ_y is trivial or a geodesic y–escape, and γ_a is a geodesic a–path of length less than L.

In the special case of $h = x^m y^n \neq 1$ every geodesic from 1 to h is of the form $\gamma_x + \gamma_y$ or $\gamma_y + \gamma_x$ where γ_x has exponent m and γ_y has exponent n, except in the case that $L = 6$ and $m = n = \pm 1$ so that $h = a^{\pm L}$, in which case there is such a geodesic, but the a–path from 1 to h is also geodesic.

Remark 3.1.2. One sees in Proposition 3.1.1 that there is a 'corner case' of low L and small powers of a that requires extra attention when describing geodesics. The situation is even worse when $L = 4$, so we have chosen to omit G_4 completely rather than deal with additional special cases. We suspect that the main results of the paper are still true for G_4. The group G_2 has quadratic Dehn function, so we already know its asymptotic cones are simply connected by Papasoglu's theorem.

Proof. A geodesic γ from 1 to h can be subdivided into toral subpaths and escapes, each of which we may assume is geodesic, since otherwise we would find a shortening of γ.

If there is more than one x–escape then by consolidating x–escapes we can replace γ by a path of the same length with the same endpoints that has adjacent x escapes. However, since x escapes are of the form $s + \gamma' + s^{-1}$, if there are two adjacent then we get an s–cancellation, so there is a shorter path from 1 to h, contradicting the fact that we started with a geodesic. By the same reasoning, there is at most one y–escape.

Suppose that there exist nontrivial geodesics that are not a single x–escape and whose endpoints differ by a power of x. Consider a shortest such geodesic, γ. By what we have already argued, γ consists of at most one x–escape, at most one y–escape, and paths, either toral path or a–escapes, whose endpoints differ by powers of a. By the 'shortest' hypothesis, γ does not contain an x–escape, because if it did we could remove it and get a shorter path whose endpoints still differ by a power of x. Let x^m be the difference between the endpoints of γ, and y^n be the difference between endpoints of the y–escape. Since the remainder of γ is paths whose endpoints differ by powers of a, we get that $x^m = a^\ell y^n$. Now, $x^m y^m = a^{mL}$, so $y^{m+n} = a^{mL-\ell}$. Since $\langle a\rangle \cap \langle y\rangle = 1$, this is only possible when $m + n = mL - \ell = 0$. However, this gives us:

$$|x^m| = |\gamma| = |y^m| + |a^{mL}|$$

By x/y–symmetry, $|x^m| = |y^m|$, which implies $mL = 0$, a contradiction. Thus, every geodesic whose endpoints differ by a power of x is a single x–escape. The corresponding statement for y follows from x/y–symmetry.

From this it follows that there are no geodesic a–escapes, for if there were we would have a geodesic γ such that, up to x/y–symmetry, $\gamma = s^{-1} + \gamma' + s$, where γ' is a geodesic whose endpoints differ by a power of x. But we have just shown that such a geodesic is a single x–escape, so $\gamma' = s + \gamma'' + s^{-1}$, which contradicts that γ is geodesic.

By consolidating toral subpaths we may replace γ by a path with the same length and the same endpoints in which all of the toral subpaths are adjacent. If any of them have different signs then there is an a–cancellation, which contradicts γ being a shortest path from 1 to h. Thus, we may suppose γ has a single toral subpath of the form a^ℓ for $|\sum_i \ell_i| = \ell \geq 0$. The toral subpath must be geodesic, since otherwise we could shorten γ. We have $|a^L| = |xy| = |sas^{-1}tat^{-1}| \leq 6$, so if $L > 6$ then no a–path of exponent at least L is geodesic. If $L = 6$ then a similar argument shows $|a^{12}| \leq 8$, so no a–path of exponent at least 11 is geodesic. Furthermore, if $\ell \geq 6$ then we can replace the toral subpath by the path $sas^{-1}tat^{-1}a^{\ell-6}$ to get a geodesic γ' with the same endpoints as γ. If $h \notin \{a^{-10}, a^{-9}, \dots, a^{10}\}$ then γ could not have been purely toral, because a geodesic toral path has endpoints that differ by a power of a with exponent less than 11 when $L = 6$. Since a–escapes are not geodesic, γ must have already had at least one x–escape or y–escape. Since γ' has one more x–escape and one more y–escape than γ, it has at least two of some flavor of escape, which contradicts the fact that γ' is geodesic. This leaves for our consideration the case that $h = a^\ell$ for $0 < \ell \leq 10$. Suppose there is a geodesic γ from 1 to h that is not toral. Then it contains either an x or y–escape, but since the endpoints are in $\langle a \rangle$ it must contain both with equal exponents. The minimum length of an escape is 3, so $|\gamma| \geq 6$, with equality only if $\ell = 6$. Thus, if $\ell < 6$ then the a–path from 1 to a^ℓ, which has exponent strictly less than L, is the unique geodesic. If $6 \leq \ell \leq 10$ and the escapes of γ have minimal length then, up to reordering, $\gamma = sas^{-1}tat^{-1}a^{\ell-6}$, which has length ℓ, so is the same length as the a–path. If the escapes are not minimal length then $\ell \geq |\gamma| \geq 8 + |a^{\ell-6p}|$ for some $p \geq 2$. The only solution, since $0 < \ell \leq 10$, is when $\ell = 10$ and $p = 2$, in which case the paths labelled a^{10}, $sas^{-1}tat^{-1}a^4$, and $sa^2s^{-1}ta^2t^{-1}a^{-2}$ all have the same length. We have shown that when $L = 6$ and $0 < \ell \leq 10$ it is not possible to find a shorter path from 1 to a^ℓ than the a–path, so $|a^\ell| = \ell$. We have also exhibited paths, either a^ℓ when $\ell < 6$ or $sas^{-1}tat^{-1}a^{\ell-6}$ when $6 \leq \ell \leq 10$, of the desired length, hence geodesic, and of the desired form: at most one x–escape, at most one y–escape, and a toral subpath of exponent strictly less than L.

Finally, consider $h = x^m y^n$ with $m \neq 0 \neq n$. Suppose a geodesic γ from 1 to h is not just an x–escape and a y–escape. By commutativity we may assume that the x and y–escapes, if any, come first, and end at a point $g \in \langle x, y \rangle$. Then $1 \neq g^{-1}h \in \langle a \rangle \cap \langle x, y \rangle = \langle a^L \rangle$. Thus, the geodesic contains a toral subpath whose exponent is a nontrivial multiple of L. As we have seen above, this is impossible except when $L = 6$ and $h = a^{\pm 6}$. In this case there exists a geodesic that is a single x–escape and a single y–escape, but there is also one that is a toral path.

Now suppose the x–escape has exponent p and the y–escape has exponent q. Then $h = x^m y^n = x^p y^q \implies x^{m-p} = y^{q-n}$, but $\langle x \rangle \cap \langle y \rangle = 1$, so $p = m$ and $q = n$. □

3.2. Geodesics between elements of $\langle a \rangle$.

Lemma 3.2.1. *If $0 \leq r < L$ and $q \in \mathbb{Z}$ then there exists a geodesic from 1 to a^{qL+r} that consists of a geodesic from 1 to either a^{qL} or $a^{(q+1)L}$, followed by a geodesic a–path.*

Proof. By Proposition 3.1.1, there is a geodesic from 1 to a^{qL+r} of the form $\gamma_x + \gamma_y + a^p$ with $|p| < L$. Suppose the endpoints of γ_x differ by x^m and the endpoints of γ_y differ by y^n. Then $x^m y^n = a^{qL+r-p}$, but since $\langle x, y\rangle \cap \langle a\rangle = \langle a^L\rangle$, this implies $m = n$ and $qL + r - p = mL$. Since $r - p = (m - q)L$ and $-L < r - p < 2L$, we have $m = q$ or $m = q + 1$. Thus, $\gamma_x + \gamma_y$ ends at either a^{qL} or $a^{(q+1)L}$. □

Corollary 3.2.2.

(1) $|a^\ell| = \ell$ *for* $0 < \ell \leq 3 + L/2$.
(2) $|a^\ell| = 6 + L - \ell$ *for* $3 + L/2 \leq \ell \leq L$.
(3) $|a^{qL}| = 4 + 2|a^q|$ *for all* $q \neq 0$.
(4) $||a^\ell| - |a^{\ell+1}|| = 1$ *for all* $\ell \in \mathbb{Z}$.
(5) $||a^{qL}| - |a^{(q+1)L}|| = 2$ *for all* $q > 0$.

Proof. If $q \neq 0$ then $a^{qL} = x^q y^q$ and by Proposition 3.1.1 there is a geodesic from 1 to a^{qL} consisting of a single x–escape and a single y–escape, both of exponent q. A geodesic x–escape of exponent q is of the form $s + \underline{a^q} + s^{-1}$, for some geodesic $\underline{a^q}$ whose endpoints differ by a^q, and similarly for the y–escape, so Item (3) follows.

By Lemma 3.2.1, if $0 < \ell < L$ then either there is a geodesic from 1 to a^ℓ that is an a–path of length ℓ, or there is a geodesic from 1 to a^ℓ that consists of a geodesic from 1 to a^L followed by an a–path of length $L - \ell$. The length of the latter is $6 + L - \ell$. When $\ell < 3 + L/2$ the former is shorter, when $\ell > 3 + L/2$ the latter is shorter, and when $\ell = 3 + L/2$ they have the same length. This proves Item (1) and Item (2).

Clearly $||a^\ell| - |a^{\ell+1}|| \leq 1$, so to prove Item (4) we only need to show it is not 0. It cannot be 0 because the relators all have even length, so two neighboring vertices cannot be equidistant to a third vertex.

Item (5) follows from Item (3) and Item (4). □

We can use Lemma 3.2.1 and its corollary to construct geodesics from 1 to powers of a with nonzero exponent inductively: Suppose that we know a geodesic from 1 to $a^{\ell'}$ for all $0 < \ell' < \ell$. By Corollary 3.2.2, this is true for $\ell \leq L + 1$, so we may assume $\ell \geq L + 1$. Write $\ell = qL + r$ for $0 \leq r < L$, so $q > 0$. By the induction hypothesis, we know a geodesic γ_{qL} from 1 to a^{qL} and a geodesic γ_{q+1} from 1 to a^{q+1}. By Lemma 3.2.1, there is a geodesic from 1 to a^ℓ that consists of a geodesic through either a^{qL} or $a^{(q+1)L}$, followed by an a–path. By Proposition 3.1.1 there exists a geodesic from 1 to $a^{(q+1)L}$ consisting of an x–escape whose endpoints differ by x^{q+1} and a y–escape whose endpoints differ by y^{q+1}. The former has the form $s + \underline{a^{q+1}} + s^{-1}$ for some geodesic $\underline{a^{q+1}}$ whose endpoints differ by a^{q+1}, and similarly for the latter. But since we know one such geodesic, γ_{q+1}, we know a geodesic $\gamma_{(q+1)L} := s + \gamma_{q+1} + s^{-1} + t + \gamma_{q+1} + t^{-1}$ from 1 to $a^{(q+1)L}$. Therefore, the shorter of $\gamma_{qL} + a^r$ and $\gamma_{(q+1)L} + a^{L-r}$ is a geodesic from 1 to a^{qL+r}.

We wrote a computer program to compute $|a^\ell|$ inductively as described. The results for $L = 10$ are shown in Figure 2. The main takeaway from this experiment is that the function $\ell \mapsto |a^\ell|$ is not monotonic, and in fact monotonicity fails at arbitrarily large scales. This essentially comes down to the fact that $|a^\ell|$ is relatively shorter when ℓ is close to being a power of L, and is somewhat larger if ℓ can only be expressed as a combination of several different powers of L. In the rest of this subsection we make the relationship between $|\ell|$ and $|a^\ell|$ as precise as possible.

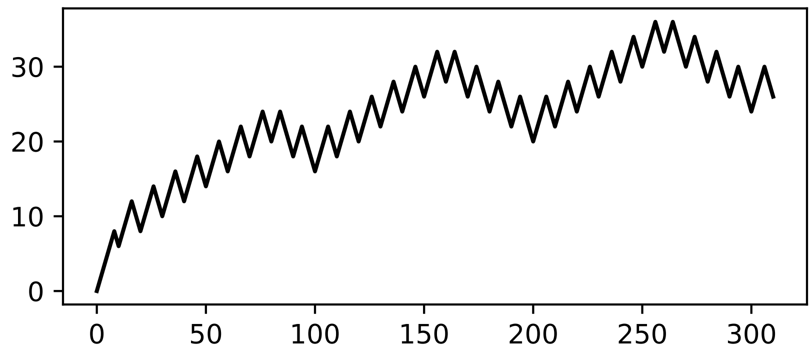

FIGURE 2. $|a^\ell|$ versus ℓ for $L = 10$. Local minima occur when $L|\ell$, second order minima occur when $L^2|\ell$, etc.

Consider an expression $0 < m = \sum_{i=0}^{j} m_i L^i$. Inductively associate to such an expression a path $\alpha + \beta + \gamma$ where γ is m_0–many a–edges, either forward or backward corresponding to the sign of m_0, and $\alpha = s + \delta + s^{-1}$ and $\beta = t + \delta + t^{-1}$ where δ is the path corresponding to $\sum_{i=0}^{j-1} m_{i+1} L^i$. This path has length:

$$\sum_{i=0}^{j} |m_i| \cdot 2^i + 4(2^j - 1) \tag{3.2.3}$$

Call $m = \sum_{i=0}^{j} m_i L^i$ a *geodesic expression* of m if the corresponding path is a geodesic. By our inductive argument, every integer admits a geodesic expression. We derive constraints on the coefficients:

Lemma 3.2.4.

- *For $0 \le \ell \le 2 + L/2$ there is a geodesic from 1 to a^ℓ consisting of an a–path of length at most $2 + L/2$.*
- *For $\ell > 2 + L/2$ there exists a geodesic from 1 to a^ℓ consisting of one x–escape, one y–escape, and an a–path of length at most $L/2$.*

Proof. The first item and the second item for $L|\ell$ follow immediately from Corollary 3.2.2 Items (1) and (3), respectively. The second item for $3 + L/2 \le \ell \le L$ follows from the proof of Corollary 3.2.2(2).

Now consider a^ℓ for $\ell \in (qL, (q+1)L)$ with $q \ge 1$. By Lemma 3.2.1, there is a geodesic from 1 to a^ℓ passing through either a^{qL} or $a^{(q+1)L}$. By Corollary 3.2.2, $||a^{qL}| - |a^{(q+1)L}|| = 2$. So if $|a^{qL}| < |a^{(q+1)L}|$ then for $\ell = qL + r$ with $r \le L/2$ there is a geodesic from 1 to a^ℓ passing through a^{qL} and then proceeding to a^ℓ via an a–path of length $r \le L/2$, while for $r \ge 1 + L/2$ there is a geodesic from 1 to a^ℓ passing through $a^{(q+1)L}$ and then proceeding to a^ℓ via an a–path of length $L - r \le L/2 - 1$. The argument for $|a^{qL}| > |a^{(q+1)L}|$ is similar. $\square$

Corollary 3.2.5. *For all $m > 0$ there is a geodesic expression $m = \sum_{i=0}^{j} m_i L^i$ satisfying:*

$$0 < m_j \le L/2 + 2 \quad \textit{and} \quad |m_i| \le L/2 \textit{ for } i < j \tag{3.2.6}$$

Note the leading coefficient has to be positive when m is because $\sum_{i=0}^{j-1} \frac{L}{2} \cdot L^i < L^j$. The conditions of (3.2.6) are not sufficient to conclude that the corresponding expression is geodesic, but they give useful general constraints.

Lemma 3.2.7. *If $0 < m = \sum_{i=0}^{j} m_i L^i$ is a geodesic expression satisfying (3.2.6) with $j \geq 1$ then $|j - \log_L m| < 1$.*

Proof.

$$|\sum_{i=0}^{j-1} m_i L^i| \leq \sum_{i=0}^{j-1} \frac{L}{2} L^i = \frac{1}{2}\frac{L}{L-1}(L^j - 1) < L^j \left(\frac{L}{2(L-1)}\right) \leq \frac{3}{5} L^j$$

So:

$$L^{j-1} < \frac{2}{5} L^j < m < L^j \left(L/2 + 2 + 3/5\right) < L^{j+1}$$ □

Lemma 3.2.8. *If $0 < m = \sum_{i=0}^{j} m_i L^i$ is a geodesic expression satisfying (3.2.6) with $j \geq 1$ then $5 \cdot 2^j - 4 \leq |a^m| \leq (L+6) \cdot 2^j - 4$.*

Proof. By (3.2.3), $|a^m| = \sum_{i=0}^{j} |m_i| \cdot 2^i + 4(2^j - 1)$. The lower bound is achieved by taking $m_j = 1$ and $m_i = 0$ for $0 \leq i < j$. The upper bound is achieved by taking $m_j = L/2 + 2$ and $m_i = L/2$ for all $0 \leq i < j$. □

We can now show that the distortion of the subgroup $\langle a \rangle$ (and therefore also of the conjugate subgroups $\langle x \rangle$ and $\langle y \rangle$) is a power function:

Theorem 3.2.9 (Power-law distortion)**.** *There is a constant C depending on L such that for $g \in \{a, x, y\}$, $|m| > 0$, and $\alpha := \log_2 L$ we have:*

$$1 \leq \frac{|g^m|}{|m|^{1/\alpha}} < C$$

Moreover, the first inequality is strict except in the case $g = a$ and $|m| = 1$.

Proof. Suppose $g = a$. By Corollary 3.2.2(1), if $0 < m < L/2 + 3$ then $|a^m| = m \geq m^{1/\alpha} \geq 1$, with equality only if $m = 1$. If $L/2 + 3 \leq m < L^{3/2}$ then by Lemma 3.2.4, there is a geodesic from 1 to a^m that contains an x–escape and a y–escape, so has length at least 6. However, $m^{1/\alpha} < (L^{3/2})^{1/\alpha} = 2^{3/2} < 3$, so $|a^m|/m^{1/\alpha} > 2$. In the other direction, $|a^m|/m^{1/\alpha} \leq m^{1-1/\alpha}$, so the upper bound for $0 < m < L^{3/2}$ is satisfied if $C \geq (L^{3/2})^{1-1/\alpha} = (L/2)^{3/2}$.

Consider the case $m \geq L^{3/2}$. There is a geodesic expression $m = \sum_{i=0}^{j} m_i L^i$ for some $j \geq 1$ satisfying (3.2.6). By Lemma 3.2.7, $L^{j-1} < m < L^{j+1}$, so $2^{j-1} < m^{1/\alpha} < 2^{j+1}$.

Lemma 3.2.8 gives:

$$m^{1/\alpha} + \frac{3}{2} m^{1/\alpha} - 4 = \frac{5}{2} m^{1/\alpha} - 4 < 5 \cdot 2^j - 4 \leq |a^m| \leq (L+6) \cdot 2^j - 4 < 2(L+6) m^{1/\alpha}$$

But $m \geq L^{3/2}$ implies $\frac{3}{2} m^{1/\alpha} - 4 > 0$, so

$$m^{1/\alpha} < |a^m| < 2(L+6) m^{1/\alpha}$$

If $g \in \{x, y\}$ and $m \neq 0$ then $|g^m| = 2 + |a^m|$ and the result follows from the result for a by taking $C := 2 + \max\{2(L+6), (L/2)^{3/2}\}$. □

In light of the claim in the introduction that the constant of Theorem 3.2.9 overwhelms the constant of the reverse Hölder inequality, and that this necessitates the labor of this paper, one might wonder whether this phenomenon is real or if it is an artifact of a suboptimal statement, or proof, of Theorem 3.2.9. Proposition 3.2.10 shows that the phenomenon is real; even if we pass to asymptotic bounds, the gap between C_{lo} and C_{hi} grows with L.

Proposition 3.2.10. *For even $L \geq 6$ consider $a \in G_L$; let $\alpha(L) := \log_2 L$, $C_{lo}(L) := \liminf_{m\to\infty} \frac{|a^m|}{m^{1/\alpha(L)}}$, and $C_{hi}(L) := \limsup_{m\to\infty} \frac{|a^m|}{m^{1/\alpha(L)}}$. Then $\frac{C_{hi}(L)}{C_{lo}(L)} > (L+6)/10$.*

When $L \geq 10$, $\frac{C_{lo}(L)}{C_{hi}(L)} \cdot 2^{1-1/\alpha(L)} < 1$.

Proof. For fixed $L \geq 6$ let $\alpha := \alpha(L)$ and $M := (L-2)/2$. For $n \geq 0$ let $m_n := ML^n - M\sum_{i=0}^{n-1} L^i$. By Corollary 3.2.2(1), $|a^{m_0}| = m_0 = M$. Notice that $m_{n+1} = Lm_n - M$. It follows from Lemma 3.2.1 and Corollary 3.2.2 parts (5) and (3) that $|a^{m_{n+1}}| = M + 4 + 2|a^{m_n}|$. Induction then shows $|a^{m_n}| = (2^{n+1}-1)M + 2^{n+2} - 4$. Thus:

$$
\begin{aligned}
\frac{|a^{m_n}|}{m_n^{1/\alpha}} &= \frac{(2^{n+1}-1)M + 2^{n+2} - 4}{\left(M\left(\frac{L^{n+1}-2L^n+1}{L-1}\right)\right)^{1/\alpha}} \\
&= \frac{(2^{n+1}-1)\left(\frac{L-2}{2}\right) + 2^{n+2} - 4}{\left(\left(\frac{L-2}{2}\right)\left(\frac{L^{n+1}-2L^n+1}{L-1}\right)\right)^{1/\alpha}} \\
&= \frac{2^n\left(\left(1-2^{-n-1}\right)(L-2) + 4 - 2^{2-n}\right)}{L^{n/\alpha}\left(\frac{1}{2}\cdot\frac{L-2}{L-1}\cdot\left(L-2+L^{-n}\right)\right)^{1/\alpha}} \\
&= \frac{\left(1-2^{-n-1}\right)(L-2) + 4 - 2^{2-n}}{\left(\frac{1}{2}\cdot\frac{L-2}{L-1}\cdot\left(L-2+L^{-n}\right)\right)^{1/\alpha}} \\
&\xrightarrow{n\to\infty} \frac{L+2}{\left(\frac{1}{2}\cdot\frac{(L-2)^2}{L-1}\right)^{1/\alpha}} \\
&= \frac{L+2}{\left(\frac{1}{2}\cdot\frac{(L-2)^2}{L-1}\right)^{\log_L 2}} \qquad (3.2.11)
\end{aligned}
$$

As a function of L, this result is greater than $L/2+3$ on $[6,\infty)$, so:

$$C_{hi}(L) \geq \lim_{n\to\infty} \frac{|a^{m_n}|}{m_n^{1/\alpha}} > L/2 + 3$$

In the other direction, induction with Corollary 3.2.2(3) gives:

$$C_{lo}(L) \leq \lim_{n\to\infty} \frac{|a^{L^n}|}{(L^n)^{1/\alpha}} = \lim_{n\to\infty} \frac{5\cdot 2^n - 4}{2^n} = 5$$

This proves the first claim. The second claim is easy to see for $L \geq 14$ using the bounds $C_{hi}(L)/C_{lo}(L) > (L+6)/10$ and $2^{-1/\alpha} < 1$. It turns out also to be true for $L \in \{10, 12\}$ using (3.2.11) and explicit computation. ∎

Remark 3.2.12. For the rest of the paper L, and consequently, α and C are fixed, and these names are only used for the constants of Theorem 3.2.9.

3.3. **Geodesics between elements of H.** Recall that x and y edges in X have length L, so geodesics consist only of a, s, and t edges.

Lemma 3.3.1. *Let $g \in \{x, y\}$. Define* $\operatorname{sign}(q)$ *to be -1, 0, or $+1$ if q is negative, zero, or positive, respectively.*

(1) *For $m \in \mathbb{N}$, $|g^m| = 2 + |a^m|$.*
(2) *For $m \in \mathbb{N}$, $||g^m| - |g^{m+1}|| = 1$.*
(3) *If $\ell = qL + r$ with $0 \leq |r| < L$ and $m, n \in \mathbb{Z}$ then:*

$$|a^\ell x^m y^n| = \min\{|r| + |x^{m+q}| + |y^{n+q}|,\, L - |r| + |x^{m+q+\operatorname{sign}(r)}| + |y^{n+q+\operatorname{sign}(r)}|\}$$

(4) *There exists a $K > 1$ such that for all ℓ and m, $K|a^\ell g^m| \geq |a^\ell| + |g^m|$.*

Proof. Item (1) follows immediately from Proposition 3.1.1, since a geodesic from 1 to x^m is a single x–escape. Item (2) follows from this and Lemma 3.2.2(4). For Item (3) the $\ell = 0$ case follows immediately from Proposition 3.1.1, while the general case is the analogue of Lemma 3.2.1: there exists a geodesic from 1 to $a^\ell x^m y^n$ passing though either $x^{m+q}y^{n+q}$ or $x^{m+q+\operatorname{sign}(r)}y^{n+q+\operatorname{sign}(r)}$, and then proceeding to $a^\ell x^m y^n$ via a geodesic a–path.

To prove Item (4), it suffices to consider $\ell \geq 0$ and $g = x$.

If $\ell = 0$ or $m = 0$ then any $K > 1$ will suffice, so assume not.

Applying Item (3):

$$|a^\ell x^m| = \min\{|r| + |x^{m+q}| + |y^q|,\, L - |r| + |x^{m+q+\operatorname{sign}(r)}| + |y^{q+\operatorname{sign}(r)}|\}$$
$$|a^\ell| + |x^m| = |x^m| + \min\{|r| + |x^q| + |y^q|,\, L - |r| + |x^{q+\operatorname{sign}(r)}| + |y^{q+\operatorname{sign}(r)}|\}$$

Thus, there are four possibilities for $K|a^\ell x^m| - (|a^\ell| + |x^m|)$, depending on which terms realize the two minima. Rewrite $K|a^\ell x^m| - (|a^\ell| + |x^m|)$ as $T' + T$ where T' contains the $|r|$ and L terms, and T contains everything else. If $r = 0$ the minima are clear and $T' = (K-1)|r| = 0$. In general for $r \neq 0$:

$$T' \in \{(K-1)|r|,\, (K+1)|r| - L,\, KL - (K+1)|r|,\, (K-1)(L - |r|)\}$$

All of these are non-negative once $K \geq L - 1$, so we assume this lower bound on K and then it suffices to find K such that the remaining part T is non-negative. The inequality $T \geq 0$ is equivalent to:

$$K \geq \frac{2|x^{q''}| + |x^m|}{|x^{q'}| + |x^{m+q'}|}$$

for some $q', q'' \in \{q, q + \operatorname{sign}(r)\}$. Notice $|q' - q''| \leq 1$.

If $q' = 0$ then $|q''| \leq 1$, so $|x^{q''}| \leq 3$, and it suffices to take $K \geq 7$.

If $0 \neq q'$ then by Item (2) we have $|x^{q''}|/|x^{q'}| \leq (|x^{q'}| + 1)/|x^{q'}| \leq 4/3$, so:

$$K' := \frac{3|x^{q'}| + |x^m|}{|x^{q'}| + |x^{m+q'}|} > \frac{2|x^{q''}| + |x^m|}{|x^{q'}| + |x^{m+q'}|}$$

Thus, it suffices to take $K \geq K'$, in the case that $\ell > 0$, $m \neq 0$, and $q' \neq 0$. We deduce upper bounds on K', hence, sufficient lower bounds on K, according to several subcases.

When $-q' = m$ we have $|x^m| = |x^{q'}|$, so $K' = 4$.

If $q' = -1$ and $m \neq 0, 1$ then:

$$K' = \frac{9 + |x^m|}{3 + |x^{m-1}|} \leq \frac{9 + |x^m|}{3 + |x^m| - 1} \leq 12/5$$

Since $\ell > 0$, we have $q' \geq -1$, so it remains to consider cases where $q' > 0$ and $m + q' \neq 0$. Suppose that $m < -q' < 0$. Then $\frac{|x^{q'}|}{|x^m|} < \frac{C(q')^{1/\alpha}}{|m|^{1/\alpha}} = C\left|\frac{q'}{m}\right|^{1/\alpha} < C$ and, using reverse Hölder and Theorem 3.2.9:

$$|x^{m+q'}| > |m + q'|^{1/\alpha} = (-m - q')^{1/\alpha} \geq (-m)^{1/\alpha} - (q')^{1/\alpha} > \frac{1}{C}|x^m| - |x^{q'}|$$

Thus:

$$K' < \frac{3|x^{q'}| + |x^m|}{|x^{q'}| + \frac{1}{C}|x^m| - |x^{q'}|} = 3C\frac{|x^{q'}|}{|x^m|} + C < C(3C + 1)$$

Now suppose $-q' < m < 0$, so $|x^m|/|x^{q'}| < C$ and:

$$K' = \frac{3 + |x^m|/|x^{q'}|}{1 + |x^{m+q'}|/|x^{q'}|} < \frac{3 + C}{1}$$

Finally, we consider $m > 0$. In this case:

$$|x^{m+q'}| > (m + q')^{1/\alpha} > 2^{-1+1/\alpha}(m^{1/\alpha} + (q')^{1/\alpha}) > C^{-1} \cdot 2^{-1+1/\alpha}(|x^m| + |x^{q'}|)$$

The corresponding estimate for K' is then:

$$\begin{aligned}
K' &< \frac{3|x^{q'}| + |x^m|}{|x^{q'}| + C^{-1} \cdot 2^{-1+1/\alpha}(|x^m| + |x^{q'}|)} \\
&= \frac{3|x^{q'}| + |x^m|}{(1 + C^{-1} \cdot 2^{-1+1/\alpha})|x^{q'}| + C^{-1} \cdot 2^{-1+1/\alpha}|x^m|} \\
&< \frac{3}{(1 + C^{-1} \cdot 2^{-1+1/\alpha})} + \frac{1}{C^{-1} \cdot 2^{-1+1/\alpha}} \\
&= C \cdot 2^{1-1/\alpha}\left(\frac{3}{1 + C \cdot 2^{1-1/\alpha}} + 1\right)
\end{aligned}$$

□

Corollary 3.3.2. *If $\ell = qL + r$ with $0 \leq |r| < L$ and $m, n \in \mathbb{Z}$ then the following inequality holds.*

$$|a^\ell x^m y^n| \geq |m + q|^{1/\alpha} + |n + q|^{1/\alpha} - 5$$

Proof. By Lemma 3.3.1(3):

$$|a^\ell x^m y^n| = \min\{|r| + |x^{m+q}| + |y^{n+q}|,\ L - |r| + |x^{m+q+\mathrm{sign}(r)}| + |y^{n+q+\mathrm{sign}(r)}|\}$$

By Theorem 3.2.9, $|m + q|^{1/\alpha} + |n + q|^{1/\alpha} - 5 \leq |x^{m+q}| + |y^{n+q}| - 5$, which is clearly less than the first term of the minimum, so it suffices to prove it is also a lower bound for the second. But $L - |r| \geq 1$ and, by Lemma 3.3.1(2) and the fact that $|x| = |y| = 3$, we have $|g^{k\pm1}| \geq |g^k| - 3$ for any $k \in \mathbb{Z}$ and $g \in \{x, y\}$. □

3.4. **Lines, intersection, projections.** The following lemmas are needed in Section 8.

Lemma 3.4.1. *For every $h \in H - \langle a \rangle$ there are exactly two closest points of $\langle a \rangle$. They are the unique element of $\langle a \rangle \cap h\langle x \rangle$ and the unique element of $\langle a \rangle \cap h\langle y \rangle$.*

Proof. The isometric action by a stabilizes $\langle a \rangle$, and $H = \coprod_{i=0}^{L-1} a^i \langle x, y \rangle$, so it suffices to assume $h = x^m y^n \in \langle x, y \rangle - \langle a \rangle$. Consider a closest point a^p of $\langle a \rangle$ to h. By Proposition 3.1.1, there is a geodesic from h to a^p of the form $\gamma_x + \gamma_y + \gamma_a$, but γ_a is clearly trivial because $\gamma_x + \gamma_y$ ends at a point of $\langle a \rangle$. Suppose γ_x and γ_y are both nontrivial. By x/y–symmetry there is a geodesic x–escape γ'_x with the same exponent as γ_y such that $\gamma' = \gamma_x + \gamma'_x$ ends on $\langle a \rangle$. Then $|\gamma'| = |\gamma_x| + |\gamma_y|$, but γ' consists of consecutive x–escapes, so can be shortened, contradicting the fact that $\gamma_x + \gamma_y$ was a shortest path to $\langle a \rangle$. Thus, either $a^p = hx^{n-m} \in H\langle x \rangle$ or $a^p = hy^{m-n} \in h\langle y \rangle$, and by x/y–symmetry, both of these choices are the same distance from h. ☐

Lemma 3.4.2. *For all $h \in H$ there exists $\ell \in \mathbb{Z}$ with $|\ell| \leq L/2$ such that $\langle x \rangle \cap ha^\ell \langle y \rangle \neq \emptyset$, in which case the intersection is a unique element.*

Proof. It suffices to consider the case $h = a^p$. Since $\langle x, y \rangle \cap \langle a \rangle = \langle a^L \rangle$, we have $\langle x \rangle \cap a^{\ell+p} \langle y \rangle \neq \emptyset$ if and only if L divides $\ell + p$, in which case the intersection is the element $x^{(\ell+p)/L} = a^{\ell+p} y^{-(\ell+p)/L}$. Choose ℓ to be an integer of smallest absolute value for which $L|(\ell + p)$. ☐

Lemma 3.4.3. *For all $n \in \mathbb{Z}$, the unique closest point of $y^n \langle x \rangle$ to 1 is y^n.*

Proof. The claim is trivial if $n = 0$, so suppose not. Suppose $y^n x^m$ is a closest point of $y^n \langle x \rangle$ to 1. If $m \neq 0$ then by Proposition 3.1.1 there is a geodesic from 1 to $x^m y^n$ consisting of a nontrivial y–escape of exponent n followed by a nontrivial x–escape. This is contradictory, since such a geodesic contains an interior point in $y^n \langle x \rangle$, so $m = 0$. ☐

Lemma 3.4.4. *If $L|p$ then $x^{p/L}$ is the unique closest point of $\langle x \rangle$ to a^p.*

Proof. If $p = 0$ the claim is trivial, so suppose not. Let x^m be a closest point of $\langle x \rangle$ to a^p. By Proposition 3.1.1 there is a geodesic from a^p to x^m of the form $\gamma_a + \gamma_y + \gamma_x$.

First, notice γ_x is trivial, because otherwise $\gamma_a + \gamma_y$ is a shorter path from a^p to $\langle x \rangle$.

Next, observe that if γ_a has exponent r then γ_y is a y–escape with endpoints a^{p+r} and x^m, so $a^{p+r} y^n = x^m$ for some n. Since $\langle x, y \rangle \cap \langle a \rangle = \langle a^L \rangle$, this implies $L|(p + r)$. By hypothesis, $L|p$, so $L|r$, but $|r| < L$, so $r = 0$. This leaves us with $a^p = x^m y^{-n}$, which is true if and only if $m = p/L = -n$. ☐

4. The snowflake Cayley graph is not strongly shortcut

In this section we prove the following theorem.

Theorem 4.0.1. *The snowflake graph X_L contains arbitrarily large geodesic loops.*

Corollary 4.0.2. *The snowflake graph X_L is not shortcut or strongly shortcut.*

Corollary 4.0.3. *There is an asymptotic cone of X_L that contains an isometrically embedded unit length circle.*

Proof of Corollary 4.0.3. Choose the observation point to be fixed at 1 and choose the scaling sequence to match the lengths of the sequence of geodesic loops of Theorem 4.0.1. □

The existence of an asymptotic cone containing an isometrically embedded unit length circle is in fact equivalent to not being strongly shortcut [23, Theorem A].

Proof of Theorem 4.0.1. Recall for each $p \geq 1$ we inductively construct snowflake paths:

$$\begin{aligned} \sigma_{1,s} &:= sas^{-1}tat^{-1} \\ \sigma_{1,t} &:= tat^{-1}sas^{-1} \\ \sigma_{p+1,s} &:= s + \sigma_{p,s} + s^{-1} + t + \sigma_{p,s} + t^{-1} \\ \sigma_{p+1,t} &:= t + \sigma_{p,t} + t^{-1} + s + \sigma_{p,t} + s^{-1} \end{aligned}$$

We aim to show snowflake loops are geodesic; that is, for all $p \geq 1$, for every pair of antipodal points on the loop $\sigma_{p,s} + \bar{\sigma}_{p,t}$ the two complementary segments of the loop are geodesics. It suffices to show that a geodesic between two antipodal points has length at least $|\sigma_{p,s}| = |\sigma_{p,t}| = |\sigma_{p,s} + \bar{\sigma}_{p,t}|/2$. Furthermore, we show that every geodesic between a pair of antipodal points on the loop passes through either 1 or a^{L^p}.

By Corollary 3.2.2(3) and induction on p, we have $|a^{L^p}| = 5 \cdot 2^p - 4 = |\sigma_{p,s}| = |\sigma_{p,t}|$, so the snowflake paths themselves are geodesic.

Next, consider the points $u = x^{L^{p-1}}$ and $v = y^{L^{p-1}}$, which are the only pair of antipodal points other than $\{1, a^{L^p}\}$ that belong to H. By Proposition 3.1.1, every geodesic γ between u and v consists of a single geodesic x–escape of exponent L^{p-1} and a single geodesic y–escape of exponent L^{p-1}, so $|u^{-1}v| = |x^{L^{p-1}}| + |y^{L^{p-1}}| = |\sigma_{p,s}|$.

For the general case, by symmetry it suffices to consider antipodal points $u, v \notin H$ such that u lies on the first half of $\sigma_{p,s}$, which is an x–escape with trace in $\langle x \rangle$, and v lies on the second half of $\sigma_{p,t}$, which is an x–escape with trace in $a^{L^p}\langle x \rangle = y^{L^{p-1}}\langle x \rangle$. Let γ be a geodesic from u to v. Decompose γ as $\gamma = \gamma_1 + \gamma_2 + \gamma_3$, where γ_1 is the shortest subpath of γ connecting u to $\langle x \rangle$, and γ_3 is the shortest subpath of γ connecting v to $y^{L^{p-1}}\langle x \rangle$. Note since $u, v \notin H$, $\gamma_1 = \gamma_1' + s^{-1}$ and $\gamma_3 = s + \gamma_3'$.

As γ_2 is a geodesic between elements of H, by Proposition 3.1.1 we can rearrange escapes and toral subpaths of γ_2 to obtain a geodesic γ_2' with the same endpoints that consists of at most one x–escape, at most one y–escape, and at most one toral subpath of exponent less than L, in that order. First, we observe that γ_2' cannot contain an x–escape as it would start with an s–edge, which would given an s–cancellation with the final edge of γ_1, contradicting the fact that γ is geodesic.

Next, observe that there is no toral subpath in γ_2', because γ_2' is a path between $\langle x \rangle$ and $a^{L^p}\langle x \rangle$, so if the toral path has exponent ℓ and the y–escape has exponent n then we would have $a^\ell y^n = a^{L^p} x^m$ for some m. This implies $a^{L^p - \ell} = x^{-m} y^n$, but $\langle a \rangle \cap \langle x, y \rangle = \langle a^L \rangle$, so ℓ is divisible by L. But $0 \leq \ell < L$, so $\ell = 0$. Thus, γ_2' is a single geodesic y–escape of exponent L^{p-1}, which implies that $\gamma_2 = \gamma_2'$ and $|\gamma_2| = |y^{L^{p-1}}| = 2 + |a^{L^{p-1}}|$, by Lemma 3.3.1(1).

We proceed by induction on p.

In the case $p = 1$ the snowflake paths are $\sigma_{1,s} = sas^{-1}tat^{-1}$ and $\sigma_{1,t} = tat^{-1}sas^{-1}$, so the pairs of antipodal points we are considering are $\{u = s,\ v = tat^{-1}sa = a^L s\}$ and

$\{u = sa = xs,\, v = tat^{-1}s = ys\}$. Observe that in both cases the points us^{-1} and vs^{-1} do not differ by a power of y, so it is not the case that both γ_1' and γ_3' are trivial. Thus $|\gamma_2| = |\gamma| - |\gamma_1'| - 1 - |\gamma_3'| - 1 \leq 6 - 3 = 3$. The only length 3 y–escapes from $\langle x\rangle$ to $a^L\langle x\rangle$ are the ones labelled tat^{-1}, so we have $\gamma = \gamma_1' + s^{-1}tat^{-1}s + \gamma_3'$. Since $|\gamma| \leq 6$, one of γ_1' or γ_3' is trivial and the other consists of a single edge. If $\{u, v\} = \{s, a^Ls\}$ then we can choose either $\gamma_1' = 1$ and $\gamma_3' = a$ to get γ to be the path from u labelled $s^{-1}tat^{-1}sa$, which goes through 1, or $\gamma_1' = a$ and $\gamma_3' = 1$ to get γ to be the path from u labelled $as^{-1}tat^{-1}s$, which goes through a^L. These are precisely the two subsegments of the snowflake loop between u and v. The calculation is similar for $\{u, v\} = \{xs, ys\}$.

Now we suppose that the claims are true up to some power p, and extend to the case of $\sigma_{p+1,s} + \bar{\sigma}_{p+1,t}$. With the setup as above, γ_1' begins at u and ends at sa^m, for some m, so $s^{-1}.\gamma_1'$ is a path from $s^{-1}u$ to a^m. Since γ_2 is a single y–escape of exponent L^p, $\bar{\gamma}_3'$ begins at $sa^ms^{-1}y^{L^p}s = x^my^{L^p}s = y^{L^p}x^ms = y^{L^p}sa^m$ and ends at v, hence $s^{-1}y^{-L^p}.\bar{\gamma}_3'$ begins at a^m and ends at $s^{-1}y^{-L^p}v$. Thus $s^{-1}.\gamma_1' + s^{-1}y^{-L^p}.\bar{\gamma}_3'$ is a path from $s^{-1}u \in \sigma_{p,s}$ to $s^{-1}y^{-L^p}v \in \sigma_{p,t}$. Furthermore, since u and v were antipodal, we claim that $s^{-1}u$ and $s^{-1}y^{-L^p}v$ are antipodal in $\sigma_{p,s} + \bar{\sigma}_{p,t}$. To see this, let α be the segment of $\sigma_{p+1,s}$ from u to $a^{L^{p+1}}$, and let β be the segment of $\bar{\sigma}_{p+1,t}$ from $a^{L^{p+1}}$ to v, so that $|\alpha| + |\beta| = |\sigma_{p+1,s}|$. The path α decomposes as $\alpha' + s^{-1} + t + \sigma_{p,s} + t^{-1}$, where $\alpha' + s^{-1}$ is the subsegment of $\sigma_{p+1,s}$ from u to x^{L^p}. We have that $s^{-1}.\alpha'$ is the subsegment of $\sigma_{p,s}$ from $s^{-1}u$ to $s^{-1}x^{L^p}s = a^{L^p}$. On the other hand, $\beta = s + \beta'$, where β' is the subsegment of $\bar{\sigma}_{p+1,t}$ from $a^{L^{p+1}}s$ to v, and $s^{-1}y^{-L^p}.\beta'$ is the subsegment of $\bar{\sigma}_{p,t}$ from $s^{-1}y^{-L^p}a^{L^{p+1}}s = a^{L^p}$ to $s^{-1}y^{-L^p}v$. Thus, $s^{-1}.\alpha' + s^{-1}y^{-L^p}.\beta'$ is the subsegment of $\sigma_{p,s} + \bar{\sigma}_{p,t}$ from $s^{-1}u$ to $s^{-1}y^{-L^p}v$ going through a^{L^p}, and it has length:

$$\begin{aligned}
|\alpha'| + |\beta'| &= |\alpha| - 3 - |\sigma_{p,s}| + |\beta| - 1 \\
&= |\sigma_{p+1,s}| - |\sigma_{p,s}| - 4 \\
&= 5 \cdot 2^{p+1} - 4 - (5 \cdot 2^p - 4) - 4 \\
&= 5 \cdot 2^p - 4 = |\sigma_{p,s}|
\end{aligned}$$

Since $s^{-1}u$ and $s^{-1}y^{-L^p}v$ are antipodal in $\sigma_{p,s} + \bar{\sigma}_{p,t}$, the induction hypothesis says that the subsegment δ of $\sigma_{p,s} + \bar{\sigma}_{p,t}$ from $s^{-1}u$ to $s^{-1}y^{-L^p}v$ passing through a^{L^p} is geodesic. Split δ at a^{L^p} as a concatenation $\delta = \delta_1 + \delta_3$, and define $\delta' := s.\delta_1 + s^{-1} + t + \sigma_{p,s} + t^{-1} + s + \bar{\delta}_3$. Then δ' is the subsegment of $\sigma_{p+1,s} + \bar{\sigma}_{p+1,t}$ from u to v that goes through $a^{L^{p+1}}$. We must show δ' is geodesic. We have:

$$\begin{aligned}
|\delta'| - |\gamma| &= |\delta_1| + |\delta_3| + 4 + |\sigma_{p,s}| - (|\gamma_1'| + |\gamma_3'| + 2 + |\gamma_2|) \\
&= |\delta_1| + |\delta_3| + 4 + |a^{L^p}| - \big(|\gamma_1'| + |\gamma_3'| + 4 + |a^{L^p}|\big) \\
&= |\delta_1| + |\delta_3| - |\gamma_1'| - |\gamma_3'|
\end{aligned}$$

On the one hand this quantity is nonnegative, because δ' is a path from u to v and γ is a geodesic with the same endpoints. On the other hand it is nonpositive, since $s^{-1}.\gamma_1' + s^{-1}y^{-L^p}.\gamma_3'$ is a path from $s^{-1}u$ to $s^{-1}y^{-L^p}v$ and $\delta = \delta_1 + \delta_3$ is a geodesic with the same endpoints. Thus, $|\delta'| = |\gamma|$, so δ' is geodesic. Since the complement to δ in $\sigma_{p+1,s} + \bar{\sigma}_{p+1,t}$ has the same length and the same endpoints, it is geodesic too. We also get that $s^{-1}.\gamma_1' + s^{-1}y^{-L^p}.\gamma_3'$ is a geodesic from $s^{-1}u$ to $s^{-1}y^{-L^p}v$, which are antipodal points on $\sigma_{p,s} + \bar{\sigma}_{p,t}$, so by the induction hypothesis $s^{-1}.\gamma_1' + s^{-1}y^{-L^p}.\gamma_3'$ passes through either 1 or a^{L^p}, necessarily at the concatenation point. This means that either γ_1 ends at 1 or γ_3 begins at $a^{L^{p+1}}$, so γ passes through either 1 or $a^{L^{p+1}}$. That completes the induction. □

5. The idea of the proof that asymptotic cones are simply connected

5.1. **The snowflake case.** Let us sketch the argument that snowflake loops can be subdivided in a way that satisfies Theorem 2.3.2. The idea in the general case will be that, for K sufficiently close to 1, K–biLipschitz loops look sufficiently similar to snowflake loops that the same strategy works.

Consider a snowflake loop γ for a^{L^p} with HNN diagram as in Figure 1. We will subdivide each region and replace it by regions with relatively short boundaries. The diagram has a central diamond, the sides of which are labelled $x^{L^{p-1}}$ and $y^{L^{p-1}}$. From (3.0.3), the length of γ is $2(5 \cdot 2^p - 4)$. We choose a subdivision constant Λ, which in this case we can take to be $\Lambda = L$. Subdivide the central diamond into Λ^2 small diamonds whose sides are labelled $x^{L^{p-2}}$ and $y^{L^{p-2}}$. If we take one of these small diamonds and replace its sides by geodesics we get a small snowflake loop whose length is $2(5 \cdot 2^{p-1} - 4) < \frac{1}{2}|\gamma|$. Propagate the subdivision into the branches of the snowflakes to get subdivisions of the neighboring triangular regions, as in Figure 3. This gives us $\sim \Lambda^2$ more short loops.

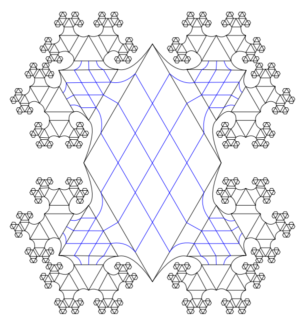

Figure 3. Subdivided snowflake to depth 1.

Obviously, we cannot continue this propagation indefinitely, since the depth of the snowflake depends on the boundary word, but to apply Theorem 2.3.2 we need the number of short loops to be uniform. Consider the situation depicted in Figure 4—we have subdivided some number of levels deeply into the snowflake, and are faced with the remaining branch. The incoming corridor has been subdivided into Λ–many pieces.

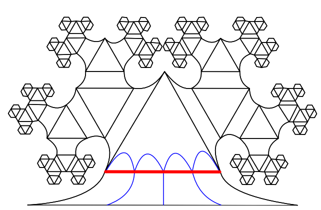

Figure 4. Capping off a branch

These pieces have been replaced by short geodesic segments. The idea is to make one short loop consisting of these Λ–many geodesics, plus the outer boundary of the branch. The incoming edge of the triangle, the red edge in Figure 4, is labelled $a^{L^{p-m}}$ if we are at depth m. Thus, the length of the outer boundary of the branch is $|a^{L^{p-m}}|$, while the length of each of the Λ–many short geodesics is $|a^{L^{p-m-1}}|$, since $\Lambda = L$. Given our formula (3.0.3), we can solve to see that $|a^{L^{p-m}}| + \Lambda|a^{L^{p-m-1}}| \leq \frac{1}{2}|\gamma|$ once $m \sim \log_2 L$. So at some depth m, *independent of* p, the paths have become short enough that we can cap off a branch with a single short loop.

This argument decomposes the snowflake loop γ into $\sim L^3$ loops of length at most $\frac{1}{2}|\gamma|$. If a similar bound were to hold for biLipschitz loops, then, by [10, Theorem 4.3.3], this would imply that the Dehn function of G_L is bounded above by $n^{3\log_2 L}$. This is consistent with the true Dehn function, which is known to be $n^{2\log_2 L}$. We have made no effort to optimize the decomposition, and do not know if it is possible to subdivide into only $\sim L^2$–many short loops.

5.2. **The general case.** We must show that for all $\lambda \in (0, 1)$ there exist M and A such that every loop γ in X can be filled by a diagram with area at most A and mesh at most $\lambda|\gamma| + M$.

Step 1, Reduce to biLipschitz loops: In Section 6 we show that if γ fails to be biLipschitz at a large scale, in a sense to be made precise, then it is easy to fill: introduce a geodesic segment between two far apart points where the biLipschitz condition fails and take an area 2 filling of the Θ graph with the 1–skeleton mapping to the union of γ and this geodesic segment.

Otherwise, if γ fails to be biLipschitz only at smaller scales then Theorem 6.0.1 says it can be tightened to a K–biLipschitz loop without changing it very much, where we are free to choose $K > 1$ as small as we like. Corollary 6.0.3 says if we can find the desired filling of the biLipschitz loop then we can extend it to the original loop without changing the area or the mesh too much. Thus, we have reduced the problem to finding some $K > 1$ for which we can fill all K–biLipschitz loops.

Interlude; how different are biLipschitz loops from snowflakes?: Figure 5 shows a schematic of an HNN diagram for a biLipschitz loop. We point out some

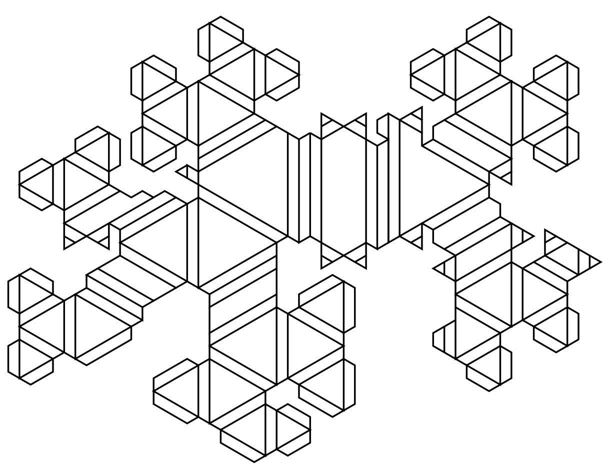

FIGURE 5. biLipschitz snowflake

differences between Figure 5 and Figure 1:

(1) Figure 5 has no central diamond.
(2) There can be adjacent corridors with no vertex region in between.
(3) Not all of the noncentral vertex regions are triangles.

We claim these differences are not severe. It turns out there is a way to choose a central region. Moreover, although regions may have any number of sides, we will show that most of them are negligibly small and are easy to account for in our filling diagram without affecting the mesh very much. More specifically, the central region has at most four long sides, and the other regions have either two or three long sides. It will take some work to make these statements precise.

Branching of the diagram played an important role in the snowflake case, so the presence of bigon regions may be concerning. We assemble maximal chains of corridor and bigon regions into subdiagrams that we call *enfilades* in Section 7.3.

Step 2, all diagrams have a central 'region': Consider an HNN diagram $D \to X$ for an embedded loop γ in X. Since γ is embedded, D is a disk. If D is a single region then call that one the central region. If not, D contains corridors. Recall that corridors have disjoint interiors and bisect D, and contain two disjoint edges in ∂D. Furthermore, corridors are 2–cells with boundary label of the form $sa^ns^{-1}x^{-n}$ or $ta^nt^{-1}y^{-n}$. We parameterize such a 2–cell as a rectangle $[0,n]\times[0,1]$ and define a map $\phi\colon D \to |T|$ from D to the geometric realization $|T|$ of the dual tree T to the corridor decomposition of D, such that ϕ restricted to a corridor parameterized $[0,n]\times[0,1]$ is projection to the second coordinate followed by a linear isometry to the geometric realization of an edge.

Since corridors contain disjoint edges on ∂D, for every $x \in |T|$, $\phi^{-1}(x)$ contains at least two points of ∂D, so $\gamma - \phi^{-1}(x)$ consists of at least two components. Define a function f on $|T|$ by:

$$x \mapsto (\text{maximum length of a component of } \gamma - \phi^{-1}(x)) - |\gamma|/2$$

The function f is typically not continuous. We claim that there is a unique point at which f achieves a non-positive value.

First, suppose that f achieves a non-positive value at x. Then $\gamma - \phi^{-1}(x)$ consists of finitely many segments γ_i, each of length at most $|\gamma|/2$. For any other $y \in |T|$, there is a component γ' of $\gamma - \phi^{-1}(y)$ and an i_0 such that $\gamma - \gamma'$ is contained in γ_{i_0}. Furthermore, γ' crosses corridors corresponding to the edges of T on the geodesic between x and y. Thus, $|\gamma'| \geq |\gamma| - |\gamma_{i_0}| + 2d_T(x,y) > |\gamma| - |\gamma_{i_0}| \geq |\gamma|/2$, so $f(y) \geq |\gamma'| - |\gamma|/2 > 0$. So if f achieves a non-positive value, it does so at a unique point of $|T|$.

Next, suppose that v is a vertex of T with $f(v) > 0$. Then there is a component γ' of $\gamma - \phi^{-1}(v)$ of length strictly greater than $|\gamma|/2$. The closure $\mathrm{cl}(\gamma')$ of γ' maps via ϕ to a loop in T at v that begins and ends by crossing some edge e incident to v. Suppose this edge is parameterized $[0,1]$ with 0 at v. Then for $x \in (0,1)$ there is a component of $\gamma - \phi^{-1}(x)$ whose closure is a subsegment of γ' of length $|\gamma'| - 2x$. So either $f(v) > 1$ and f is linearly decreasing and positive on $[0,1)$, or $f(v) = 1$ and f achieves value 0 at the midpoint of e. In both cases, $f(v) > 0$ implies that $f(v)$ is not a local minimum.

Finally, suppose that f is positive and decreasing on some edge parameterized $[0,1]$. Then for each $x \in (0,1)$ there is a component γ_x of $\gamma - \phi^{-1}(x)$ such that $|\gamma_x| > |\gamma|/2$ and as $x \to 1$ the closed segments $\mathrm{cl}(\gamma_x)$ form a decreasing nested family all containing

$\phi^{-1}(1) \cap \partial D$. The limit γ' of this family as $x \to 1$ is a closed subsegment of γ of length at least $|\gamma|/2$ containing $\phi^{-1}(1) \cap \partial D$. There are two possibilities: either $\phi^{-1}(1) \cap \partial D$ is exactly two points and $f(1) = |\gamma'| - |\gamma|/2$, so $f|_{(0,1]}$ is continuous at 1, or $\phi^{-1}(1) \cap \partial D$ has more than two points and the components of $\gamma - \phi^{-1}(1)$ are either $\gamma - \gamma'$ or proper subsegments of γ'. In this case $f(1) \leq |\gamma'| - |\gamma|/2$, so $f(1)$ is a strict lower bound for f on $(0,1)$.

Since there are finitely many vertices, we conclude that f achieves a minimum value. If $f(x) > 0$ then x is not a local minimum, so the minimum value achieved by f is non-positive.

If f achieves value 0 on the midpoint of an edge then we call the corresponding corridor the central region R of D. If f achieves its minimum value at a vertex v then we define $R = \phi^{-1}(v)$ to be the central region of D. This includes a degenerate possibility that R is not really a region; it can be that $\phi^{-1}(v)$ is a tree in the 1-skeleton of D with leaves on ∂D. The important point is that the map $D \to X$ sends $\phi^{-1}(v)$ into a single coset of H.

Remark 5.2.1. There is a natural map from the dual tree in the above argument into the Bass-Serre tree of G, so to every vertex $v \in T$ there is associated a coset $g_v H$. However, we cannot assume this map is injective. In particular, if v is a vertex of T, we cannot conclude that the closures of components of $\gamma - \phi^{-1}(v)$ are *escapes* from $g_v H$. One of these components could return to $g_v H$ in its interior. We need a more general definition to describe these paths.

Definition 5.2.2. Let γ be a path in X that intersects a coset gH. Define a *compound escape* of γ from gH to be a subpath γ' of γ with both endpoints in gH such that one of the following holds:

- γ' begins with s, ends with s^{-1}, and has endpoints that differ by a power of x.
- γ' begins with t, ends with t^{-1}, and has endpoints that differ by a power of y.
- γ' begins with s^{-1}, ends with s, and has endpoints that differ by a power of a.
- γ' begins with t^{-1}, ends with t, and has endpoints that differ by a power of a.

The first two cases we call compound x and y–escapes, respectively, and the last two compound a–escapes.

So our usual, simple, escapes are also compound escapes, but a compound escape may return to gH in its interior.

In the case where γ is a K-biLipschitz (and hence embedded) loop, we gain two things by identifying the central region:

- If R is the central region, each component of $\gamma - R$ is a K-biLipschitz path with endpoints in a coset of H.
- If R is a non-central region then at most one component γ' of $\gamma - R$ can fail to be K–biLipschitz, and $\gamma - \gamma'$ is a single K–biLipschitz path with endpoints in a coset of H.

We analyzed *geodesics* between elements of H in Section 3.3, and now we must:

Step 3, Analyze biLipschitz paths between elements of H: This is Section 7.1. The underlying idea is that for such a path to be efficient it should make as much use of the distortion of H as possible, and the way that that happens is when the path is almost entirely either one long escape or two long escapes that are an x–escape and a y–escape.

Step 4, Apply the previous step to analyze central and non-central regions of the diagram: This is done in Section 7.2 and Section 7.3. The conclusions, as alluded to above, are that the central region has at most four long sides, and they are configured in one of 6 possible ways, and every other region has at most 3 long sides, and in the case of 3 they approximately form a triangle of a, x, and y–escapes just like in the snowflake case. Furthermore, we show that when we lump together adjacent bigon regions and corridors into enfilades, the enfilades are metrically thin.

Step 5, Construct a new filling diagram: We have established that the structure of the diagram is a central region with at most 4 adjacent enfilades, each of which leads to a triangular region. Each of these has two outgoing sides with adjacent enfilades leading to more triangular regions, etc. The strategy now will be the same as in the snowflake case: choose a way to subdivide the central region and propagate this subdivision out across the original diagram in a way that the mesh is controlled and such that after a uniform number of steps we can cap off the remaining branches with single 2–cells. This is done in Section 8.

6. Reduction to biLipschitz cycles

The following theorem is a specialized form of a result of Hoda [23].

Theorem 6.0.1 (Circle Tightening Lemma [23, Theorem G])**.** *Let $N > 1$ and $K > 1$, and let $\theta > 1$ be small enough (depending on N and K) and let $M > 0$ be large enough (depending on N, K, and θ). Let $\alpha\colon S \to X$ be a 1-Lipschitz map from a Riemannian circle S to a geodesic metric space X. If*

$$d_X\big(\alpha(p), \alpha(\bar{p})\big) \geq \frac{1}{\theta} d_S(p, \bar{p})$$

for every antipodal pair $p, \bar{p} \in S$ and $|S| > M$ then there exists a countable collection $\{Q_i\}_i$ of pairwise disjoint closed segments in S such that the following conditions hold.

1. $\sum_i |Q_i| < \frac{|S|}{N}$
2. *For each i, we have $d_X\big(\alpha(p_i), \alpha(q_i)\big) < |Q_i|$ where p_i and q_i denote the endpoints of Q_i.*
3. *There is a collection of geodesics $\{\gamma_i\colon \bar{Q}_i \to X\}_i$ such that γ_i has endpoints $\alpha(p_i)$ and $\alpha(q_i)$ and replacing each $Q_i \to X$ in α with $\bar{Q}_i \to X$ results in a K-biLipschitz embedding α' of a circle that is also 1-Lipschitz.*

Remark 6.0.2. If X is a graph and α is a combinatorial map then no Q_i can be contained in a single edge, as this would contradict $d_X\big(\alpha(p_i), \alpha(q_i)\big) < |Q_i|$. Then each Q_i contains a vertex in its interior and it follows that the family Q_i is necessarily finite. Moreover, since α' is bilipschitz, it is also a combinatorial map.

Corollary 6.0.3. *Let X be a Cayley graph. Suppose there exist $K > 1$, $0 < \lambda < 1$, M, and A such that every K–biLipschitz loop α admits a filling of area at most A and mesh at most $\lambda|\alpha| + M$. Then there exists $0 < \lambda' < 1$ and M' such that every 1–Lipschitz loop α admits a filling of area at most $A + 3$ and mesh at most $\lambda'|\alpha| + M'$.*

Proof. Take $N > 12$. Let $\theta > 1$ be as in Theorem 6.0.1 with respect to N and K. Let M' be the larger of M and the M of Theorem 6.0.1. Define:

$$\lambda' := \max\left\{\lambda,\, \frac{1+\theta}{2\theta},\, 2\left(\frac{1}{3}+\frac{2}{N}\right)\right\} < 1$$

Consider a 1–Lipschitz loop $\alpha\colon S \to X$. If there exist a pair of antipodal points p and $\bar{p} \in S$ such that $d_X(\alpha(p), \alpha(\bar{p})) < \frac{1}{\theta}\frac{|S|}{2}$ then there is a diagram of area 2 filling α obtained by taking one 2–cell to have boundary the segment of α restricted to the interval of S from p to $\bar{p}$ followed by a geodesic δ from $\alpha(\bar{p})$ to $\alpha(p)$, and taking the other to have boundary $\bar{\delta}$ followed by the remaining subsegment of α. These loops have length $|S|/2 + |\delta| < \frac{1+\theta}{2\theta}|S| \leq \lambda'|S|$.

If there is no such pair of antipodal points then Theorem 6.0.1 applies. We use notation as in the theorem. By hypothesis, there is a filling of α' of area at most A and mesh at most $\lambda|S'| + M \leq \lambda'|S| + M'$. We need to extend this to a filling of α. Pick points s_0, s_1, and s_2 in $S - \cup_i \mathring{Q}_i$ such that for all i, subscripts mod 3, we have $d_S(s_i, s_{i+1}) \leq \left(\frac{1}{3}+\frac{2}{N}\right)|S|$. Then we get 3 loops of the form: segment of α restricted to the interval of S from s_i to s_{i+1} followed by reverse of the segment of α' from s_i to s_{i+1}. The length of such a loop is at most twice the α part, since α' is a tightening of α, so it is bounded above by $2\left(\frac{1}{3}+\frac{2}{N}\right)|S| \leq \lambda'|S|$. Adding three 2–cells with these boundary loops to the diagram for α gives us the desired diagram for α. □

7. BiLipschitz cycles in snowflake groups

Recall, Remark 3.2.12, that the group G_L is deemed to be fixed, so L, C, and α are constant. The other 'constants' in this section implicitly depend on the choice of L.

In Section 7.1 we analyze biLipschitz paths with endpoints in H. Sections 7.2 and 7.3 are preparatory for Section 8. In those sections we establish properties for central and non-central regions of a putative filling of a biLipschitz loop γ. Since 'region' is a term applied to an already existing filling, we will phrase these properties in a way that is intrinsic to γ.

7.1. BiLipschitz paths with endpoints in H.

The main result of this subsection is:

Theorem (Theorem 7.1.24)**.** *For all $R > 1$ there exist $J > 1$ and $1 < K < 2$ such that if γ is a K–biLipschitz path with endpoints in $H = \langle a, x, y\rangle$ then either $|\gamma| \leq J$ or γ has either one or two long escapes that collectively account for at least $\frac{R-1}{R}$ fraction of its length. Furthermore, in the case of two long escapes they are one x–escape and one y–escape.*

If the endpoints of γ differ by a power of x or y, then there is only one long escape, and it is of the corresponding flavor, and if the endpoints of γ differ by a power of a then either there is one long a–escape or there is one long x–escape and one long y–escape.

We build up to this theorem through a string of auxiliary results. Most follow the same template: given a target R that quantifies the desired ratio of domination, it is possible to choose $K > 1$ sufficiently close to 1 so that any K–optimal path γ with endpoints in H must have one or two escapes that dominate the others. The complexity of the assumed structure of γ increases with each lemma.

There is also an issue that in the theorem the domination is phrased in terms of length, but for most of the auxiliary results it is more convenient to work with exponents, so we will have to make a conversion. Because the relationship between exponent and length is not monotonic, this conversion is nontrivial.

For the first step, we suppose that γ consists of two escapes of the same flavor:

Lemma 7.1.1. *There exists $J > 1$ such that for all $R > 1$ there exists $1 < K < 2$ such that for all $|m|, |n| \geq J$, if $g \in \{a, x, y\}$ and*

$$|g^m| + |g^n| \leq K|g^{m+n}|$$

then $\max\{\frac{|n|}{|m|}, \frac{|m|}{|n|}\} > R$.

Proof. First assume $g = a$. Let $J := 1+(L+3)/2$. Let $m = \sum_{i=0}^{j} m_i L^i$ and $n = \sum_{i=0}^{k} n_i L^i$ be geodesic expressions for m and n satisfying Condition (3.2.6). Since $|m|, |n| \geq J$, we have $j, k > 0$. Without loss of generality, assume $k \geq j$ and $n > 0$ so that $n_k \geq 1$.

We approximate as follows:

$$\begin{aligned}
\frac{|n|}{|m|} &= \frac{|\sum_{i=0}^{k} n_i L^i|}{|\sum_{i=0}^{j} m_i L^i|} \\
&= \frac{|n_k L^k + \sum_{i=0}^{k-1} n_i L^i|}{|m_j L^j + \sum_{i=0}^{j-1} m_i L^i|} \\
&\geq \frac{L^k + \sum_{i=0}^{k-1} -(L/2)L^i}{(L/2+2)L^j + \sum_{i=0}^{j-1}(L/2)L^i} && \text{by (3.2.6)} \\
&= \frac{L^k - \frac{1}{2}\frac{L}{L-1}(L^k - 1)}{\frac{1}{2}(L+4)L^j + \frac{1}{2}\frac{L}{L-1}(L^j - 1)} \\
&= \frac{2(L-1)L^k - L(L^k - 1)}{(L-1)(L+4)L^j + L(L^j - 1)} \\
&= \frac{L^{k+1} - 2L^k + L}{L^{j+2} + 4L^{j+1} - 4L^j - L} \\
&= \frac{(L-2)L^{k-1} + 1}{(L+4)L^j - 4L^{j-1} - 1}
\end{aligned}$$

Thus, $|n|/|m| > R$ if:

$$(L-2)L^{k-1} + 1 - R\left((L+4)L^j - 4L^{j-1} - 1\right) > 0$$

The left hand side is bigger than $(L-2)L^{k-1} - R(L+4)L^j$, so the claim holds if:

$$k - j > 1 + \log_L\left(\frac{R(L+4)}{L-2}\right) \tag{7.1.2}$$

Otherwise, if $0 \leq k - j \leq 1 + \log_L(R(L+4)/(L-2))$, we choose K sufficiently close to 1 to make $|a^m| + |a^n| \leq K|a^{m+n}|$ impossible. To show that this can be done we use the fact that $m + n = \sum_{i=0}^{k}(m_i + n_i)L^i$, where $m_i = 0$ for $i > j$, to provide an upper bound for $|a^{m+n}|$.

$$
\begin{aligned}
|a^m| + |a^n| - K|a^{m+n}| &\geq |a^m| + |a^n| - K\left(\sum_{i=0}^{k} |m_i + n_i| 2^i + 4(2^k - 1)\right) \\
&= 4(2^j - 1) + 4(2^k - 1) - 4K(2^k - 1) \\
&\qquad + \sum_{i=0}^{j} (|m_i| + |n_i| - K|m_i + n_i|) 2^i && \text{by (3.2.3)} \\
&\geq 4(2^j - 1) - (K-1)4(2^k - 1) \\
&\qquad + \sum_{i=0}^{k} -(K-1)2^i(|m_i| + |n_i|) && \text{by tri. ineq.} \\
&\geq 4(2^j - 1) - (K-1)4(2^k - 1) \\
&\qquad - (K-1)\sum_{i=0}^{k} 2^i L && \text{by (3.2.6)} \\
&\qquad - (K-1)(2^{k+1} + 2^{j+1}) \\
&= 4(2^j - 1) - (K-1)\left(4(2^k - 1) + L(2^{k+1} - 1) + 2^{k+1} + 2^{j+1}\right) \\
&= 2^{j+2} - (K-1)\left(2^{k+2} + L(2^{k+1} - 1) + 2^{k+1} + 2^{j+1}\right) - 4(2 - K)
\end{aligned}
$$

To make this expression positive, it suffices to have:

$$
1 - \frac{2-K}{2^j} > 2^{k-j}(K-1)\left(1 + \frac{L}{2} + 2^{-1} + 2^{j-1-k}\right) \tag{7.1.3}
$$

The left hand side is at least 1/2, and the right hand side is bounded above by:

$$
(1/2) \cdot 2^{k-j}(K-1)(L+4)
$$

Thus, applying the bound on $k - j$ from the negation of (7.1.2), we see that (7.1.3) is satisfied for

$$
K < 1 + \frac{1}{2^{k-j}(L+4)} \leq 1 + \frac{1}{2(L+4)} \cdot \left(\frac{R(L+4)}{L-2}\right)^{-1/\alpha}
$$

This completes the proof when $g = a$.

If $g \in \{x, y\}$ then $|g^p| = |a^p| + 2$ (by Lemma 3.3.1), so $|g^m| + |g^n| \leq K|g^{m+n}|$ implies:

$$
|a^m| + |a^n| = |g^m| + |g^n| - 4 \leq K|g^{m+n}| - 4 = K|a^{m+n}| + 2K - 4 \leq K|a^{m+n}|
$$

Thus, the result follows from the result for a. □

Remark 7.1.4. In Lemma 7.1.1 we provide a condition to show that two quantities, let us call them A and B, are related by $A/B > R$ for some $R > 0$. We will frequently pass without comment between equivalent formulations of this relation that we note here to avoid any confusion:

$$
A/B > R \iff A > RB \iff A > \frac{R}{R+1}(A+B) \iff B < \frac{1}{R+1}(A+B)
$$

Next, we consider multiple escapes, all of the same flavor and with all exponents positive:

Corollary 7.1.5. *For all $R > 1$ there exist $J > 1$ and $1 < K < 2$ such that if $g \in \{a, x, y\}$ and $m_1 \geq m_2 \geq \cdots \geq m_k > 0$ and $\sum_{i=1}^k m_i \geq J$ and*

$$\sum_{i=1}^{k} |g^{m_i}| \leq K |g^{\sum_{i=1}^k m_i}|$$

then $m_1 > \frac{R}{R+1} \sum_{i=1}^k m_i$.

Proof. Replace R by $\max\{R, 5\}$. Observe that the result for the new R implies the result for the original R. Let $J' := 1 + (L+3)/2$ as in Lemma 7.1.1, let $J := J'(R+1)$, and let K be a constant satisfying Lemma 7.1.1 with respect to R. By Lemma 7.1.1, we have one of the following possibilities:

- $\frac{m_1}{m_2+m_3+\ldots+m_k} > R$
- $m_2 + m_3 + \ldots + m_k < J'$
- $\frac{m_2+m_3+\ldots+m_k}{m_1} > R$
- $m_1 < J'$

Since $\sum_{i=1}^k m_i \geq J$, either of the first two conditions imply $m_1 > \frac{R}{R+1} \sum_{i=1}^k m_i$. The disjunction of the last two conditions implies $m_2 + m_3 + \cdots + m_k > \frac{R}{R+1} \sum_{i=1}^k m_i$. Thus it suffices to rule out this latter possibility.

Suppose $m_2 + m_3 + \cdots + m_k > \frac{R}{R+1} \sum_{i=1}^k m_i$. Let ℓ be least such that $\sum_{i=1}^{\ell} m_i \geq \frac{1}{2} \sum_{i=1}^k m_i$. Then, for all i, we have $m_i \leq m_1 < \frac{1}{R} \sum_{i=1}^k m_i$ and so

$$\frac{1}{2} \sum_{i=1}^{k} m_i \leq \sum_{i=1}^{\ell} m_i < \frac{1}{2} \sum_{i=1}^{k} m_i + m_\ell < \frac{R+2}{2R} \sum_{i=1}^{k} m_i$$

holds. Then $\sum_{i=1}^{\ell} m_i \geq \frac{1}{2} \sum_{i=1}^k m_i \geq J/2 > J'$ and $\sum_{i=\ell+1}^k m_i > \frac{R-2}{2R} \sum_{i=1}^k m_i \geq \frac{R-2}{2R} J > J'$, since $R \geq 5$, so by Lemma 7.1.1, either (I) $\sum_{i=1}^{\ell} m_i > R \sum_{i=\ell+1}^k m_i$ or (II) $\sum_{i=\ell+1}^k m_i > R \sum_{i=1}^{\ell} m_i$. We will show that either case results in a contradiction. In case (I) we have

$$\frac{R+2}{2R} \sum_{i=1}^{k} m_i > \sum_{i=1}^{\ell} m_i > R \sum_{\ell+1}^{k} m_i > \frac{R(R-2)}{2R} \sum_{i=1}^{k} m_i$$

which contradicts $R \geq 5$. In case (II) we have

$$\frac{1}{2} \sum_{i=1}^{k} m_i \geq \sum_{i=\ell+1}^{k} m_i > R \sum_{1}^{\ell} m_i \geq \frac{R}{2} \sum_{i=1}^{k} m_i$$

which again contradicts $R \geq 5$. □

Next we will generalize to the case that γ consists of escapes of the same flavor, this time allowing both positive and negative exponents. First, there is an auxiliary result, Corollary 7.1.6, that says either the positive exponents or the negative exponents dominate. Then, in Corollary 7.1.7, we show that a single escape dominates.

Corollary 7.1.6. *For all $R > 1$ there exist $J > 1$ such that for any sufficiently small $1 < K < 2$, independent of J, if $g \in \{a, x, y\}$ and $\sum_{i=1}^{k} |m_i| \geq J$ and*

$$\sum_{i=1}^{k} |g^{m_i}| \leq K |g^{\sum_{i=1}^{k} m_i}|$$

then for $I = \{i : m_i > 0\}$ and for one of $I^* \in \{I, I^c\}$ we have

$$\left|\sum_{i \in I^*} m_i\right| > \frac{R}{R+1} \sum_{i=1}^{k} |m_i|$$

and

$$\sum_{i \in I^*} |g^{m_i}| < \big(K + (K-1)CR^{(-1/\alpha)}\big) \big|g^{\sum_{i \in I^*} m_i}\big|$$

Proof. Let $J' := 1 + (L+3)/2$ and $J := J'(R+1)$ as in the previous corollary. By Lemma 7.1.1, if $K > 1$ is sufficiently small, then whenever $K|g^{m+n}| \geq |g^m| + |g^n|$ either we have

$$|n| > \frac{R}{R+1}\big(|m| + |n|\big) \text{ or } |m| < J' \text{ or } |m| > \frac{R}{R+1}\big(|m| + |n|\big) \text{ or } |n| < J'.$$

When $|m| + |n| \geq J$, the second condition implies the first condition and the fourth condition implies the third. So, if

$$K|g^{\sum_{i=1}^{k} m_i}| \geq \sum_{i=1}^{k} |g^{m_i}|$$

and $\sum_{i=1}^{k} |m_i| \geq J$ then, since

$$\sum_{i=1}^{k} |g^{m_i}| = \sum_{i \in I} |g^{m_i}| + \sum_{i \notin I} |g^{m_i}| \geq |g^{\sum_{i \in I} m_i}| + |g^{\sum_{i \notin I} m_i}|$$

we can set $n = \sum_{i \in I} m_i$ and $m = \sum_{i \notin I} m_i$ to obtain one of the two following conditions.

$$\left|\sum_{i \in I} m_i\right| > \frac{R}{R+1} \sum_{i=1}^{k} |m_i|$$

$$\left|\sum_{i \notin I} m_i\right| > \frac{R}{R+1} \sum_{i=1}^{k} |m_i|$$

By symmetry, the first condition holds without loss of generality so it remains to prove

$$\big(K + (K-1)CR^{(-1/\alpha)}\big)|g^{\sum_{i \in I} m_i}| > \sum_{i \in I} |g^{m_i}|$$

We have:

$$|g^{\sum_{i \in I} m_i}| \geq |g^{\sum_{i=1}^{k} m_i}| - |g^{\sum_{i \notin I} m_i}|$$

$$\geq \frac{1}{K}\sum_{i\in I}|g^{m_i}| + \frac{1}{K}\sum_{i\notin I}|g^{m_i}| - |g^{\sum_{i\notin I} m_i}|$$
$$\geq \frac{1}{K}\sum_{i\in I}|g^{m_i}| + \frac{1}{K}|g^{\sum_{i\notin I} m_i}| - |g^{\sum_{i\notin I} m_i}|$$
$$= \frac{1}{K}\sum_{i\in I}|g^{m_i}| - \frac{K-1}{K}\cdot|g^{\sum_{i\notin I} m_i}|$$

So:

$$\sum_{i\in I}|g^{m_i}| \leq K|g^{\sum_{i\in I} m_i}| + (K-1)|g^{\sum_{i\notin I} m_i}|$$
$$\leq \left(K + (K-1)\cdot\frac{|g^{\sum_{i\notin I} m_i}|}{|g^{\sum_{i\in I} m_i}|}\right)|g^{\sum_{i\in I} m_i}|$$

Finally, since we know from Theorem 3.2.9 that the distortion of $\langle g\rangle$ obeys a power law, $\left|\sum_{i\notin I} m_i\right| < \left|\sum_{i\in I} m_i\right|/R$ implies $\frac{|g^{\sum_{i\notin I} m_i}|}{|g^{\sum_{i\in I} m_i}|} < CR^{(-1/\alpha)}$. □

Corollary 7.1.7. *For all $R>1$ there exist J, $K>1$ such that if $g\in\{a,x,y\}$ and $\sum_{i=1}^k|m_i|\geq J$ and*

$$\sum_{i=1}^k|g^{m_i}| \leq K|g^{\sum_{i=1}^k m_i}|$$

then $\max_i|m_i| > \frac{R}{R+1}\sum_{i=1}^k|m_i|$.

Proof. We may assume $0 < m_1 = \max_i m_i$ and $0 > m_k = \min_i m_i$. Let $I := \{i \mid m_i > 0\}$. We will let $R' \geq 5$ be large enough that $\left(\frac{R'}{R'+1}\right)^2 > \frac{R}{R+1}$. Let $J_{7.1.6}$, $K_{7.1.6}$, and $J_{7.1.5}$ and $K_{7.1.5}$ be the numbers provided by Corollaries 7.1.6 and 7.1.5 respect to R'. (Actually, $J_{7.1.6} = J_{7.1.5}$.) We claim it suffices to take any $J \geq \frac{R'+1}{R'}J_{7.1.5} > J_{7.1.6}$ and any $1 < K \leq \min\{K_{7.1.6}, \frac{K_{7.1.5}+C(R')^{(-1/\alpha)}}{1+C(R')^{(-1/\alpha)}}\}$.

To see this, we first apply Corollary 7.1.6. Since $K \leq K_{7.1.6}$, K is sufficiently small for Corollary 7.1.6, so, since

$$\sum_{i=1}^k|m_i| \geq J > J_{7.1.6} \quad\text{and}\quad \sum_{i=1}^k|g^{m_i}| \leq K\left|g^{\sum_{i=1}^k m_i}\right|$$

there is an $I^* \in \{I, I^c\}$ such that:

$$\left|\sum_{i\in I^*} m_i\right| > \frac{R'}{R'+1}\sum_{i=1}^k|m_i|$$

and

$$(K + (K-1)C(R')^{(-1/\alpha)})|g^{\sum_{i\in I^*} m_i}| > \sum_{i\in I^*}|g^{m_i}|$$

Now, $K \leq \frac{K_{7.1.5}+C(R')^{(-1/\alpha)}}{1+C(R')^{(-1/\alpha)}}$ if and only if $(K+(K-1)C(R')^{(-1/\alpha)}) \leq K_{7.1.5}$, so $K_{7.1.5}\left|g^{\sum_{i\in I^*} m_i}\right| \geq \sum_{i\in I^*}|g^{m_i}|$. Furthermore:

$$\sum_{i\in I^*}|m_i| = \left|\sum_{i\in I^*} m_i\right| > \frac{R'}{R'+1}\sum_{i=1}^{k}|m_i| \geq \frac{R'}{R'+1}J \geq J_{7.1.5}$$

Thus, the hypotheses of Corollary 7.1.5 for I^* with respect to R' are satisfied, and we get:

$$\max_i |m_i| \geq \max_{i\in I^*}|m_i| > \frac{R'}{R'+1}\left|\sum_{i\in I^*} m_i\right| > \left(\frac{R'}{R'+1}\right)^2\sum_{i=1}^{k}|m_i| > \frac{R}{R+1}\sum_{i=1}^{k}|m_i| \qquad \square$$

In the previous results we picked out a 'dominant' escape in terms of exponents. In the next result we show it is still dominant in terms of length.

Corollary 7.1.8. *For all $R>1$ there exist $J, K>1$ such that if $g\in\{a,x,y\}$ and $\gamma=\gamma_1\gamma_2\cdots\gamma_k$ is a concatenation of paths such that*

(1) *for all i, the endpoints of γ_i differ by g^{m_i},*
(2) $J \leq |\gamma| \leq K|g^{\sum_{i=1}^k m_i}|$

then $\max_i|\gamma_i| > \frac{R}{R+1}\cdot|\gamma|$.

Proof. Let $R_0>1$ and let $J_0, K_0>1$ be such that the conclusion of Corollary 7.1.7 holds for $(R,J,K)=(R_0,J_0,K_0)$. Suppose $\gamma=\gamma_1\gamma_2\cdots\gamma_k$ satisfies conditions (1) and (2) for some $K\in(1,K_0)$, some $J>J_0^{1/\alpha}KC$ and some $g\in\{a,x,y\}$. Then we have

$$K|g^{\sum_{i=1}^k m_i}| \geq |\gamma| = \sum_{i=1}^{k}|\gamma_i| \geq \sum_{i=1}^{k}|g^{m_i}|$$

and

$$J_0^{1/\alpha} < \frac{J}{KC} \leq \frac{|\gamma|}{KC} \leq \frac{|g^{\sum_{i=1}^k m_i}|}{C} \leq \left|\sum_{i=1}^{k} m_i\right|^{1/\alpha} \leq \left(\sum_{i=1}^{k}|m_i|\right)^{1/\alpha}$$

so, by Corollary 7.1.7, we have $\max_i|m_i| > \frac{R_0}{R_0+1}\sum_{i=1}^k|m_i|$. If $i=\iota$ maximizes $|m_i|$ then this inequality is equivalent to $\sum_{i\neq\iota}|m_i| < \frac{1}{R_0}\cdot|m_\iota|$ and we have

$$\begin{aligned}
\frac{1}{C}\cdot|g^{\sum_{i\neq\iota} m_i}| &\leq \left|\sum_{i\neq\iota} m_i\right|^{\frac{1}{\alpha}}\\
&\leq \left(\sum_{i\neq\iota}|m_i|\right)^{\frac{1}{\alpha}}\\
&< \frac{1}{R_0^{1/\alpha}}\cdot|m_\iota|^{\frac{1}{\alpha}}\\
&\leq \frac{1}{R_0^{1/\alpha}}\cdot|g^{m_\iota}|\\
&\leq \frac{1}{R_0^{1/\alpha}}\cdot\left(|g^{\sum_{i\neq\iota} m_i}| + |g^{\sum_{i=1}^k m_i}|\right)
\end{aligned}$$

from which we can obtain

$$|g^{\sum_{i\neq\iota} m_i}| < \frac{C}{R_0^{1/\alpha} - C} \cdot |g^{\sum_{i=1}^k m_i}|$$

as long as $R_0 > C^\alpha$. Thus

$$|g^{\sum_{i=1}^k m_i}| \leq |g^{m_1}| + |g^{\sum_{i\neq\iota} m_i}| < |\gamma_\iota| + \frac{C}{R_0^{1/\alpha} - C} \cdot |g^{\sum_{i=1}^k m_i}|$$

and so

$$\max_i |\gamma_i| \geq |\gamma_\iota| > \frac{R_0^{1/\alpha} - 2C}{R_0^{1/\alpha} - C} \cdot |g^{\sum_{i=1}^k m_i}| \geq \frac{R_0^{1/\alpha} - 2C}{K(R_0^{1/\alpha} - C)} \cdot |\gamma|$$

and the factor $\frac{R_0^{1/\alpha}-2C}{K(R_0^{1/\alpha}-C)}$ tends to 1 as K tends to 1 and R_0 tends to infinity.

To complete the proof of the corollary, we need to explain how we obtain the $J, K > 1$ of the corollary statement. To obtain $J, K > 1$ we pick $R_0 > C^\alpha$ large enough that $\frac{R_0^{1/\alpha}-2C}{(R_0^{1/\alpha}-C)} > \frac{R}{R+1}$. Next, we obtain $K_0, J_0 > 1$ such that the conclusion of Corollary 7.1.7 holds for $(R, J, K) = (R_0, J_0, K_0)$. Finally, we choose $K \in (1, K_0)$ so that $\frac{R_0^{1/\alpha}-2C}{K(R_0^{1/\alpha}-C)} > \frac{R}{R+1}$ and then choose $J > J_0^{1/\alpha} KC$. □

We will now start allowing escapes of different flavors. The first result says if there is exactly one escape of each flavor and the a–escape is not tiny then it dominates.

Lemma 7.1.9. *For all $R > 1$ there exist $J, K > 1$ such that if $|\ell| + |m| + |n| \geq J$ and*

$$|a^\ell| + |x^m| + |y^n| \leq K|a^\ell x^m y^n|$$

and

$$|\ell| > \frac{|\ell| + |m| + |n|}{R}$$

then $|m|, |n| \leq \frac{|\ell|+|m|+|n|}{R}$.

Proof. The result for large R yields J and K for which the same result is true for all smaller R, so we may assume in the proof that $R > 2$. We can multiply all three exponents by -1 without changing the hypothesized inequalities, so we may assume $\ell > 0$. Further, by the x–y symmetry we may assume $|n| \leq |m|$.

There exist integers $p > 0$ and q with $|q| \leq L/2$ such that $\ell = pL+q$ and $|a^\ell| = |q|+|a^{pL}|$, by (3) of Lemma 3.3.1. The strategy for the proof is to compare the approximation of $|a^\ell x^m y^n|$ by $|a^\ell|+|x^m|+|y^n|$ (illustrated by the solid line in Figure 6), to the approximation given by $|a^q| + |x^{m+p}| + |y^{n+p}|$ (illustrated by the dotted line in Figure 6).

Notice that if $\ell \geq L + 1$ then we can verify the following bounds:

$$\frac{2}{L+2} \cdot \frac{1}{L} \leq \frac{p}{\ell} \leq \frac{L+2}{2} \cdot \frac{1}{L} \tag{7.1.10}$$

Let $J' = (L + 5)/2$ as in Lemma 7.1.1. Let $J := R(1 + LJ')$. Let $R' := (1/2)L(L + 2)(R - 1)$, and let K' be as in Lemma 7.1.1 with respect to R'. We will choose $K > 1$ to be sufficiently small that the below inequalities labelled (♣) and (♢) are contradicted, and the below inequality labelled (♡) is satisfied.

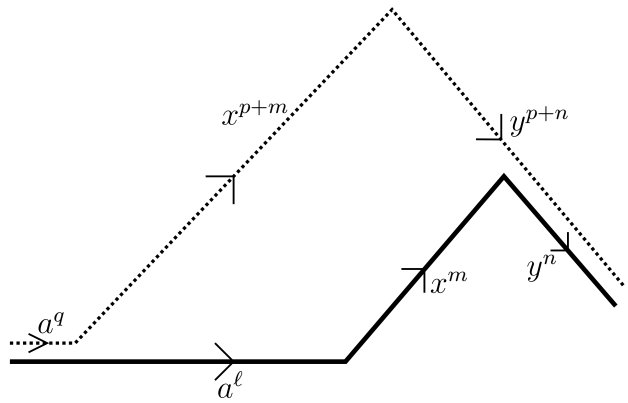

FIGURE 6. Illustration of the two decompositions of $a^\ell x^m y^n$.

Suppose that $|m| > \frac{\ell+|m|+|n|}{R}$. We will derive a contradiction. First observe that we have the bounds

$$1/(R-1) < \ell/|m| < R-1. \tag{7.1.11}$$

Thus, by combining equations (7.1.10) and (7.1.11) we deduce that

$$\frac{1}{R'} < \frac{p}{|m|} < \frac{(L+2)(R-1)}{2L} < \frac{L(L+2)(R-1)}{2} = R' \tag{7.1.12}$$

As both $|m|$ and p are larger than J', we can combine Lemma 7.1.1 with Equation (7.1.12) to see that

$$|x^m| + |x^p| > K'|x^{m+p}|. \tag{7.1.13}$$

We now deduce that

$$\begin{aligned}
|q| + |x^p| + |x^m| + |y^p| + |y^n| &\leq |a^l| + |x^m| + |y^n| && \text{By 3 of Lemma 3.3.1.}\\
&\leq K|a^\ell x^m y^n| && \text{By assumption.}\\
&= K(|a^q x^{m+p} y^{n+p}|)\\
&\leq K|q| + K(|x^{p+m}| + |y^{p+n}|). && \text{Triangle inequality.}
\end{aligned}$$

Combining this with (7.1.13) yields

$$(1-\frac{K}{K'})(|x^p| + |x^m|) + |y^p| + |y^n| - K|y^{p+n}| < (K-1)L/2 \tag{7.1.14}$$

First, suppose that either $|n| < J'$ or $|n| < p/R'$. Both of these conditions imply $|n| < p$, so by Theorem 3.2.9 we have $|y^n| < C|n|^{1/\alpha} < Cp^{1/\alpha} < C|y^p|$. Continuing from (7.1.14), we have:

$$\begin{aligned}
(K-1)L/2 &> (1-\frac{K}{K'})(|x^p| + |x^m|) + |y^p| + |y^n| - K|y^{p+n}|\\
&\geq (1-\frac{K}{K'})(|x^p| + |x^m|) - (K-1)(|y^p| + |y^n|)\\
&\geq (1-\frac{K}{K'})(|x^p| + |x^m|) - (K-1)|y^p|(1+C)
\end{aligned}$$

$$= (1 - \frac{K}{K'} - (K-1)(1+C))|x^p| + (1 - \frac{K}{K'})|x^m|$$

To ensure that the coefficients in this final expression are non-negative we will have assumed that K is chosen to satisfy the inequalities:

$$(\heartsuit) \qquad 1 < K < \min\{K',\, 1 + \frac{K'-1}{(C+1)K'+1}\}$$

By Theorem 3.2.9, the lower bounds on p and $|m|$ imply $|x^p|, |x^m| > (J')^{1/\alpha}$, so:

$$(K-1)L/2 > \left(1 - \frac{K}{K'} - (K-1)(1+C) + 1 - \frac{K}{K'}\right)(J')^{1/\alpha}$$

Solving for K gives us:

$$(\clubsuit) \qquad K > \frac{LK' + 2(J')^{1/\alpha}\cdot(K'(1+C)+2K')}{LK' + 2(J')^{1/\alpha}\cdot(K'(1+C)+2)} > 1$$

Having assumed that $K > 1$ is chosen to be small enough that ($\clubsuit$) does not hold, we must in fact have $|n| \ge J'$ and $|n| \ge p/R'$. Then Lemma 7.1.1 implies $|y^p| + |y^n| > K'|y^{p+n}|$. In this case, continuing from (7.1.14) we have:

$$\begin{aligned}(K-1)L/2 &> (1 - \frac{K}{K'})\,(|x^p| + |x^m| + |y^p| + |y^n|)\\ &> (1 - \frac{K}{K'})(4(J')^{1/\alpha})\end{aligned}$$

Solving for K gives

$$(\diamondsuit) \qquad K > \frac{8K'(J')^{1/\alpha} + LK'}{8(J')^{1/\alpha} + LK'} > 1.$$

By having assumed that $K > 1$ is chosen small enough that ($\diamondsuit$) does not hold, this cannot happen. Thus, for $J := R(1 + LJ')$ and K as specified, the hypotheses imply $|n| \le |m| \le \frac{|\ell|+|m|+|n|}{R}$. □

The next result, Lemma 7.1.15 is a stepping stone. It says that if we have a mixture of different flavors of escapes, then whenever one flavor makes up a nontrivial amount of the total, then there is an escape of that flavor that is dominant *among the other escapes of that flavor*. Moreover, if the a–escapes make up a nontrivial amount of the total then the x–escapes and y–escapes are negligible.

Lemma 7.1.15. *For all $R > 1$ there exist $J, K > 1$ such that if $T = \sum_i |\ell_i| + \sum_j |m_j| + \sum_k |n_k| \ge J$ and*

$$(7.1.16) \qquad \sum_i |a^{\ell_i}| + \sum_j |x^{m_j}| + \sum_k |y^{n_k}| \le K|a^{\sum_i \ell_i} x^{\sum_j m_j} y^{\sum_k n_k}|$$

then the following implications hold.

$$\sum_i |\ell_i| > \frac{1}{R}\cdot T \implies \max_i |\ell_i| > \frac{R-1}{R}\sum_i |\ell_i|$$

$$\sum_j |m_j| > \frac{1}{R} \cdot T \implies \max_j |m_j| > \frac{R-1}{R} \sum_j |m_j|$$

$$\sum_k |n_k| > \frac{1}{R} \cdot T \implies \max_k |n_k| > \frac{R-1}{R} \sum_k |n_k|$$

Moreover, if $\sum_i |\ell_i| > \frac{1}{R} \cdot T$ *then* $\sum_j |m_j| \leq \frac{1}{R} \cdot T$ *and* $\sum_k |n_k| \leq \frac{1}{R} \cdot T$.

Proof. We will prove the first implication. The remaining implications are proved similarly. Assume that (7.1.16) and the left-hand side of the first implication holds with:

$$1 < K < 1 + \left(\frac{1}{2}\right)^{1+\frac{\alpha-1}{\alpha}} \cdot \frac{1}{CR^{1/\alpha}} \tag{7.1.17}$$

Claim 7.1.18. $|x^{\sum_j m_j} y^{\sum_k n_k}| < 2^{1-1/\alpha} C \left(\sum_j |m_j| + \sum_k |n_k|\right)^{1/\alpha}$

Proof of claim.

$$\begin{aligned}
\left(\sum_j |m_j| + \sum_k |n_k|\right)^{1/\alpha} &\geq \left(\left|\sum_j m_j\right| + \left|\sum_k n_k\right|\right)^{1/\alpha} \\
&\geq \left(\frac{1}{2}\right)^{\frac{\alpha-1}{\alpha}} \left(\left|\sum_j m_j\right|^{1/\alpha} + \left|\sum_k n_k\right|^{1/\alpha}\right) && \text{Fact 1.0.1} \\
&> \frac{1}{C}\left(\frac{1}{2}\right)^{\frac{\alpha-1}{\alpha}} \left(|x^{\sum_j m_j}| + |y^{\sum_k n_k}|\right) && \text{Theorem 3.2.9} \\
&\geq \frac{1}{C}\left(\frac{1}{2}\right)^{\frac{\alpha-1}{\alpha}} |x^{\sum_j m_j} y^{\sum_k n_k}| && \diamondsuit
\end{aligned}$$

Claim 7.1.19. $|\sum_i \ell_i| > \frac{1}{(4C)^\alpha R} \cdot T$

Proof of claim. For the sake of finding a contradiction, assume $|\sum_i \ell_i| \leq \frac{1}{(4C)^\alpha R} \cdot T$. Then, since $T < R \sum_i |\ell_i|$, we have $|\sum_i \ell_i| < \frac{1}{(4C)^\alpha} \sum_i |\ell_i|$. Then we have

$$\begin{aligned}
|a^{\sum_i \ell_i}| &< C \Big|\sum_i \ell_i\Big|^{1/\alpha} && \text{by Theorem 3.2.9} \\
&< C\Big(\frac{1}{(4C)^\alpha} \sum_i |\ell_i|\Big)^{1/\alpha} && \text{by the above} \\
&\leq \frac{1}{4} \sum_i |\ell_i|^{1/\alpha} && \text{by Fact 1.0.1} \\
&< \frac{1}{4} \sum_i |a^{\ell_i}| && \text{by Theorem 3.2.9}
\end{aligned}$$

thus $\sum_i |a^{\ell_i}| + |x^{\sum_j m_j} y^{\sum_k n_k}| \leq \sum_i |a^{\ell_i}| + \sum_j |x^{m_j}| + \sum_k |y^{n_k}| \leq K|a^{\sum_i \ell_i} x^{\sum_j m_j} y^{\sum_k n_k}| \leq K|a^{\sum_i \ell_i}| + K|x^{\sum_j m_j} y^{\sum_k n_k}| < \frac{K}{4} \sum_i |a^{\ell_i}| + K|x^{\sum_j m_j} y^{\sum_k n_k}|$ which implies

$$\frac{1}{2} \sum_i |a^{\ell_i}| < (K-1)|x^{\sum_j m_j} y^{\sum_k n_k}|$$

since (7.1.17) implies $K < 2$.

On the other hand, by Theorem 3.2.9, Claim 7.1.18 and Fact 1.0.1, we have

$$\begin{aligned}
\sum_i |a^{\ell_i}| &> \sum_i |\ell_i|^{1/\alpha} && \text{by Theorem 3.2.9} \\
&\geq \big(\sum_i |\ell_i|\big)^{1/\alpha} && \text{by Fact 1.0.1} \\
&> \frac{1}{R^{1/\alpha}} \cdot T^{1/\alpha} && \text{by assumption} \\
&\geq \frac{1}{R^{1/\alpha}} \big(\sum_j |m_j| + \sum_k |n_k|\big)^{1/\alpha} \\
&\geq \frac{1}{CR^{1/\alpha}} \big(\frac{1}{2}\big)^{\frac{\alpha-1}{\alpha}} |x^{\sum_j m_j} y^{\sum_k n_k}| && \text{by Claim 7.1.18}
\end{aligned}$$

thus

$$\frac{1}{2} \sum_i |a^{\ell_i}| < (K-1)|x^{\sum_j m_j} y^{\sum_k n_k}| < 2^{1-1/\alpha} CR^{1/\alpha}(K-1) \sum_i |a^{\ell_i}| < \frac{1}{2} \sum_i |a^{\ell_i}|$$

where the last inequality follows from (7.1.17). This is a contradiction. $\diamondsuit$

Then we have:

$$\begin{aligned}
|a^{\sum_i \ell_i}| &> |\sum_i \ell_i|^{1/\alpha} && \text{by Theorem 3.2.9} \\
&> \frac{1}{4CR^{1/\alpha}} \cdot T^{1/\alpha} && \text{Claim 7.1.19} \\
&\geq \frac{1}{4CR^{1/\alpha}} \cdot \big(\sum_j |m_j| + \sum_k |n_k|\big)^{1/\alpha} && \text{by assumption} \\
&\geq \frac{1}{4C^2 R^{1/\alpha}} \cdot \big(\frac{1}{2}\big)^{\frac{\alpha-1}{\alpha}} \cdot |x^{\sum_j m_j} y^{\sum_k n_k}| && \text{by Claim 7.1.18}
\end{aligned}$$

This gives us:

$$|x^{\sum_j m_j} y^{\sum_k n_k}| < 2^{3-1/\alpha} C^2 R^{1/\alpha} |a^{\sum_i \ell_i}|.$$

On the other hand:

$$\begin{aligned}
\sum_i |a^{\ell_i}| + |x^{\sum_j m_j} y^{\sum_k n_k}| &\leq \sum_i |a^{\ell_i}| + \sum_j |x^{m_j}| + \sum_k |y^{n_k}| \\
&\leq K|a^{\sum_i \ell_j} x^{\sum_j m_j} y^{\sum_k n_k}| \\
&\leq K|a^{\sum_i \ell_j}| + K|x^{\sum_j m_j} y^{\sum_k n_k}|
\end{aligned}$$

So:

$$
\begin{aligned}
\sum_i |a^{\ell_i}| &\leq K|a^{\sum_i \ell_j}| + (K-1)|x^{\sum_j m_j} y^{\sum_k n_k}| \\
&< K|a^{\sum_i \ell_j}| + 2^{3-1/\alpha} C^2 R^{1/\alpha}(K-1)|a^{\sum_i \ell_i}| \\
&= \big(K + 2^{3-1/\alpha} C^2 R^{1/\alpha}(K-1)\big)|a^{\sum_i \ell_j}| \qquad (\dagger) \\
&\xrightarrow{K\to 1} |a^{\sum_i \ell_j}|.
\end{aligned}
$$

Noting that if $T \geq J$ then $\sum_i |\ell_i| > \frac{1}{R} \cdot T \geq \frac{J}{R}$. Thus, by Corollary 7.1.7, if J is large enough and $K > 1$ is small enough that ($\dagger$) satisfies the requisite assumption — all depending only on R and L — then $\max_i |\ell_i| > \frac{R-1}{R} \sum_i |\ell_i|$.

We now assume $\sum_i |\ell_i| > \frac{1}{R} \cdot T$ to prove the "moreover part." We will show that $\sum_j |m_j| \leq \frac{1}{R} \cdot T$. A similar argument can be used to show that $\sum_k |n_k| \leq \frac{1}{R} \cdot T$. For the sake of finding a contradiction, assume that $\sum_j |m_j| > \frac{1}{R} \cdot T$. Without loss of generality, we have $\max_i |\ell_i| = |\ell_1|$ and $\max_j |m_j| = |m_1|$. Then

$$
|\ell_1| > \frac{R-1}{R} \sum_i |\ell_i| > \frac{R-1}{R^2} \cdot T \quad \text{and} \quad |m_1| > \frac{R-1}{R} \sum_j |m_j| > \frac{R-1}{R^2} \cdot T. \tag{7.1.20}
$$

Then, by Fact 1.0.1 and Theorem 3.2.9, we have

$$
\begin{aligned}
&|a^{\ell_1}| \\
&> |\ell_1|^{1/\alpha} && \text{Theorem 3.2.9} \\
&> \Big(\frac{R-1}{R^2}\Big)^{1/\alpha} \cdot T^{1/\alpha} && \text{Equation (7.1.20)} \\
&\geq \Big(\frac{R-1}{R^2}\Big)^{1/\alpha} \cdot \Big(\Big|\sum_{i\geq 2} \ell_i\Big| + \Big|\sum_{j\geq 2} m_j\Big| + \Big|\sum_k n_k\Big|\Big)^{1/\alpha} && \text{assumption} \\
&\geq \Big(\frac{R-1}{R^2}\Big)^{1/\alpha} \cdot \Big(\frac{1}{3}\Big)^{\frac{\alpha-1}{\alpha}} \cdot \Big(\Big|\sum_{i\geq 2} \ell_i\Big|^{1/\alpha} + \Big|\sum_{j\geq 2} m_j\Big|^{1/\alpha} + \Big|\sum_k n_k\Big|^{1/\alpha}\Big) && \text{Fact 1.0.1} \\
&> \Big(\frac{R-1}{R^2}\Big)^{1/\alpha} \cdot \Big(\frac{1}{3}\Big)^{\frac{\alpha-1}{\alpha}} \cdot \frac{1}{C} \cdot \big(|a^{\sum_{i\geq 2} \ell_i}| + |x^{\sum_{j\geq 2} m_j}| + |y^{\sum_k n_k}|\big) && \text{Theorem 3.2.9} \\
&\geq \Big(\frac{R-1}{R^2}\Big)^{1/\alpha} \cdot \Big(\frac{1}{3}\Big)^{\frac{\alpha-1}{\alpha}} \cdot \frac{1}{C} \cdot |a^{\sum_{i\geq 2} \ell_i} x^{\sum_{j\geq 2} m_j} y^{\sum_k n_k}|
\end{aligned}
$$

and, similarly, we have $|x^{m_1}| > \big(\frac{R-1}{R^2}\big)^{1/\alpha} \cdot \big(\frac{1}{3}\big)^{\frac{\alpha-1}{\alpha}} \cdot \frac{1}{C} \cdot |a^{\sum_{i\geq 2} \ell_i} x^{\sum_{j\geq 2} m_j} y^{\sum_k n_k}|$.

By Lemma 3.3.1(4), for sufficiently small $K' > 1$ we have:

(7.1.21)

$$
|a^{\ell_1} x^{m_1}| > \frac{1}{K'}(|a^{\ell_1}| + |x^{m_1}|) = \big(\frac{R-1}{R^2}\big)^{1/\alpha} \cdot \big(\frac{1}{3}\big)^{\frac{\alpha-1}{\alpha}} \cdot \frac{2}{CK'} \cdot |a^{\sum_{i\geq 2} \ell_i} x^{\sum_{j\geq 2} m_j} y^{\sum_k n_k}|
$$

But:

$$
\begin{aligned}
|a^{\ell_1}| + |x^{m_1}| + |a^{\sum_{i\geq 2} \ell_i} x^{\sum_{j\geq 2} m_j} y^{\sum_k n_k}| &\leq \sum_i |a^{\ell_i}| + \sum_j |x^{m_j}| + \sum_k |y^{n_k}| \\
&\leq K|a^{\sum_i \ell_i} x^{\sum_j m_j} y^{\sum_k n_k}|
\end{aligned}
$$

$$\leq K|a^{\ell_1}x^{m_1}| + K|a^{\sum_{i\geq 2}\ell_i}x^{\sum_{j\geq 2}m_j}y^{\sum_k n_k}|$$

so that

$$\begin{aligned}
|a^{\ell_1}| + |x^{m_1}| &\leq K|a^{\ell_1}x^{m_1}| + (K-1)|a^{\sum_{i\geq 2}\ell_i}x^{\sum_{j\geq 2}m_j}y^{\sum_k n_k}| \\
&< K|a^{\ell_1}x^{m_1}| + 3^{\frac{\alpha-1}{\alpha}}\left(\frac{R^2}{R-1}\right)^{1/\alpha}\cdot\frac{CK'}{2}(K-1)|a^{\ell_1}x^{m_1}| \quad \text{Equation (7.1.21)} \\
&= \left(K + 3^{\frac{\alpha-1}{\alpha}}\left(\frac{R^2}{R-1}\right)^{1/\alpha}\cdot\frac{CK'}{2}(K-1)\right)|a^{\ell_1}x^{m_1}| \\
&\xrightarrow{K\to 1} |a^{\ell_1}x^{m_1}|
\end{aligned}$$

Also, if $T \geq J$ then $|\ell_1| + |m_1| > \frac{2(R-1)}{R^2}\cdot T \geq \frac{2(R-1)}{R^2}\cdot TJ$. Thus, by Lemma 7.1.9, if J is large enough and $K > 1$ is small enough—depending only on R, K', C and L—then $|m_1| < \frac{1}{R}|\ell_1| < \frac{1}{R}\cdot T$, which is a contradiction. Since K' and C depend only on L, we are done. ☐

Lemma 7.1.22. *If $R \geq 2$ and $|n_1| > \frac{R-1}{R}\sum_{i=1}^{j}|n_i|$ then:*

$$\left|\frac{\sum_{i=1}^{j} n_i}{n_1} - 1\right| < \frac{1}{R-1}$$

and

$$\frac{R-2}{R} < \frac{|\sum_{i=1}^{j} n_i|}{\sum_{i=1}^{j}|n_i|} \leq 1$$

Proof. The first and last inequalities are easy. For the remaining inequality, we have $|n_1| > (R-1)\sum_{i=2}^{j}|n_i|$, so:

$$\frac{|\sum_{i=1}^{j} n_i|}{\sum_{i=1}^{j}|n_i|} \geq \frac{|n_1| - \sum_{i=2}^{j}|n_i|}{|n_1| + \sum_{i=2}^{j}|n_i|} > \frac{|n_1| - \frac{1}{R-1}|n_1|}{|n_1| + \frac{1}{R-1}|n_1|} = \frac{R-2}{R}$$ ☐

Now we put it all together. Proposition 7.1.23 and Theorem 7.1.24 say basically the same thing: either there is a single dominant escape or there are two and they are an x–escape and a y–escape. The difference in the two results is that in Proposition 7.1.23 'dominance' is in terms of magnitude of exponent and in Theorem 7.1.24 it is in terms of length.

Proposition 7.1.23. *Suppose $R \geq 3L + 4$ and J and K are as in Lemma 7.1.15 and:*

$$\sum_i |a^{\ell_i}| + \sum_j |x^{m_j}| + \sum_k |y^{n_k}| \leq K|a^{\sum_i \ell_i}x^{\sum_j m_j}y^{\sum_k n_k}|$$

Suppose $T := \sum_i |\ell_i| + \sum_j |m_j| + \sum_k |n_k| \geq J$.

1. *If $\sum_i |\ell_i| > T/R$ or exactly one of $\sum_j |m_j|$ and $\sum_k |n_k|$ is strictly greater than T/R then there is one maximal term whose absolute value is strictly greater than $\frac{(R-1)(R-2)}{R^2}T$.*
2. *If $\sum_j |m_j| > T/R$ and $\sum_k |n_k| > T/R$ then $\max_j |m_j| + \max_k |n_k| > \left(\frac{R-1}{R}\right)^2 T$.*
3. *If $x^z = a^{\sum_i \ell_i}x^{\sum_j m_j}y^{\sum_k n_k}$, then $\sum_j |m_j| > T/R$ and $\sum_i |\ell_i|$, $\sum_k |n_k| \leq T/R$.*

(4) *If* $a^z = a^{\sum_i \ell_i} x^{\sum_j m_j} y^{\sum_k n_k}$, *then either:*
- $\sum_i |\ell_i| > T/R$ *and* $\sum_j |m_j|$, $\sum_k |n_k| \leq T/R$, *or*
-
  - $\sum_j |m_j|$, $\sum_k |n_k| > T/R$,
  - $\sum_i |\ell_i| \leq T/R$,
  - $\max_j |m_j|$, $\max_k |n_k| > \frac{1}{2} \cdot \frac{(R-1)^2(R-2)}{R^3} \cdot T$, *and*
  - $\left(\frac{R-2}{R+2}\right)^2 < \frac{\max_j |m_j|}{\max_k |n_k|} < \left(\frac{R+2}{R-2}\right)^2$.

Proof. The first case follows from Lemma 7.1.15, since if two of the sums are bounded above by T/R then the third is bounded below by $\frac{R-2}{R}T$.

The second case also follows immediately from Lemma 7.1.15, since:

$$\max_j |m_j| + \max_k |n_k| > \frac{R-1}{R}\left(\sum_j |m_j| + \sum_k |n_k|\right) \geq \frac{R-1}{R}\left(T - \sum_i |\ell_i|\right) \geq \frac{R-1}{R}\left(1 - \frac{1}{R}\right)T$$

In Case (3), we have $\sum_i \ell_i = pL$ and $z = p + \sum_j m_j$ and $0 = p + \sum_k n_k$. Suppose that $\sum_i |\ell_i| > T/R$. By Lemma 7.1.15,

$$\max_i |\ell_i| > \frac{R-1}{R} \sum_k |\ell_k| \quad \text{and} \quad \sum_j |m_j|, \sum_k |n_k| \leq T/R,$$

the latter implying $\sum_i |\ell_i| \geq \frac{R-2}{R}T$. Applying Lemma 7.1.22:

$$\frac{T}{R} \geq \sum_k |n_k| \geq \left|\sum_k n_k\right| = |p| = \frac{|\sum_i \ell_i|}{|L|} > \frac{1}{L} \cdot \frac{R-2}{R} \cdot \sum_i |\ell_i| \geq \frac{1}{L} \cdot \left(\frac{R-2}{R}\right)^2 T$$

This gives a contradiction if $R \geq 3L + 4$.

Suppose that $\sum_k |n_k| > T/R$. By Lemma 7.1.15, $\sum_i |\ell_i| \leq T/R$ and $\max_k |n_k| > \frac{R-1}{R} \sum_k |n_k|$ so, applying Lemma 7.1.22:

$$\frac{T}{R} \geq \sum_i |\ell_i| \geq \left|\sum_i \ell_i\right| = L|p| = L\left|\sum_k n_k\right| > L \cdot \frac{R-2}{R} \cdot \sum_k |n_k| > L \cdot \frac{R-2}{R} \cdot \frac{T}{R}$$

This implies $R < \frac{2L}{L-1} \leq 12/5$, which is a contradiction.

Since $R > 3$, we are left with the possibility that only $\sum_j |m_j|$ is strictly greater than T/R.

In Case (4), if $\sum_i |\ell_i| > T/R$ then Lemma 7.1.15 lets us revert to Case (1), so assume $\sum_i |\ell_i| \leq T/R$. Without loss of generality, assume $\sum_j |m_j| \geq \sum_k |n_k|$, so that $\sum_j |m_j| \geq \frac{R-1}{2R} \cdot T > \frac{T}{R}$. By Lemma 7.1.15 $\max_j |m_j| > \frac{R-1}{R} \sum_j |m_j| \geq \frac{1}{2} \cdot \left(\frac{R-1}{R}\right)^2 \cdot T$.

The constraint $a^z = a^{\sum_i \ell_i} x^{\sum_j m_j} y^{\sum_k n_k}$ implies $\sum_j m_j = \sum_k n_k = (z - \sum_i \ell_i)/L$, so, applying Lemma 7.1.22:

$$\sum_k |n_k| \geq \left|\sum_k n_k\right| = \left|\sum_j m_j\right| \geq \frac{R-2}{R} \sum_j |m_j| \geq \frac{(R-1)(R-2)}{2R^2} \cdot T$$

The given lower bound on R is enough to imply that this quantity is greater than T/R, so Lemma 7.1.15 applies to give:

$$\max_k |n_k| > \frac{R-1}{R} \sum_k |n_k| \geq \frac{(R-1)^2(R-2)}{2R^3} \cdot T$$

It remains to estimate $\max_j |m_j| / \max_k |n_k|$:

$$\begin{aligned}\frac{\max_j |m_j|}{\max_k |n_k|} &\leq \frac{\sum_j |m_j|}{\frac{R-1}{R}\sum_k |n_k|} \\ &\leq \frac{T - \sum_k |n_k|}{\frac{R-1}{R}\sum_k |n_k|} \\ &\leq \frac{R}{R-1}\left(\frac{2R^2}{(R-1)(R-2)} - 1\right) \\ &< \left(\frac{R+2}{R-2}\right)^2\end{aligned}$$

The last inequality is true, in particular, when $R > 2$. A similar computation gives the lower bound. □

Theorem 7.1.24. *For any $R' > 1$ there exist $J' > 1$ and $2 > K > 1$ such that if γ is a K–biLipschitz path with endpoints in $\langle a, x, y\rangle$ then either $|\gamma| \leq J'$ or γ has either one or two long escapes that collectively account for at least $\frac{R'-1}{R'}$ fraction of its length. Furthermore, in the case of two long escapes ϵ_0 and ϵ_1 they are one x–escape and one y–escape.*

If the endpoints of γ differ by a power of x or y, then there is only one long escape, and it is of the corresponding flavor, and if the endpoints of γ differ by a power of a then either there is one long a–escape or there is one long x–escape and one long y–escape.

Proof. Since γ is K–biLipschitz for $K < 2$, γ does not use any x or y edges, so toral subpaths are just powers of a. Thus, the a–escapes and/or maximal toral subpaths have endpoints that differ by $a^{\ell_1}, a^{\ell_2}, \dots$ and the x–escapes and y–escapes have endpoints that differ by $x^{m_1}, x^{m_2}, \dots$ and $y^{n_1}, y^{n_2}, \dots$, respectively.

Given R' we will determine in the course of the proof a bound such that the rest of the argument works provided R is larger than that bound and K and J are chosen as in Lemma 7.1.15 with respect to R. Since we are allowed to enlarge R we may assume $R \geq 3L + 4$ so that Proposition 7.1.23 applies. Let T be the usual sum of absolute values. Let $J' := JK$. If $T < J$ then $|\gamma| \leq KT < KJ$, so it suffices to take $|\gamma| \geq J'$ to guarantee $T \geq J$ so that we may apply Lemma 7.1.15.

By Lemma 7.1.15 there are either one or two long escapes. Proposition 7.1.23 bounds these in terms of the exponent of the difference between their endpoints. It remains only to recast these bounds in terms of path length.

Suppose there are two long escapes ϵ_1 and ϵ_2, the strategy in the other cases being similar. By Proposition 7.1.23, $\max_j |m_j| + \max_k |n_k| > \left(\frac{R-1}{R}\right)^2 T$. The complement of these two escapes in γ consists of at most three subpaths, δ_1, δ_2, and δ_3. Let $I_{a,1}$ be the set of indices i such that the escape of γ corresponding to the term a^{ℓ_i} belongs to δ_1. Similarly, define $I_{a,2}$, $I_{a,3}$, $I_{x,1}$, etc.

$$\frac{|\delta_1| + |\delta_2| + |\delta_3|}{|\gamma|} \leq \frac{K\sum_{h=1}^{3} |a^{\sum_{i\in I_{a,h}} \ell_i} x^{\sum_{j\in I_{x,h}} m_j} y^{\sum_{k\in I_{y,h}} n_k}|}{|\delta_1| + |\epsilon_1| + |\delta_2| + |\epsilon_2| + |\delta_3|}$$

$$
\begin{aligned}
&\leq \frac{K\sum_{h=1}^{3}|a^{\sum_{i\in I_{a,h}}\ell_i}|+|x^{\sum_{j\in I_{x,h}}m_j}|+|y^{\sum_{k\in I_{y,h}}n_k}|}{|\epsilon_1|+|\epsilon_2|}\\
&\leq \frac{KC\sum_{h=1}^{3}|\sum_{i\in I_{a,h}}\ell_i|^{1/\alpha}+|\sum_{j\in I_{x,h}}m_j|^{1/\alpha}+|\sum_{k\in I_{y,h}}n_k|^{1/\alpha}}{(\max_j|m_j|)^{1/\alpha}+(\max_k|n_k|)^{1/\alpha}}\\
&\leq \frac{KC\cdot 9^{1-1/\alpha}(\sum_{h=1}^{3}|\sum_{i\in I_{a,h}}\ell_i|+|\sum_{j\in I_{x,h}}m_j|+|\sum_{k\in I_{y,h}}n_k|)^{1/\alpha}}{(\max_j|m_j|+\max_k|n_k|)^{1/\alpha}}\\
&\leq \frac{KC\cdot 9^{1-1/\alpha}(\sum_{h=1}^{3}\sum_{i\in I_{a,h}}|\ell_i|+\sum_{j\in I_{x,h}}|m_j|+\sum_{k\in I_{y,h}}|n_k|)^{1/\alpha}}{(\max_j|m_j|+\max_k|n_k|)^{1/\alpha}}\\
&< \frac{KC\cdot 9^{1-1/\alpha}\left(\left(1-\left(\frac{R-1}{R}\right)^2\right)T\right)^{1/\alpha}}{\left(\left(\frac{R-1}{R}\right)^2T\right)^{1/\alpha}}\\
&= KC\cdot 9^{1-1/\alpha}\left(\frac{2R-1}{(R-1)^2}\right)^{1/\alpha}\\
&< 2C\cdot 9^{1-1/\alpha}\left(\frac{2R-1}{(R-1)^2}\right)^{1/\alpha}\xrightarrow{R\to\infty}0
\end{aligned}
$$

Thus, given $R'>1$, for sufficiently large R we have $\frac{|\delta_1|+|\delta_2|+|\delta_3|}{|\gamma|}<\frac{1}{R'}$, or, conversely, $\frac{|\epsilon_1|+|\epsilon_2|}{|\gamma|}>\frac{R'-1}{R'}$. □

7.2. **The central 'region' of a biLipschitz cycle.** The goal of this subsection is to show, as promised in Section 5.1, that the central region has at most four long sides.

Definition 7.2.1. Let $\gamma\colon S\to X$ be a cycle such that $\gamma\cap H\neq\emptyset$ and such that all of the escapes of γ from H have length at most $|\gamma|/2$. Let $\{\gamma|_{P_1},\gamma|_{P_2},\dots,\gamma|_{P_k}\}$ be a set of distinct escapes from H. The set is *manageable* if one of the following conditions referencing Figure 7 holds.

- $k=2$ and
  (7A) $\gamma|_{P_1}$ and $\gamma|_{P_2}$ are of the same flavor with opposite sign.
- $k=3$ and
  (7B) the $\gamma|_{P_i}$ are all of the same flavor but are not all of the same sign, or
  (7C) there is exactly one escape of each flavor among the $\gamma|_{P_i}$ and the a-escape has sign opposite to that of the x-escape and the y-escape.
- $k=4$ and three consecutive escapes $\gamma|_{P_{i_1}}$, $\gamma|_{P_{i_2}}$ and $\gamma|_{P_{i_3}}$, alternate between x and y flavors and the fourth escape $\gamma|_{P_{i_4}}$ has sign opposite to $\gamma|_{P_{i_2}}$ and either
  (7D) $\gamma|_{P_{i_4}}$ is an a-escape and the escapes $\gamma|_{P_{i_1}}$ and $\gamma|_{P_{i_3}}$ have opposite sign, or
  (7E) $\gamma|_{P_{i_4}}$ is an a-escape and the escapes $\gamma|_{P_{i_1}}$ and $\gamma|_{P_{i_3}}$ have the same sign, or
  (7F) $\gamma|_{P_{i_4}}$ is of the same flavor as $\gamma|_{P_{i_2}}$ and the escapes $\gamma|_{P_{i_1}}$ and $\gamma|_{P_{i_3}}$ have opposite sign.

Proposition 7.2.2. *For any $M\geq 24C+1$ and $R>M-1$ there are $J>0$ and a $K\in(1,2)$ such that the following holds.*

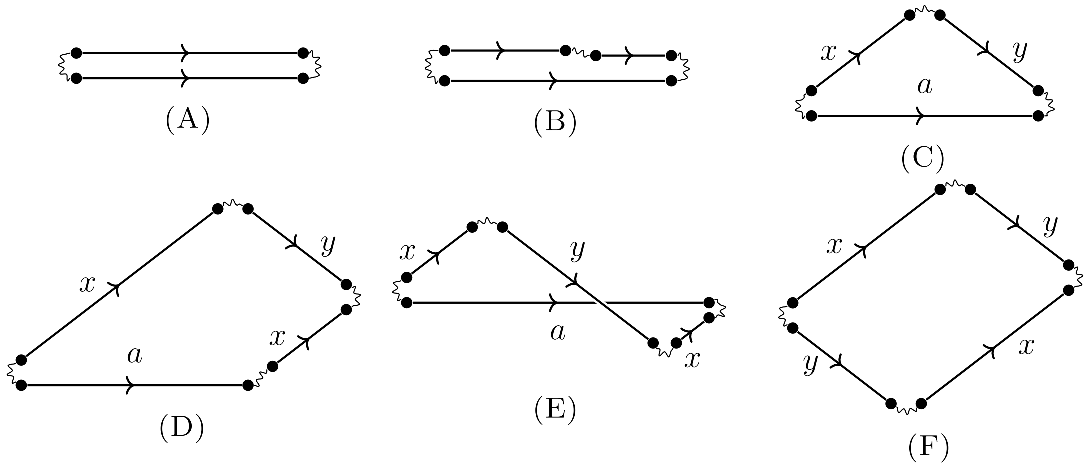

FIGURE 7. The possible configurations, up to symmetry, of the long escapes of a central region of the minimal area disk diagram of a biLipschitz cycle. The directed segments represent the oriented corridors of the long escapes with labels indicating the flavor of the escape. (In the configurations without labels, all long escapes must have the same flavor but each of the three flavors is possible.) The squiggly paths represent the complement of the long escapes in the cycle.

Let $\gamma\colon S \to X$ be a K-biLipschitz cycle of length $|\gamma| \geq J$ such that $\gamma \cap H \neq \emptyset$ and every escape of γ from H has length at most $|\gamma|/2$. Let $\gamma|_{P_1}, \gamma|_{P_2}, \ldots, \gamma|_{P_k}$ be distinct escapes from H such that $k \leq 5$ and $\sum_{i=1}^{k}\big|\gamma|_{P_i}\big| \geq \frac{R-1}{R} \cdot |\gamma|$. Then:

(I) $k > 1$
(II) *If $k \in \{2,3,4,5\}$ then either the $\gamma|_{P_i}$ are manageable or $\big|\gamma|_{P_i}\big| \leq \frac{M-1}{R} \cdot |\gamma|$ for some i.*

Proof. Given M and R as in the statement, let J and K be large enough with respect to R so that Theorem 7.1.24 is satisfied, and so that $J \geq R$.

We have $\sum_{i=1}^{k}\big|\gamma|_{P_i}\big| \geq \frac{R-1}{R} \cdot |\gamma| > \frac{1}{2} \cdot J > 0$ so $k > 0$. If $k = 1$ then by hypothesis $\frac{|\gamma|}{2} \geq \big|\gamma|_{P_1}\big| \geq \frac{R-1}{R} \cdot |\gamma| > \frac{1}{2} \cdot |\gamma|$, a contradiction. This establishes (I).

Let $\{Q_i\}_{i=1}^{k}$ be the set of closures of components of $S \setminus \bigcup_{i=1}^{k} P_i$ and let $\beta\colon Q \to X$ be the path obtained by concatenating translates of the $\gamma|_{Q_i}$. Note that if the endpoints of the concatenation of translates of the $\gamma|_{P_i}$ differ by $g \in G_L$ then the endpoints of β differ by g^{-1}.

For the cases $k \in \{2,3,4\}$, it will suffice to prove that if the $\gamma|_{P_i}$ are not manageable then $|\beta| \geq \frac{1}{2}|r|^{1/\alpha} - 5$ where g^r is the difference between the endpoints of some $\gamma|_{P_i}$ with $g \in \{a, x, y\}$. Indeed, then we have

$$\begin{aligned}\frac{|\gamma|}{R} &\geq |\gamma| - \sum_{i=1}^{k}\big|\gamma|_{P_i}\big| \\ &= |\beta|\end{aligned}$$

$$\begin{aligned} &\geq \frac{1}{2}|r|^{1/\alpha} - 5 \\ &\geq \frac{1}{2C} \cdot |g^r| - 5 \\ &\geq \frac{1}{2KC} \cdot \big|\gamma|_{P_i}\big| - 5 \end{aligned}$$

so that, as long as $J \geq R$, we have

$$\begin{aligned} \big|\gamma|_{P_i}\big| &\leq 2KC \cdot \left(\frac{|\gamma|}{R} + 5\right) \\ &< 4C \cdot \left(\frac{1}{R} + \frac{5}{J}\right) \cdot |\gamma| \\ &\leq \frac{24C}{R} \cdot |\gamma| \end{aligned}$$

and so we need only ensure that $M \geq 24C + 1$ to obtain $\big|\gamma|_{P_i}\big| \leq \frac{M-1}{R} \cdot |\gamma|$.

Consider the case $k = 2$. If the $\gamma|_{P_i}$ are unmanageable then either they differ in flavor or they have the same sign. Suppose that $\gamma|_{P_1}$ and $\gamma|_{P_2}$ have different flavors. Without loss of generality, $\gamma|_{P_1}$ is an x-escape and $\gamma|_{P_2}$ is either a y-escape or an a-escape. Let x^m be the difference between the endpoints of $\gamma|_{P_1}$ and let y^n and a^ℓ be the same for $\gamma|_{P_2}$ in each of the two cases. In the first case, Corollary 3.3.2 tells us that

$$|\beta| \geq |x^m y^n| \geq |m|^{1/\alpha} - 5$$

so we are done. In the second case, choose p and q so that $\ell = pL + q$ with $0 \leq |q| < L$ and either $q = 0$ or q and ℓ have opposite sign. Corollary 3.3.2 tells us that

$$|\beta| \geq |a^\ell x^m| \geq |p|^{1/\alpha} - 5$$

but our choice of p and q ensures that $|p| = \frac{|\ell-q|}{L} = \frac{|\ell|+|q|}{L} \geq \frac{|\ell|}{L}$ and so we have $|\beta| \geq \frac{|\ell|^{1/\alpha}}{L^{1/\alpha}} - 5 = \frac{1}{2}|\ell|^{1/\alpha} - 5$. It remains to consider the case where $\gamma|_{P_1}$ and $\gamma|_{P_2}$ have the same flavor $g \in \{x, y, a\}$ and the same sign. Suppose the endpoints of $\gamma|_{P_1}$ differ by g^{m_1} and those of $\gamma|_{P_2}$ differ by g^{m_2}. Then $|\beta| \geq |g^{m_1+m_2}| \geq |m_1 + m_2|^{1/\alpha} \geq |m_1|^{1/\alpha}$. This completes the proof for $k = 2$.

Consider the case $k = 3$. We split into subcases based on the number of flavors that appear among the the $\gamma|_{P_i}$: (i) exactly one flavor, (ii) exactly two flavors or (iii) exactly three flavors. If the $\gamma|_{P_i}$ are unmanageable then in case (i) they all have the same sign, in case (ii) up to symmetry the flavors that appear are (x, a, a), (x, x, a) or (x, x, y) and in case (iii) up to symmetry the x-escape and the a-escape have the same sign. Case (i) is treated similarly to the case $k = 2$ with all escapes having the same flavor and sign. In case (iii), let the endpoints of the escapes differ by a^ℓ, x^m and y^n. If p and q so that $\ell = pL + q$ with $0 \leq |q| < L$ then ℓ and p have the same sign so that, by Corollary 3.3.2, we have

$$|\beta| \geq |a^\ell x^m y^n| \geq |m + p|^{1/\alpha} - 5 = \big(|m| + |p|\big)^{1/\alpha} - 5 \geq |m|^{1/\alpha} - 5$$

so we are done. For case (ii), the (x,x,a) and (x,x,y) subcases are treated by again applying Corollary 3.3.2 to obtain

$$|\beta| \geq |m_1+m_2+p|^{1/\alpha} + |p|^{1/\alpha} - 5 \geq |p|^{1/\alpha} - 5 \geq \frac{|\ell|^{1/\alpha}}{L^{1/\alpha}} - 5 = \frac{|\ell|^{1/\alpha}}{2} - 5$$

(where the last inequality is obtained as in the (x,a) case of $k=2$ above) and

$$|\beta| \geq |m_1+m_2|^{1/\alpha} + |n|^{1/\alpha} - 5 \geq |n|^{1/\alpha} - 5$$

respectively. It remains to consider the (x,a,a) subcase for which Corollary 3.3.2 gives us the following inequality.

$$|\beta| \geq |m+p_1+p_2|^{1/\alpha} + |p_1+p_2|^{1/\alpha} - 5$$

If $|m| \leq |p_1+p_2|$ we are done so assume that $|p_1+p_2| \leq |m|$. Then, by the triangle inquality we have $|m+p_1+p_2| \geq |m| - |p_1+p_2| \geq 0$ and so $|m+p_1+p_2|^{1/\alpha} \geq \big(|m|-|p_1+p_2|\big)^{1/\alpha} \geq |m|^{1/\alpha} - |p_1+p_2|^{1/\alpha}$ by Fact 1.0.1. Thus we have

$$|\beta| \geq |m|^{1/\alpha} - |p_1+p_2|^{1/\alpha} + |p_1+p_2|^{1/\alpha} - 5 = |m|^{1/\alpha} - 5$$

as required.

Consider the case $k=4$. Assume that the $\gamma|_{P_i}$ are unmanageable. Renumber the segments so that P_1, P_2, P_3 and P_4 appear consecutively along S. Then either $P_1 \cup P_2$ is contained in a segment of length at most $\frac{|S|}{2}$ of S or $P_3 \cup P_4$ is contained in such a segment and similarly for $P_2 \cup P_3$ and $P_1 \cup P_4$. We again renumber the segments so that the first possibility holds in each case. Apply Theorem 7.1.24 to the minimal geodesic segments respectively containing $P_1 \cup P_2$ and $P_2 \cup P_3$ to conclude that either $\big|\gamma|_{P_i}\big| \leq \frac{M-1}{R} \cdot |\gamma|$ for some i or that $\gamma|_{P_1}$, $\gamma|_{P_2}$ and $\gamma|_{P_3}$ alternate between x and y flavors. Then, up to symmetry, we can assume that $\gamma|_{P_1}$ and $\gamma|_{P_3}$ are x-escapes and $\gamma|_{P_2}$ is a y-escape. If $\gamma|_{P_4}$ were an x-escape then, applying Corollary 3.3.2 we would obtain:

$$|\beta| \geq |m_1+m_3+m_4|^{1/\alpha} + |n_2|^{1/\alpha} - 5 \geq |n_2|^{1/\alpha} - 5$$

as needed. It remains to consider the cases where $\gamma|_{P_4}$ is a (i) y-escape or an (ii) a-escape. In case (i), since the $\gamma|_{P_i}$ are unmanageable, either the escapes $\gamma|_{P_1}$ and $\gamma|_{P_3}$ have the same sign or the escapes $\gamma|_{P_2}$ and $\gamma|_{P_4}$ have the same sign. Up to symmetry we can assume the former so that Corollary 3.3.2 gives us

$$|\beta| \geq |m_1+m_3|^{1/\alpha} + |n_2+n_4|^{1/\alpha} - 5 \geq |m_1|^{1/\alpha} - 5$$

as needed. In case (ii), since the $\gamma|_{P_i}$ are unmanageable, the escapes $\gamma|_{P_2}$ and $\gamma|_{P_4}$ must have the same sign but then Corollary 3.3.2 gives us

$$|\beta| \geq |m_1+m_3+p_4|^{1/\alpha} + |n_2+p_4|^{1/\alpha} - 5 \geq |n_2|^{1/\alpha} - 5$$

as needed.

Consider the case $k=5$. The $\gamma|_{P_i}$ are unmanageable so we need to show that $\big|\gamma|_{P_i}\big| \leq \frac{M-1}{R} \cdot |\gamma|$ for some i. Suppose this does not hold. Apply Theorem 7.1.24 to conclude that no three consecutive escapes among the $\gamma|_{P_i}$ are contained in a subsegment of γ of length at most $\frac{|\gamma|}{2}$ of γ. Then any two consecutive segments among the $\gamma|_{P_i}$ are contained in a subsegment of γ of length at most $\frac{|\gamma|}{2}$. Then Theorem 7.1.24 implies that, for any two consecutive escapes, one of them is an x-escape and the other one is a y-escape. Since k is odd this is a contradiction. □

Corollary 7.2.3. *For all $M \geq 24C+1$ and $R > M-1$ there exist $J > 0$ and $1 < K < 2$ such that the following holds.*

Let $\gamma\colon S \to X$ be a K-biLipschitz cycle of length $|\gamma| \geq J$ such that $\gamma \cap H \neq \emptyset$ and every escape of γ from H has length at most $|\gamma|/2$. Let $\gamma|_{P_1}, \gamma|_{P_2}, \ldots, \gamma|_{P_k}$ be distinct escapes from H such that $k \leq 5$ and $\sum_{i=1}^{k} \big|\gamma|_{P_i}\big| \geq \frac{R-1}{R} \cdot |\gamma|$. Then a subset $T \subseteq \big\{\gamma|_{P_i}\big\}_{i=1}^{k}$ of $|T| \in \{2,3,4\}$ longest escapes is manageable and satisfies $\sum_{\gamma|_P \in T} \big|\gamma|_P\big| \geq \frac{R-M^3}{R} \cdot |\gamma|$ and $\min_{\gamma|_P \in T} \big|\gamma|_P\big| \geq (M-1) \max\Big\{\frac{|\gamma|}{R}, |\gamma| - \sum_{\gamma|_P \in T} \big|\gamma|_P\big|\Big\}$.

Proof. Let $R_0 > M^4(M-1)$, and let $R_i := R_0 M^{-i}$ for $i \leq 4$, so that for all i, M and R_i satisfy the hypotheses of Proposition 7.2.2. Let $K \in (1,2)$ be close enough to 1 and let $J > 0$ be large enough that Proposition 7.2.2 holds with respect to M and R_i, for all $0 \leq i \leq 4$.

Let $\gamma\colon S \to X$ be a K-biLipschitz cycle of length $|\gamma| \geq J$ such that $\gamma \cap H \neq \emptyset$ and every escape of γ from H has length at most $|\gamma|/2$. Let $\gamma|_{P_1}, \gamma|_{P_2}, \ldots, \gamma|_{P_k}$ be distinct escapes from H such that $k \leq 5$ and $\sum_{i=1}^{k} \big|\gamma|_{P_i}\big| \geq \frac{R_0-1}{R_0} \cdot |\gamma|$.

If every escape of $T_0 = \big\{\gamma|_{P_i}\big\}_{i=1}^{k}$ has length greater than $\frac{M-1}{R_0} \cdot |\gamma|$ then applying Proposition 7.2.2 with $R = R_0$ the escapes of T_0 must be manageable. Moreover, in this case we would have

$$\min_{\gamma|_P \in T_0} \big|\gamma|_P\big| > (M-1) \cdot \left(|\gamma| - \frac{R_0 - 1}{R_0} \cdot |\gamma| \right) \geq (M-1) \cdot \left(|\gamma| - \sum_{\gamma|_P \in T_0} \big|\gamma|_P\big| \right)$$

so we would have the required conclusion with $R = R_0$ and $T = T_0$. Hence we may assume that some escape of T_0 has length at most $\frac{M-1}{R_0} \cdot |\gamma|$.

Let T_1 be obtained from T_0 by removing a shortest escape. We have

$$\sum_{\gamma|_P \in T_1} \big|\gamma|_P\big| \geq \left(\frac{R_0 - 1}{R_0} - \frac{M-1}{R_0} \right) \cdot |\gamma| = \frac{R_0 - M}{R_0} \cdot |\gamma| = \frac{R_1 - 1}{R_1} \cdot |\gamma|$$

so, applying Proposition 7.2.2 with $R = R_1$, we can conclude that $2 \leq |T_1| = |T_0| - 1 \leq 4$. Moreover, if every escape of T_1 had length greater than $\frac{M-1}{R_1} \cdot |\gamma|$ then T_1 would be manageable and, as argued above, we would have $\min_{\gamma|_P \in T_1} \big|\gamma|_P\big| \geq (M-1) \cdot \Big(|\gamma| - \sum_{\gamma|_P \in T_1} \big|\gamma|_P\big| \Big)$. Thus we would have the required conclusion with $R = R_0$ and $T = T_1$. Hence we may assume that some escape of T_1 has length at most $\frac{M-1}{R_1} \cdot |\gamma|$.

Continuing in this way, we obtain T_2 from T_1 by removing a shortest escape and if $T = T_2$ is not as needed then we again remove a shortest escape to obtain T_3. By the same arguments, we have $\sum_{\gamma|_P \in T_3} \big|\gamma|_P\big| \geq \frac{R_3-1}{R_3} \cdot |\gamma| = \frac{R_0-M^3}{R_0} \cdot |\gamma|$ and $|T_3| = 2$. If the shorter escape of T_3 had length at most $\frac{M-1}{R_3} \cdot |\gamma|$ then the remaining escape would have length at least $\frac{R_4-1}{R_4} \cdot |\gamma|$ which, by Proposition 7.2.2 with $R = R_4$, is a contradiction. Thus the escapes of T_3 must all have length greater than $\frac{M-1}{R_3} \cdot |\gamma| \geq (M-1) \cdot \Big(|\gamma| - \sum_{\gamma|_P \in T_3} \big|\gamma|_P\big| \Big)$.

Applying Proposition 7.2.2 with $R = R_3$ the escapes of T_3 must also be manageable, so we are done with $R = R_0$ and $T = T_3$. $\square$

Corollary 7.2.4. *For all $R > 0$ there exist $J > 0$ and $1 < K < 2$ such that if $\gamma\colon S \to X$ is a K-biLipschitz cycle of length $|\gamma| \geq J$ with $\gamma \cap H \neq \emptyset$ and all escapes of γ from H have length at most $|\gamma|/2$ then there is a manageable set T of longest escapes of γ from H that satisfies $\sum_{\gamma|_P \in T} \big|\gamma|_P\big| \geq \frac{R-1}{R} \cdot |\gamma|$ and $\min_{\gamma|_P \in T} \big|\gamma|_P\big| \geq R \cdot \max\Big\{\frac{|\gamma|}{J}, |\gamma| - \sum_{\gamma|_P \in T} \big|\gamma|_P\big|\Big\}$.*

Proof. Let $M \geq R + 1$ be large enough that we can apply Corollary 7.2.3 and let R' be large enough that $\frac{R'-M^3}{R'} \geq \frac{R-1}{R}$ and large enough that we can apply Corollary 7.2.3 with M and R'. Assume that $J \geq R'$ is large enough and $K > 1$ is close enough to 1 that the second paragraph of Corollary 7.2.3 holds.

Let $\gamma\colon S \to X$ be a K-biLipschitz cycle of length $|\gamma| \geq J$. Let v be a vertex of S that maps to H. Let $\bar{v}$ be the antipode of v in S. Since the relators of G_L all have even length so then does S and so $\bar{v}$ is a vertex of S. Let Q_1' and Q_2' be the two geodesic segments of S between v and $\bar{v}$. If $\bar{v} \in P$ for some escape $\gamma|_P$ of A then, for each i, let $Q_i = Q_i' \setminus P^\circ$ where P° is the interior of P; otherwise, for each i, let $Q_i = Q_i'$. If J is large enough and K is close enough to 1, Theorem 7.1.24 implies that at most four escapes occupy an $\frac{R'-1}{R'}$ proportion of $\gamma|_{Q_1}$ and $\gamma|_{Q_2}$. Thus a set T' of five longest escapes of A have length at least $\frac{R'-1}{R'} \cdot |\gamma|$. Applying Corollary 7.2.3 to T' we obtain a manageable set T of longest escapes of A such that:

$$\sum_{\gamma|_P \in T} \big|\gamma|_P\big| \geq \frac{R' - M^3}{R'} \cdot |\gamma| \geq \frac{R-1}{R} \cdot |\gamma|$$

and

$$\min_{\gamma|_P \in T} \big|\gamma|_P\big| \geq (M-1) \cdot \Big(|\gamma| - \sum_{\gamma|_P \in T} \big|\gamma|_P\big|\Big) \geq R \cdot \Big(|\gamma| - \sum_{\gamma|_P \in T} \big|\gamma|_P\big|\Big)$$

and

$$\min_{\gamma|_P \in T} \big|\gamma|_P\big| \geq (M-1) \cdot \frac{|\gamma|}{R'} \geq R \cdot \frac{|\gamma|}{J}$$ $\square$

7.3. **Non-central 'regions'.** Recall compound escapes from Definition 5.2.2. Fix R and let J and K be the corresponding constants from Theorem 7.1.24, and suppose that $\gamma\colon S \to X$ is a K–biLipschitz cycle. Suppose that $\gamma \cap gH \neq \emptyset$ and suppose that γ has a designated compound escape $\gamma|_P$ from gH that has length greater than $|\gamma|/2$. Call $\gamma|_P$ the "central escape". We wish to describe the configuration of non-central escapes of γ from gH. This is easier than in the previous subsection because $\big|\gamma\big| - \big|\gamma|_P\big| < |\gamma|/2$, so all of the non-central escapes are contained in a common K–biLipschitz path. This fact eliminates most of the cases considered in Figure 7; only the analogues of cases (7A) and (7C) can occur. Specifically, according to Theorem 7.1.24, there are only three possibilities:

1. $\big|\gamma\big| - \big|\gamma|_P\big| < J$. In this case say *the non-central part of γ at gH is very small.*
2. The non-central part is not very small, the central escape is a compound a–escape, and there are a non-central x–escape and non-central y–escape whose lengths sum to at least $\frac{R-1}{R}\big(\big|\gamma\big| - \big|\gamma|_P\big|\big)$. In this case say that the non-central part of γ is *branching at gH*.

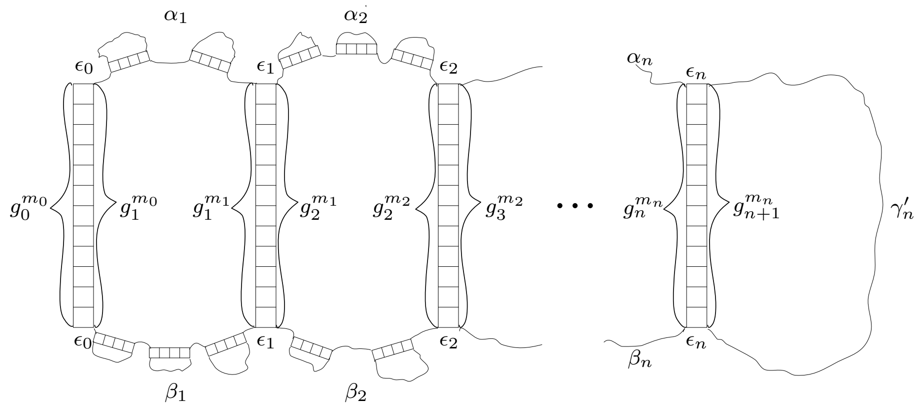

FIGURE 8. Enfilade of length n.

(3) The non-central part is not very small and there is exactly one escape of length at least $\frac{R-1}{R}\left(|\gamma| - |\gamma|_P|\right)$, and it is of the same flavor as the central escape.

Instances of the third case can be chained together to form super-regions that we now describe:

Definition 7.3.1. Let $R > 2$. Let γ be a g-escape for some $g \in \{a, x, y\}$. The *R–enfilade decomposition* of γ is the factoring of γ as:

$$\gamma_0 := \gamma = \epsilon_0 + \alpha_1 + \epsilon_1 + \cdots + \alpha_n + \epsilon_n + \gamma_n' + \epsilon_n^{-1} + \beta_n + \cdots + \epsilon_1^{-1} + \beta_1 + \epsilon_0^{-1}$$

such that the following conditions hold (see Figure 8).

- Each α_i or β_i is a path whose endpoints differ by an element of H.
- For each i, we have $\epsilon_i \in \{s^{\pm 1}, t^{\pm 1}\}$ and γ_i' is defined to be the path such that $\gamma_i = \epsilon_i + \gamma_i' + \epsilon_i^{-1}$.
- For each $i \in \{0, 1, \dots, n-1\}$, we have $|\gamma_{i+1}| \geq \frac{R-1}{R} \cdot |\gamma_i'|$.
- For each $i \in \{0, 1, 2, \dots, n\}$
$$\gamma_i = \epsilon_i + \alpha_{i+1} + \cdots + \epsilon_n + \gamma_n' + \epsilon_n^{-1} + \cdots + \beta_{i+1} + \epsilon_i^{-1}$$
is a g_i-escape, for some $g_i \in \{a, x, y\}$, whose endpoints differ by $g_i^{m_i}$ for some $m_i \in \mathbb{Z}$.
- n is maximal such that γ admits a decomposition satisfying these conditions.

Call the subsegment γ_n' the *end* of the enfilade.

Note that since $R > 2$ there is at most one candidate for γ_{i+1} for each i, so the decomposition is unique.

Lemma 7.3.2. *If $R > 2$ and $1 < K < 2$ and γ is a K–biLipschitz g–escape for some $g \in \{a, x, y\}$ then in the R–enfilade decomposition of γ all of the exponents m_i have the same sign.*

Proof. If m_{i-1} and m_i have different signs for some i then $|\beta_i| \geq |g_i^{m_{i-1}}| - |\alpha_i| + |g_i^{m_i}|$, but $\gamma_{i-1}' = \alpha_i + \gamma_i + \beta_i$, so:

$$|\gamma_{i-1}'| - |\gamma_i| = |\alpha_i| + |\beta_i| \geq |g_i^{m_{i-1}}| + |g_i^{m_i}| \geq \frac{1}{K}(|\gamma_{i-1}'| + |\gamma_i|) \implies |\gamma_i| \leq \frac{K-1}{K+1}|\gamma_{i-1}'|$$

But $|\gamma_i| > \frac{R-1}{R}|\gamma_{i-1}'|$, so $\frac{1}{2} < \frac{R-1}{R} < \frac{K-1}{K+1} < \frac{1}{3}$, and we have a contradiction. $\square$

Lemma 7.3.3. *Assume that γ begins at 1 and that we have an enfilade decomposition of γ with notation as above. Let $h_i \in H$ be the difference between the endpoints of α_i. For any $k \in \mathbb{Z}$, we have that $g_0^k.(\epsilon_0 + \sum_{i=1}^n \alpha_i + \epsilon_i)$ is a path from g_0^k to $(\epsilon_0 \prod_{i=1}^n h_i \epsilon_i) g_{n+1}^k$.*

Proof. This follows by induction on n using that facts that $g_i = \epsilon_{i-1}^{-1} g_{i-1} \epsilon_{i-1}$ and g_i and h_i commute. □

Remark 7.3.4. Let $R > 2$, let $2 > K > 1$, let γ be a K-biLipschitz g–escape for some $g \in \{a, x, y\}$ and let

$$\gamma = \epsilon_0 + \alpha_1 + \cdots + \epsilon_n + \gamma'_n + \epsilon_n^{-1} + \cdots + \beta_1 + \epsilon_0^{-1}$$

be the R-enfilade decomposition of γ. By Theorem 7.1.24, there exists a $J > 1$ such that if K is close enough to 1 then either $|\gamma'_n| \leq J$ or the endpoints of γ'_n differ by a power of a and γ'_n has an x–escape and a y–escape that collectively account for an at least $\frac{R-1}{R}$ fraction of its length.

Proposition 7.3.5 (Enfilades are short)**.** *Let $R > 3$. There exists a $2 > K > 1$ and $J > 2$ such that if γ is a K-biLipschitz g-escape for some $g \in \{a, x, y\}$ and $|\gamma| \geq J$ and*

$$\gamma = \epsilon_0 + \alpha_1 + \cdots + \epsilon_n + \gamma'_n + \epsilon_n^{-1} + \cdots + \beta_1 + \epsilon_0^{-1}$$

is the R-enfilade decomposition of γ then $|\gamma'_n| \geq \frac{R-3}{R} \cdot |\gamma|$.

Proof. Since $R > 3$, $\frac{R-1}{R} \cdot \frac{R-2}{R} > \frac{R-3}{R}$. Let $R_0 > 1$ be large enough to satisfy $\frac{R_0}{R_0+1} > \frac{2}{R}$ and $\frac{R-1}{R} \cdot \frac{R_0}{R_0+1} > \frac{R-2}{R}$. Let $J > 2$, $2 > K > 1$ be such that the conclusion of Corollary 7.1.8 holds with $(R, J, K) = (R_0, J, K)$ and so that all of the following hold:

- $\frac{2}{R} + \frac{4}{J} < \frac{R_0}{R_0+1}$
- $\frac{R-1}{R} \cdot \left(\frac{R_0}{R_0+1} - \frac{2}{J}\right) > \frac{R-2}{R}$.
- $\frac{R-1}{R} \cdot \frac{R_0}{R_0+1} - \frac{4}{J} \geq \frac{R-2}{R}$
- $\frac{R-1}{R} \cdot \frac{J-2}{J} \geq \frac{R-2}{R}$
- $\frac{R-1}{R} \cdot \frac{R-2}{R} \cdot \frac{J-2}{J} > \frac{R-3}{R}$

Let γ be a K-biLipschitz g-escape for some $g \in \{a, x, y\}$, let $|\gamma| \geq J$ and consider the R-enfilade decomposition of γ with the same notation as in Definition 7.3.1.

First assume that $g_0 = a$, and notice that then $g_i = a$ whenever i is even. We have $\alpha_i + g_i^{m_i} + \beta_i = g_i^{m_{i-1}}$, for each $i \in \{1, 2, \ldots n\}$. By commutativity of H, the endpoints of $\alpha_i + \beta_i$ differ by $g_i^{m_{i-1} - m_i}$. Define $\delta_{2i} := \epsilon_{2i-2} + \alpha_{2i-1} + \epsilon_{2i-1} + \alpha_{2i} + \beta_{2i} + \epsilon_{2i-1}^{-1} + \beta_{2i-1} + \epsilon_{2i-2}^{-1}$. By the previous observation and an argument similar to Lemma 7.3.3, the endpoints of δ_{2i} differ by $a^{m_{2i-2} - m_{2i}}$, so the endpoints of $\delta_{2i} + \gamma_{2i}$ differ by $a^{m_{2i-2} - m_{2i}} = a^{m_{2i-2}}$, which is the same as the difference between the endpoints of γ_{2i-2}. Moreover, we have:

$$\begin{aligned}
|\delta_{2i} + \gamma_{2i}| &= |\epsilon_{2i-2} + \alpha_{2i-1} + \epsilon_{2i-1} + \alpha_{2i} + \beta_{2i} + \epsilon_{2i-1}^{-1} + \beta_{2i-1} + \epsilon_{2i-2}^{-1}| + |\gamma_{2i}| \\
&= |\epsilon_{2i-2} + \alpha_{2i-1} + \epsilon_{2i-1} + \alpha_{2i} + \gamma_{2i} + \beta_{2i} + \epsilon_{2i-1}^{-1} + \beta_{2i-1} + \epsilon_{2i-2}^{-1}| \\
&= |\gamma_{2i-2}|
\end{aligned}$$

By induction, the path $\delta_2 + \delta_4 + \cdots + \delta_{2i} + \gamma_{2i}$ has the same length and the same endpoints as γ. Let $k \in \mathbb{Z}$ be defined by $n-1 \leq 2k \leq n$ and consider the path $\delta_2 + \delta_4 + \cdots + \delta_{2k} + \gamma_{2k}$. Since γ is K-biLipschitz, we have $J \leq |\gamma| = |\delta_2 + \delta_4 + \cdots + \delta_{2k} + \gamma_{2k}| = |\gamma| \leq K|a^{m_0}|$. Also the endpoints of δ_{2i} differ by $a^{m_{2i-2} - m_{2i}}$, for each i, and the endpoints of γ_{2k} differ by $a^{m_{2k}}$, so, by Corollary 7.1.8, either $|\delta_{2i}| > \frac{R_0}{R_0+1} \cdot |\gamma|$, for some $i \in \{1, 2, \dots, k\}$, or $|\gamma_{2k}| > \frac{R_0}{R_0+1} \cdot |\gamma|$. But

$$\begin{aligned}
|\delta_{2i}| &= |\epsilon_{2i-2} + \alpha_{2i-1} + \epsilon_{2i-1} + \alpha_{2i} + \beta_{2i} + \epsilon_{2i-1}^{-1} + \beta_{2i-1} + \epsilon_{2i-2}^{-1}| \\
&= |\epsilon_{2i-2} + \alpha_{2i-1} + \beta_{2i-1} + \epsilon_{2i-2}^{-1}| + |\epsilon_{2i-1} + \alpha_{2i} + \beta_{2i} + \epsilon_{2i-1}^{-1}| \\
&= \left(2 + |\gamma'_{2i-2}| - |\gamma_{2i-1}|\right) + \left(2 + |\gamma'_{2i-1}| - |\gamma_{2i}|\right) \\
&\leq |\gamma'_{2i-2}| - \frac{R-1}{R} \cdot |\gamma'_{2i-2}| + |\gamma'_{2i-1}| - \frac{R-1}{R} \cdot |\gamma'_{2i-1}| + 4 \\
&= \frac{1}{R} \cdot |\gamma'_{2i-2}| + \frac{1}{R} \cdot |\gamma'_{2i-1}| + 4 \\
&\leq \frac{2}{R} \cdot |\gamma| + 4 \\
&= \left(\frac{2}{R} + \frac{4}{|\gamma|}\right) \cdot |\gamma| \\
&\leq \left(\frac{2}{R} + \frac{4}{J}\right) \cdot |\gamma| \\
&< \frac{R_0}{R_0+1} \cdot |\gamma|
\end{aligned}$$

where the first inequality follows from the definition of R-enfilade decomposition. Thus:

$$\frac{R_0}{R_0+1} \cdot |\gamma| < |\gamma_{2k}| = |\gamma'_{2k}| + 2 \leq \frac{R}{R-1} \cdot |\gamma_n| + 2$$

We conclude:

$$\begin{aligned}
|\gamma'_n| &= |\gamma_n| - 2 \\
&> \frac{R-1}{R} \cdot \left(\frac{R_0}{R_0+1} \cdot |\gamma| - 2\right) - 2 \\
&= \frac{R-1}{R} \cdot \frac{R_0}{R_0+1} \cdot |\gamma| - 2 \cdot \frac{2R-1}{R} \\
&> \frac{R-1}{R} \cdot \frac{R_0}{R_0+1} \cdot |\gamma| - 4 \\
&= \left(\frac{R-1}{R} \cdot \frac{R_0}{R_0+1} - \frac{4}{|\gamma|}\right) |\gamma| \\
&\geq \left(\frac{R-1}{R} \cdot \frac{R_0}{R_0+1} - \frac{4}{J}\right) |\gamma| \\
&\geq \frac{R-2}{R} \cdot |\gamma|
\end{aligned}$$

If $g_0 \neq a$ then $g_0 \in \{x, y\}$. If $n = 0$ we are done, so suppose not. Since $g_0 \neq a$, $g_1 = a$ and $g_i = a$ for all odd i. Apply the previous argument to γ_1 to get:

$$|\gamma'_n| \geq \frac{R-2}{R} \cdot |\gamma_1|$$

$$\begin{aligned}
&\geq \frac{R-2}{R} \cdot \frac{R-1}{R} \cdot |\gamma_0'| \\
&= \frac{R-2}{R} \cdot \frac{R-1}{R} \cdot (|\gamma| - 2) \\
&= \frac{R-2}{R} \cdot \frac{R-1}{R} \cdot \frac{J-2}{J} \cdot |\gamma| \\
&\geq \frac{R-3}{R} \cdot |\gamma| \qquad \square
\end{aligned}$$

8. Constructing fillings

We will show that for all $\lambda \in (0,1)$ we have that for all sufficiently large R and Λ there exist $1 < K < 2$ and $A, J, M > 0$ such that every K–biLipschitz loop γ can be filled by a diagram of mesh at most $\lambda|\gamma| + M$ of area at most A. We do so inductively. An overview of the inductive argument is given in Section 8.1. In Section 8.2 we establish basic filling results for the approximate polygons that will occur as vertex regions. In Section 8.3 we handle the base case: identifying and filling a central region. In Section 8.4 we cover three possible types of induction steps: small enough parts, enfilades, and branching regions. In many of these steps we will need to make assumptions on the relationships between the various constants. These are boxed for emphasis. In Theorem 9.0.1 we put all of the pieces of the proof together, including observing that all of the boxed relations can be satisfied simultaneously, so that we can actually, quantitatively, perform the induction described in Section 8.1.

8.1. **Overview: Constructing a filling inductively.** In Lemma 8.3.1 we identify a coset gH from which γ has a manageable collection of at most 4 long escapes. Call these *the* 0*-th level escapes*. We resect those escapes and replace each with its trace in gH. We then subdivide each of the traces into segments of bounded exponent and replace each segment by a geodesic with the same endpoints. We find a filling diagram for the resulting loop γ' of controlled mesh and area. Call the filling diagram for γ' the 0*-th shell*.

It remains to take each of the 0-th level escapes, complete it to a loop using the same concatenation of geodesic subsegments as used to build γ', and construct a filling diagram of that loop.

For the induction, suppose we have an n-th level escape $\gamma|_P$ of γ and an n-th shell that includes a filling diagram with a boundary segment that is a subdivision of the trace of $\gamma|_P$. If $\gamma|_P$ is "small enough" we can fill it with a single 2–cell. This is quantified explicitly in (8.1.3) below. We will see in Section 8.4 that very small parts are small enough. If $\gamma|_P$ is not small enough then we look at its enfilade decomposition. Let $\gamma|_{P'}$ be the end of the enfilade, and let δ be the toral segment between the endpoints of $\gamma|_{P'}$. In Section 8.4 we describe how to fill the enfilade up to δ, which also yields a subdivision of δ. Then according to Section 7.3 there are two possibilities: either $\gamma|_{P'}$ is short enough to cap off with a single 2–cell, or it is branching. If it is branching then $\gamma|_{P'}$ has two long escapes and their traces make an approximate triangle with δ. We fill that triangle. The fillings of the enfilade part and the short/branching part together make up a component of the $(n+1)$-st shell. In the case of branching, the two long escapes are added to the list of $(n+1)$-st level escapes.

We finish the argument by showing that after finitely many steps, independent of γ, every remaining branch is small enough that it can be capped off with a single 2–cell, so that no escapes get added to a deeper level of the induction. The diagram filling γ is the union of the shells, identified along common segments. The induction hypothesis is:

(8.1.1) For an n–th level escape that is not small enough to cap off, the n–th shell provides a subdivision of its trace into at most $2(\Lambda+1)$–many subsegments of exponent at most $E|\gamma|^\alpha \cdot (3/L)^n$, where E is the constant of Lemma 8.3.1, which is independent of γ.

Lemma 8.3.1 establishes (8.1.1) for $n=0$. The inductive step is proved in Section 8.4. Let us suppose that (8.1.1) is true for all n and see how to finish the argument.

$$\boxed{\text{Assume } R > 12C(\Lambda+1)/\lambda.} \tag{8.1.2}$$

Suppose γ is a K–biLipschitz loop and gH is a coset such that:

(8.1.3) γ has a central escape, a compound escape from gH of length at least $|\gamma|/2$, whose trace is subdivided into at most $2(\Lambda+1)$–many subsegments of exponent bounded by $L\left(\frac{|\gamma|}{R}\right)^\alpha$.

Choose geodesic segments $\delta_1, \dots, \delta_m$, $m \leq 2(\Lambda+1)$, with the same endpoints as the subdivision segments. Let $\gamma|_P$ be the complement of the central escape. It is K–biLipschitz, with the same endpoints as $\delta_1 + \cdots + \delta_m$, so $|\gamma|_P| \leq K\sum_{i=1}^m |\delta_i|$. Since the exponents of the δ_i are bounded, we apply Theorem 3.2.9 to get $|\delta_i| < C\left(L\left(\frac{|\gamma|}{R}\right)^\alpha\right)^{1/\alpha} = 2C|\gamma|/R$. Thus:

$$\begin{aligned}
|\gamma|_P| + \sum_{i=1}^m |\delta_i| &\leq (K+1)\sum_{i=1}^m |\delta_i| \\
&< 3 \cdot 2(\Lambda+1) \cdot 2C|\gamma|/R \\
&= 12C(\Lambda+1) \cdot |\gamma| \cdot \frac{1}{R} \\
&< 12C(\Lambda+1) \cdot |\gamma| \cdot \frac{\lambda}{12C(\Lambda+1)} \\
&= \lambda|\gamma|
\end{aligned}$$

Thus, if (8.1.3) is satisfied then $\gamma|_P + \bar{\delta}_m + \cdots + \bar{\delta}_1$ is a loop of length less than $\lambda|\gamma|$, so it is small enough to cap off with a single 2–cell satisfying the desired mesh bound.

The induction hypothesis (8.1.1) says that an n–th level escape has trace subdivided into segments of exponent at most $E|\gamma|^\alpha \cdot (3/L)^n$, so it is guaranteed to be small enough to cap off with a single 2–cell once we have:

$$E|\gamma|^\alpha \cdot (3/L)^n \leq L\left(\frac{|\gamma|}{R}\right)^\alpha \iff n \geq \log_{L/3}(ER^\alpha/L) \tag{8.1.4}$$

Since E and R are independent of γ, (8.1.4) gives a uniform upper bound on the number of shells we need to fill before we can cap off all remaining branches with a single 2–cell apiece.

Suppose that we have area bounds $\mathcal{C}$, $\mathcal{E}$, and $\mathcal{B}$ for our fillings of the central region, enfilades, and branching regions, respectively, by diagrams of controlled mesh. The worst-case scenario is that the central region has four long escapes, each belonging to an enfilade terminating in a branching region, and for each of these branching regions the two long escapes belong to enfilades terminating in a branching region, etc, carried out to the n–th shell, where n is the least integer satisfying (8.1.4), at which point all remaining regions are small enough and can be capped off with one additional 2–cell. The area of the resulting diagram is bounded above by:

$$\mathcal{C} + 4(\mathcal{E} + \mathcal{B})(2^n - 1) + 2^{n+2} \tag{8.1.5}$$

Thus, if we control the mesh and area of the filling diagrams used in the induction steps then we can assemble a uniformly bounded number of them to get a filling diagram for γ of controlled mesh and uniformly bounded area.

8.2. **Approximate polygons and fillings.** The construction of fillings for the different pieces of the argument can be unified in the framework of filling approximate polygons. An approximate polygon, for us, will mean a cycle, in H, of segments of a–lines, x–lines, and y–lines such that the terminal endpoint of one is close to the initial endpoint of the next. We construct fillings of certain approximate polygons. These will be the building blocks for fillings of biLipschitz loops constructed in the next two sections.

Approximate polygons are close to true polygons. We will quantify approximate polygons as D*–approximate* to mean that the distance between consecutive segments is as most D. A *true* polygon is a 0–approximate polygon.

Definition 8.2.1. Let a D*–approximate triangle* mean a collection of elements g_0, g_1, g_2 of $\langle a, x, y\rangle$ and numbers $m_0, m_1, m_2 \in \mathbb{Z}$ such that the distances $d(g_0x^{m_0}, g_1)$, $d(g_1y^{m_1}, g_2)$, and $d(g_2a^{m_2}, g_0)$ are at most D.

Lemma 8.2.2 (Approximate triangles)**.** *For every such D–approximate triangle there exists a true triangle described by $g_0', g_1', g_2' \in \langle a, x, y\rangle$ and $m_0', m_1', m_2' \in \mathbb{Z}$ such that the distance between every corresponding pair of points is at most $2D + L$.*

Proof. By Lemma 3.4.2, there exists $p \in \mathbb{Z}$ with $|p| \le L/2$ such that $g_0\langle x\rangle \cap g_1a^p\langle y\rangle \neq \emptyset$. Choose such a p, and let $g_1' := g_0\langle x\rangle \cap g_1a^p\langle y\rangle$. By Lemma 3.4.1, we can set $g_0' := g_0\langle x\rangle \cap g_2\langle a\rangle$ and $g_2' := g_2\langle a\rangle \cap g_1a^p\langle y\rangle = g_2\langle a\rangle \cap g_1'a^p\langle y\rangle$. Define m_i' so that $g_0'x^{m_0'} = g_1'$, $g_1'y^{m_1'} = g_2'$, and $g_2'a^{m_2'} = g_0'$. Note that $m_0' = m_1'$ and $m_2' = -Lm_0'$. See Figure 9.

It remains to bound the distance between corresponding points. We verify what we claim to be the worst case, and leave the remaining verifications to the reader.

$$\begin{aligned}
d(g_2, g_2') &\le d(g_2, g_1y^{m_1}) + d(g_1y^{m_1}, g_2') \\
&\le D + d(g_1y^{m_1}, g_2') \\
&= D + d(g_1y^{m_1}, g_1'y^{m_1'}) \\
&\le D + d(g_1y^{m_1}, g_1a^py^{m_1}) + d(g_1a^py^{m_1}, g_1'y^{m_1'})
\end{aligned}$$

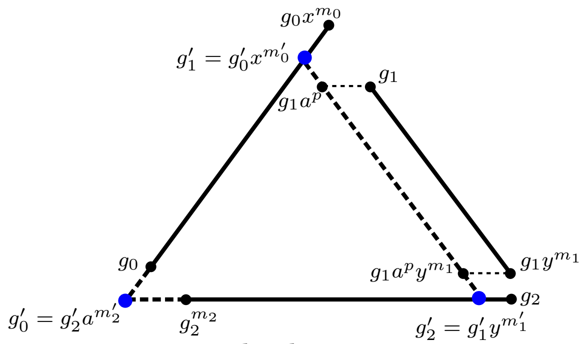

FIGURE 9. True triangle close to an approximate triangle

$$\begin{aligned}
&= D + d(g_1y^{m_1}, g_1a^py^{m_1}) + d(g_1a^py^{m_1}, g_2\langle a\rangle)\\
&\le D + 2d(g_1y^{m_1}, g_1a^py^{m_1}) + d(g_1y^{m_1}, g_2\langle a\rangle)\\
&\le D + L + d(g_1y^{m_1}, g_2\langle a\rangle)\\
&\le D + L + d(g_1y^{m_1}, g_2) \le 2D + L
\end{aligned}$$
□

Lemma 8.2.3 (Approximate diamonds)**.** *Let a D–*approximate diamond *mean a collection of elements g_1, g_2, h_1, $h_2 \in \langle a, x, y\rangle$ and numbers m_1, m_2, n_1, $n_2 \in \mathbb{Z}$ such that $d(g_1x^{m_1}, h_1)$, $d(h_1y^{n_1}, g_2)$, $d(g_2x^{m_2}, h_2)$, and $d(h_2y^{n_2}, g_1)$ are all at most D.*

For every such D–approximate diamond there exits a true diamond described by g'_1, g'_2, h'_1, $h'_2 \in \langle a, x, y\rangle$ and m'_1, m'_2, n'_1, $n'_2 \in \mathbb{Z}$ such that the distance between every corresponding pair of points is at most $D + 3L/2$.

Proof. By Lemma 3.4.2, there exist numbers p_1, p_2, and p_3 with all $|p_i| \le L/2$ such that $g_1\langle x\rangle \cap h_1a^{p_1}\langle y\rangle \ne \emptyset$, $g_1\langle x\rangle \cap h_2a^{p_2}\langle y\rangle \ne \emptyset$, and $g_2a^{p_3}\langle x\rangle \cap h_1a^{p_2}\langle y\rangle \ne \emptyset$. Choose such p_i. Define $h'_1 := g_1\langle x\rangle \cap h_1a^{p_1}\langle y\rangle$. Define $g'_2 := g_2a^{p_3}\langle x\rangle \cap h'_1\langle y\rangle$. Define n'_1 so that $h'_1y^{n'_1} = g'_2$. Define $h'_2 := g'_2\langle x\rangle \cap h_2a^{p_2}\langle y\rangle$. Define m'_2 so that $h'_2 = g'_2x^{m'_2}$. Define $g'_1 := h'_2\langle y\rangle \cap g_1\langle x\rangle == h_2a^{p_2}\langle y\rangle \cap g_1\langle x\rangle$. Define n'_2 so that $g'_1 = h'_2y^{n'_2}$. Define m'_1 so that $g'_1x^{m'_1} = h'_2$. Finally, note that $m'_2 = -m'_1$ and $n'_2 = -n'_1$. See Figure 10.

It remains to bound the distance between corresponding points. We will check what we claim is the worst case, and leave the other, similar, verifications to the reader.

$$\begin{aligned}
d(h_2, h'_2) &\le d(h_2, h_2a^{p_2}) + d(h_2a^{p_2}, h'_2)\\
&= d(h_2, h_2a^{p_2}) + d(h_2a^{p_2}, g'_2x^{m'_2})\\
&\le d(h_2, h_2a^{p_2}) + d(h_2a^{p_2}, g'_2\langle x\rangle)\\
&\le d(h_2, h_2a^{p_2}) + d(h_2a^{p_2}, g_2\langle x\rangle) + d_{\mathrm{Haus}}(g_2\langle x\rangle, g'_2\langle x\rangle)\\
&\le L + d(h_2a^{p_2}, g_2\langle x\rangle)\\
&\le L + d(h_2a^{p_2}, g_2x^{m_2})\\
&\le L + d(h_2a^{p_2}, h_2) + d(h_2, g_2x^{m_2}) \le L + L/2 + D
\end{aligned}$$
□

Filling approxiate polygons. Let a *D–approximate bigon* mean a collection of elements $g_0, g_1 \in \langle a, x, y\rangle$, $g \in \{a, x, y\}$, and numbers $m_0, m_1 \in \mathbb{Z}$ such that $d(g_ig^{m_i}, g_{i+1}) \le D$ for all $0 \le i \le 1$ with indices mod 2.

For an approximate polygon, a collection of "corner paths" refers to a collection of paths connecting successive endpoints of sides.

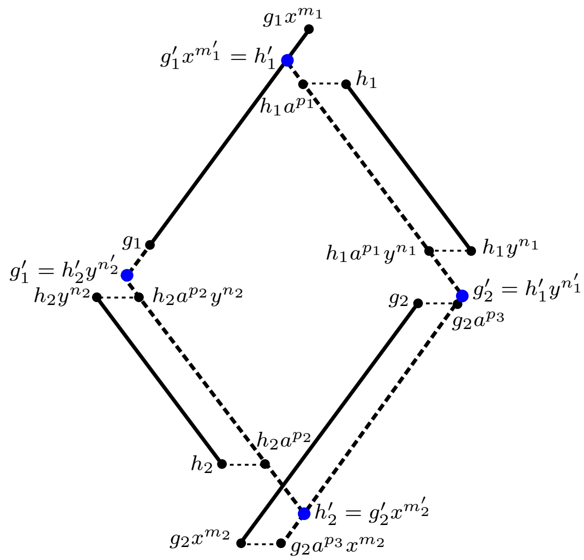

FIGURE 10. True diamond close to an approximate diamond

Lemma 8.2.4 (Filling bigons)**.** *There exist constants M_0, M_1, and M_2 such that for all positive Λ, E, and D, given an approximate bigon, a collection of corner paths of length at most D, and a subdivision of one side of the bigon into Λ–many subsegments, each of exponent at most E, the following hold. There exists a subdivision of the opposite side of the bigon into Λ–many subsegments of exponent bounded by $E + LD^\alpha$. Furthermore, if we construct a loop γ out of the bigon with corner paths by replacing each of the subsegments of the sides by some geodesic, then there is a diagram for γ with mesh at most $M_0 + M_1D + M_2E^{1/\alpha}$ and area at most Λ. In fact, it suffices to take $M_0 := 0$, $M_1 := 2(2C + 1)$, and $M_2 := 2C$.*

Proof. Assume that we have been given a subdivision of the g_0–side of the bigon. We refer to the g_0–side of the bigon as the "bottom" and the g_1–side as the "top". Up to isometry we may assume $g_0 = 1$ and $m_0 \geq 0$. Set $h := g_1$.

Let $s_0 := 0$ and let $s_i \geq 0$ be the sum of the first i exponents of the bottom, so that the bottom consists of g–segments $[g^{s_{i-1}}, g^{s_i}]$ for $0 < i \leq \Lambda$. Note that $s_\Lambda = m_0$. Let δ_0 be the given corner path from 1 to hg^{m_1}, and let δ_Λ be the corner path from g^{s_Λ} to h. Define p to be the lesser of $\Lambda - 1$ and the greatest index such that s_p is contained in the closed interval defined by 0 and m_1 (i.e. $[m_1, 0]$ or $[0, m_1]$ depending on the sign of m_1).

There are two cases according to whether or not $m_0 > -m_1$. See Figure 11.

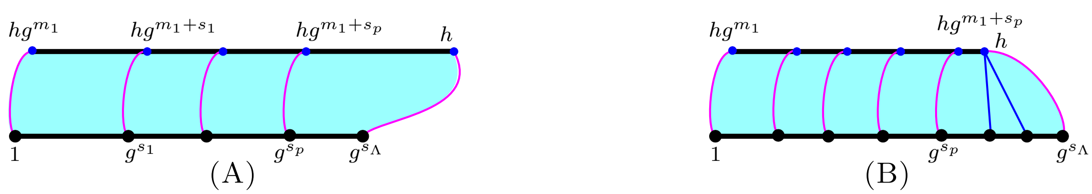

FIGURE 11. Two cases for filling a bigon

First suppose, as in Figure (11A), that $m_0 \leq -m_1$, so that $m_1 \leq 0$ and $p = \Lambda - 1$. For each $0 < i \leq p$, define $\delta_i = g^{s_i}.\delta_0$, so that δ_i is a path of length at most D between g^{s_i} and $g^{s_i}hg^{m_1} = hg^{m_1+s_i}$.

For each $i < p$ define a 2–cell with boundary consisting of a geodesic from $g^{s_{i-1}}$ to g^{s_i}, δ_i, a geodesic from $hg^{m_1+s_i}$ to $hg^{m+2+s_{i-1}}$, and $\bar{\delta}_{i-1}$. The δ sides have length at most D, while the other two sides have length bounded above by $CE^{1/\alpha}$, since $s_i - s_{i-1} \leq E$, so these 2–cells have perimeter of length at most $2D + 2CE^{1/\alpha} < M_1D + M_2E^{1/\alpha}$.

Now define a 2–cell whose boundary consists of a geodesic from g^{s_p} to g^{s_Λ}, δ_Λ, a geodesic from h to $hg^{m_1+s_p}$, and $\bar{\delta}_p$. The bottom has length less than $CE^{1/\alpha}$, since $p = \Lambda - 1$, and the vertical sides each have length at most D by hypothesis. We have:

$$|m_1+s_\Lambda|^{1/\alpha} < |g^{m_1+s_\Lambda}| = |(hg^{m_1+s_\Lambda})^{-1}h| \leq d(hg^{m_1+s_\Lambda}, g^{s_\Lambda})+d(g^{s_\Lambda}, h) \leq |\delta_0|+|\delta_\Lambda| \leq 2D$$

So $|m_1 + s_\Lambda| < (2D)^\alpha$, which implies $|m_1 + s_p| < E + (2D)^\alpha = E + LD^\alpha$ and the length of a geodesic between $hg^{m_1+s_p}$ and h is less than $CE^{1/\alpha} + 2CD$, so the perimeter has length less than $2(C + 1)D + 2CE^{1/\alpha} < M_1D + M_2E^{1/\alpha}$.

These 2–cells glue together along common δ_i to give the desired diagram.

Now suppose $m_0 > -m_1$, as in Figure (11B). In this case it is possible that $m_1 \geq 0$ with $p = 0$. For $i \leq p$ define δ_i as in the previous case. For each $i < p$, as in the previous case, define a 2–cell with boundary consisting of a geodesic from $g^{s_{i-1}}$ to g^{s_i}, δ_i, a geodesic from $hg^{m_1+s_i}$ to $hg^{m+2+s_{i-1}}$, and $\bar{\delta}_{i-1}$.

For $p < i < \Lambda$ choose a geodesic δ_i from g^{s_i} to h. As in the previous case, $0 < s_\Lambda + m_1 \leq (2D)^\alpha$, so for all $p < i \leq \Lambda$ we also have $0 \leq s_i + m_1 \leq (2D)^\alpha$. This implies that for $i > p$ we have $|\delta_i| \leq (2C + 1)D$. It also implies that, when $m_1 \geq 0$, we have $|g^{m_1}| < C|m_1|^{1/\alpha} \leq 2D$.

Define a 2–cell with boundary consisting of a geodesic from g^{s_p} to $g^{s_{p+1}}$, δ_{p+1}, a geodesic from h to $hg^{m_1+s_p}$, and $\bar{\delta}_p$. The bottom of this 2–cell has exponent bounded by E, so has length less than $CE^{1/\alpha}$. When $m_1 < 0$, the top of the 2–cell similarly has length bounded by $CE^{1/\alpha}$. Otherwise, the top has length $|g^{m_1}| < 2D$. The sides have length bounded by D and $(2C + 1)D$, so the perimeter has length less than $(2C + 4)D + 2CE^{1/\alpha} < 2(2C + 1)D + 2CE^{1/\alpha} = M_1D + M_2E^{1/\alpha}$.

Finally, for $p < i < \Lambda$ define a 2–cell[3] with boundary consisting of a geodesic from g^{s_i} to g^{s_i+1}, δ_{i+1}, and $\bar{\delta}_i$. It has length less than $CE^{1/\alpha} + 2(2C + 1)D < M_1D + M_2E^{1/\alpha}$.

Again, glue the 2–cells together along common δ_i to get the desired diagram. □

Lemma 8.2.5 (Filling triangles)**.** *There exist constants M_0, M_1, and M_2 such that for all positive Λ, E, and D, given an approximate triangle, corner paths of length at most D, and a subdivision of the a–side of the triangle into Λ-many subsegments, each of exponent at most E, the following hold. There exist subdivisions of the x–side and y–side into Λ–many subsegments of exponent bounded by $1 + E/L + D^\alpha$. Furthermore, if we construct a loop γ by replacing each of the subsegments by some geodesic then there is a diagram for γ with mesh at most $M_0 + M_1D + M_2E^{1/\alpha}$ and area at most $(\Lambda^2 + 9\Lambda + 6)/2$. In fact, it suffices to take $M_0 := 4C$, $M_1 := 6C + 2$ and $M_2 := 2C$.*

[3] We are constrained by the hypothesis that the bottom of γ uses geodesics along the given subdivision of the bottom side, so if we just flip the construction from Figure (11A) we cannot use the estimate for the length of a geodesic along the long side of the last 2–cell in the mesh calculation. We add the extra 2–cells and accept more area to get finer mesh.

Proof. By Lemma 8.2.2 there is a true triangle with corresponding points at distance at most $2D+L$. That is, for each of the three sides, the corresponding pairs of sides from the approximate and true triangle form a $(2D+L)$–approximate bigon. We construct a filling by filling the true triangle, using Lemma 8.2.4 to fill the three approximate bigons, and then adding one more 2–cell at each corner to close the corner path.

Apply Lemma 8.2.4 between the a–side approximate bigon. This gives a decomposition of the a–side of the true triangle into at most Λ–many subsegments of exponent at most $E+(2D)^\alpha$, and a diagram of area Λ and mesh at most $2(2C+1)D+2CE^{1/\alpha} < M_1D+M_2E^{1/\alpha}$.

It would be preferable, because we want to apply Lemma 3.4.4, if the subsegments of the a–side all had exponents that were multiples of L. This can be achieved by moving the endpoints slightly along the side, each moving distance at most $L/2$. For the purposes of the diagram, we add an extra strip of 2–cells along the previous strip, the bottom of the new strip is identified with the top of the old strip and the top of the new strip is the a–side of the triangle with its new subdivision. A vertical division into 2–cells can be obtained by connecting the original subdivision points with the new ones by geodesics. The exponents of the new subdivision segments increase by at most L from the previous bound. The new strip has area Λ and mesh bounded by:

$$\begin{aligned} C(E+(2D)^\alpha)^{1/\alpha}+&C(L+E+(2D)^\alpha)^{1/\alpha}+L/2+L/2 \\ &\leq 2CE^{1/\alpha}+4CD+CL^{1/\alpha}+L \\ &= 2CE^{1/\alpha}+4CD+2C+L \\ &< M_0+M_1D+M_2E^{1/\alpha} \end{aligned}$$

Having made this adjustment, by Lemma 3.4.4, every subdivision point p of the a–side of the triangle has a unique closest point q on the x–side. Furthermore, from the proof of Lemma 3.4.4, every geodesic from p to q consists of a single geodesic y–escape, so they all have the same trace: it is the y–segment between p and q. A similar argument holds for p and the closest point on the y–side of the triangle.

Subdivide the triangle by taking the trace of a geodesic from each subdivision point of the a–side to its closest point on the x–side and the y–side. This divides the triangle into $(\Lambda^2-\Lambda)/2$–many small diamonds and Λ–many small triangles. See Figure 12.

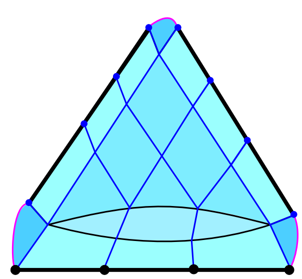

FIGURE 12. Filling an approximate triangle

The small triangles have as a–sides one of the subsegments of the a–side of the triangle, so we know they have exponent at most $L+E+(2D)^\alpha$. From Lemma 3.4.4, the resulting subdivisions of the x and y–sides have exponent that decreases by a factor of L, so all x and y–sides of all of the small triangles and small diamonds have exponents bounded by $(L+E+(2D)^\alpha)/L = 1+E/L+(2^\alpha/L)D^\alpha = 1+E/L+D^\alpha$.

From this subdivision of the triangle define a diagram with one 2–cell for each of the small diamonds and small triangles, where the 1–skeleton of the diagram is obtained by replacing each side of each of the small polygons by a geodesic with the same endpoints. The mesh of this diagram is at most:

$$\begin{aligned} 4\cdot C((L+E+(2D)^\alpha)/L)^{1/\alpha} &= 4C\cdot L^{-1/\alpha}(L^{1/\alpha}+E^{1/\alpha}+2D) \\ &= 4C\cdot(1/2)(2+E^{1/\alpha}+2D) \\ &< M_0+M_1D+M_2E^{1/\alpha} \end{aligned}$$

The next step is to use Lemma 8.2.4 to fill the approximate bigons formed by the x–side of the approximate triangle and the x–side of the true triangle, and similarly for the y–sides. This results in subdivisions of the x–side and y–side of the approximate triangle with Λ–many pieces of exponent at most $(L+E+(2D)^\alpha)/L$ and two diagrams with area Λ and mesh at most:

$$\begin{aligned} &M_{1,8.2.4}D+M_{2,8.2.4}\left((L+E+(2D)^\alpha)/L\right)^{1/\alpha} \\ &\quad\le M_{1,8.2.4}D+M_{2,8.2.4}\left(1+E^{1/\alpha}/2+D\right) \\ &\quad= M_{2,8.2.4}+(M_{1,8.2.4}+M_{2,8.2.4})D+(M_{2,8.2.4}/2)E^{1/\alpha} \\ &\quad= 2C+(6C+2)D+CE^{1/\alpha} \\ &\quad< M_0+M_1D+M_2E^{1/\alpha} \end{aligned}$$

To complete the diagram, at each corner add one 2–cell whose boundary is the given path between the sides of the approximate triangle, followed by a geodesic from one endpoint of one side of the approximate triangle to the corner of the true triangle, followed by a geodesic to the endpoint of the other side of the approximate triangle. The boundary of this 2–cell has length at most $D+2(2D+L)<M_0+M_1D$.

We have verified that the perimeter of every 2–cell of the diagram has length at most $M_0+M_1D+M_2E^{1/\alpha}$. The total area of our diagram is:

$$\Lambda+\Lambda+(\Lambda^2-\Lambda)/2+\Lambda+2\Lambda+3=(\Lambda^2+9\Lambda+6)/2$$ □

Lemma 8.2.6 (Filling diamonds)**.** *There exist constants M_0, M_1, and M_2 such that for all positive Λ, E, and D, given an approximate diamond, corner paths of length at most D, and subdivisions of one x–side and one y–side into at most Λ-many subsegments of exponent at most E, the following hold. There exist subdivisions of the other two sides into at most Λ–many subsegments of exponent at most $E+2LD^\alpha$. Furthermore, if we construct a loop γ by replacing each of the subsegments by some geodesic then there is a diagram for γ with mesh at most $M_0+M_1D+M_2E^{1/\alpha}$ and area at most $\Lambda^2+4\Lambda+4$. In fact, it suffices to take $M_0:=3L$, $M_1:=8C+2$, and $M_2:=4C$.*

Proof. The strategy is the same as in the triangle case. By Lemma 8.2.3 there is a true diamond whose corners are within distance $D+3L/2$ of the ends of the corresponding sides of the approximate diamond. Use Lemma 8.2.4 with the given subdivided sides of the approximate diamond to get subdivisions of two sides of the true diamond. Each of these consists of at most Λ–many segments of exponent at most $E + (2D)^\alpha$. In terms of diagrams we get two strips each with area at most Λ and mesh at most $2(2C+1)D + 2CE^{1/\alpha} < M_1 D + M_2 E^{1/\alpha}$.

By Lemma 3.4.3 for each of the subdivision points p on the given x–side of the true diamond, there is a unique closest point q on the opposite x–side. Furthermore, by Proposition 3.1.1, every geodesic between them is a single geodesic y–escape, so all have the same trace: it is the y–segment between p and q. A similar statement holds for the y–sides.

Subdivide the diamond by taking the trace of a geodesic between each subdivision point and its closest point on the opposite side of the diamond. This divides the diamond into at most Λ^2–many small diamonds whose sides have the same exponent bound as we started with, $E + (2D)^\alpha$. See Figure 13.

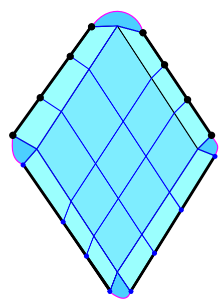

FIGURE 13. Filling an approximate diamond

From the subdivision of the diamond define a diagram with one 2–cell for each of the small diamonds, where the 1–skeleton is obtained by replacing each side of each small diamond by a geodesic. The mesh of this diagram is at most:

$$4 \cdot C\left(E + (2D)^\alpha\right)^{1//\alpha} \leq 4CE^{1/\alpha} + 8D < M_1 D + M_2 E^{1/\alpha}$$

The next step is to use Lemma 8.2.4 to relate the remaining x and y–side of the true diamond with the corresponding sides of the approximate diamond. Each adds a subdiagram of area at most Λ and mesh at most:

$$2(2C+1)D + 2C(E + (2D)^\alpha)^{1/\alpha} \leq 2CE^{1/\alpha} + (8C+2)D < M_1 D + M_2 E^{1/\alpha}$$

The resulting subdivision of the sides of the approximate diamond have exponent at most:

$$E + (2D)^\alpha + (2D)^\alpha = E + 2LD^\alpha$$

To complete the diagram, add a corner 2–cell at each of the four corners are in the triangle case. The boundaries of these 2–cells have length at most $D + 2(D + 3L/2) = 3D + 3L < M_0 + M_1 D$.

We have verified that the perimeter of every 2–cell of our diagram has length bounded by $M_0 + M_1 D + M_2 E^{1/\alpha}$. Its area is $2\Lambda + \Lambda^2 + 2\Lambda + 4$. $\square$

8.3. **Base case: identifying and filling a central region.**

Lemma 8.3.1. *For all $\lambda \in (0,1)$ and all sufficiently large Λ depending on λ and all sufficiently large R depending on λ and Λ there exist $K > 1$ depending on R, A depending on Λ, and $E := \left(\frac{1}{L\Lambda} + \frac{2L}{R^\alpha}\right)$ and J depending on R and Λ such that for any K–biLipschitz loop γ of length $|\gamma| > J$ we can construct a loop γ' from γ as follows:*

1. *Identify a coset gH such that every escape of γ from gH has length at most $|\gamma|/2$.*
2. *Select a manageable collection of long escapes of γ from gH.*
3. *Subdivide the trace of each long escape into at most $2(\Lambda+1)$–many segments of exponent at most $E|\gamma|^\alpha$.*
4. *Define γ' to be the loop obtained by replacing each long escape of γ by a concatenation of geodesics connecting the endpoint of these segments.*

The loop γ' can be filled by a diagram of area at most A and mesh at most $\lambda|\gamma| + 4C$.

Proof. Define:

$$
\begin{aligned}
M_0 &:= \max\{M_{0,8.2.4}, M_{0,8.2.5}, M_{0,8.2.6}\} = 4C\\
M_1 &:= \max\{M_{1,8.2.4}, M_{1,8.2.5}, M_{1,8.2.6}\}\\
M_2 &:= \max\{M_{2,8.2.4}, M_{2,8.2.5}, M_{2,8.2.6}\}/2
\end{aligned}
$$

Assume that $\Lambda > (2M_2/\lambda)^\alpha$ and that $R > \max\{2M_1/\lambda, \left(\frac{L^2\Lambda}{L-1}\right)^{1/\alpha}\}$. Let J and K be as in Corollary 7.2.4 with respect to R, and further increase J if necessary so that $J \geq \left(\frac{L-1}{L^2\Lambda} - \frac{1}{R^\alpha}\right)^{-1/\alpha}$.

Assume $|\gamma| > J$. As described in Step 2 of Section 5.2, any HNN diagram for γ has a central region. The boundary of the central region maps to a loop in some coset gH of the vertex group. Up to isometry, we may assume $g = 1$. By definition, the components of γ complementary to the central region have length at most $|\gamma|/2$. These components are compound escapes of γ from H, and they contain the simple escapes from H as subpaths, so all of the escapes of γ from H have length at most $|\gamma|/2$. Corollary 7.2.4 gives us a manageable collection of 2, 3, or 4 R–long escapes from H. Call the subsegments of γ between these long escapes the "junk". The total length of the junk is strictly less than $|\gamma|/R$.

Together the traces of the long escapes form an approximate 2, 3, or 4–gon, and the junk segments give corner paths of length less than $|\gamma|/R$. Furthermore, since each escape from the central region has length at most $|\gamma|/2$, its trace has exponent at most $(|\gamma|/2)^\alpha$. We will apply Lemmas 8.2.4, 8.2.5, and 8.2.6, in all cases with $D_{8.*} = |\gamma|/R$, $E_{8.*} = (|\gamma|/2)^\alpha/\Lambda$, and $\Lambda_{8.*} = \Lambda + 1$. Then all three lemmas produce a diagram with:

$$
\begin{aligned}
&\text{mesh} \leq M_0 + M_1|\gamma|/R + M_2|\gamma|/\Lambda^{1/\alpha}\\
&\text{area} \leq (\Lambda+1)^2 + 4(\Lambda+1) + 4
\end{aligned}
\tag{8.3.2}
$$

To construct subdivisions and fillings there are six cases to consider, according to the configuration of traces of the escapes of the manageable collection as in Figure 7.

Case (7A)**:** Approximate bigon: Choose a subdivision of one side into at most $(\Lambda+1)$–many segments of exponent at most $(|\gamma|/2)^\alpha/\Lambda$. Apply Lemma 8.2.4. This yields a subdivision of the opposite side into at most $(\Lambda+1)$–many segments of exponent at most $|\gamma|^\alpha \left(\frac{1}{L\Lambda} + \frac{L}{R^\alpha}\right)$ and a filling diagram with mesh and area bounded by (8.3.2).

Case (7C)**:** Approximate triangle: Choose a subdivision of the a–side into at most $(\Lambda+1)$–many subsegments of exponent at most $(|\gamma|/2)^\alpha/\Lambda$. Apply Lemma 8.2.5. This yields subdivisions of the other two sides into at most $(\Lambda+1)$–many segments of exponent at most $1+|\gamma|^\alpha\left(\frac{1}{L^2\Lambda}+\frac{1}{R^\alpha}\right)$ and a filling diagram with mesh and area bounded by (8.3.2).

Case (7F)**:** Approximate diamond: Choose subdivisions of one x–side and one y–side into at most $\Lambda+1$ many segments of exponent at most $(|\gamma|/2)^\alpha/\Lambda$. Apply Lemma 8.2.6. This yields subdivisions of the other two sides into $(\Lambda+1)$–many segments of exponent at most $|\gamma|^\alpha\left(\frac{1}{L\Lambda}+\frac{2L}{R^\alpha}\right)$ and a filling diagram with mesh and area bounded by (8.3.2).

Case (7B)**:** The traces of the manageable escapes can be described as if they were an approximate triangle by elements g_0, g_1, g_2 and numbers m_0, m_1, m_2, with the exception that instead of the sides alternating x, y, a, they are all of the same flavor $g\in\{a,x,y\}$. Let us assume the g_2–side is the long side. Let δ_i be the junk segment from $g_{i-1}g^{m_{i-1}}$ to g_i. Then $g^{m_0}\delta_0$ is a path from $g_2g^{m_2+m_0}$ to $g_0g^{m_0}$.

We treat this configuration as a pair of approximate bigons. One of these has side δ_0, top the g_0–side, side $g^{m_0}\bar{\delta}_0$, and bottom the part of the g_2–side from $g_2g^{m_2+m_0}$ to $g_2g^{m_2}$. The two sides have length $|\delta_0|<|\gamma|/R$. The second bigon has side $g^{m_0}\delta_0+\delta_1$, top the g_1–side, side $\bar{\delta}_2$, and bottom the part of the g_2–side from g_2 to $g_2g^{m_2+m_0}$. One side has length $|\delta_2|<|\gamma|/R$. The other has length $|\delta_0|+|\delta_1|$, which, since our junk bound is actually on the total length of the junk and not the individual segments, is still less than $|\gamma|/R$.

Choose a subdivision of the g_0 and g_1 sides into at most $(\Lambda+1)$–many subsegments of exponent at most $(|\gamma|/2)^\alpha/\Lambda$. Apply Lemma 8.2.4 to each of the two approximate bigons. The constants involved are exactly the same as in Case (7A), except that the bounds for the area and number of induced subsegments of the g_2–side are doubled.

Case (7D)**:** Use the same trick as in Case (7B): use the group action to translate the y–side and its attached junk segments to the opposite end of the shorter x–side, and view this configuration as a combination of an approximate diamond and an approximate triangle, and fill them separately.

Case (7E)**:** In this case think of the configuration as two approximate triangles meeting at the point where the a–side and y–side intersect. Fill them each separately and combine the fillings.

In all cases we produce diagrams with mesh bounded by $M_0+M_1|\gamma|/R+M_2|\gamma|/\Lambda^{1/\alpha}$, so since $M_0=4C$, $R>2M_1/\lambda$, and $\Lambda>(2M_2/\lambda)^\alpha$, we have mesh bounded by $\lambda|\gamma|+4C$.

In all cases we fill at most two approximate polygons, each with a diagram of area at most $(\Lambda+1)^2+4(\Lambda+1)+4$, so it suffices to take A to be double this bound.

Scanning the six cases for exponent bounds, we have that the hypotheses $R>\left(\frac{L^2\Lambda}{L-1}\right)^{1/\alpha}$ and $|\gamma|>J\geq\left(\frac{L-1}{L^2\Lambda}-\frac{1}{R^\alpha}\right)^{-1/\alpha}$ imply that the largest of the bounds for the exponents of the subdivision segments is at most $|\gamma|^\alpha\left(\frac{1}{L\Lambda}+\frac{2L}{R^\alpha}\right)$, so it suffices to take $E:=\left(\frac{1}{L\Lambda}+\frac{2L}{R^\alpha}\right)$. □

8.4. **Inductive steps.**

Inductive step: capping off small enough parts. Recall (8.1.3). There γ had a central escape, from some coset gH, whose trace in gH had been subdivided into at most

$2(\Lambda+1)$–many subsegments of exponent at most $L\left(\frac{|\gamma|}{R}\right)^\alpha$, which were then replaced by geodesics $\delta_1,\dots,\delta_m$. Then if $\gamma|_P$ was the part of γ complementary to the central escape, we argued that the length of $\gamma|_P+\bar{\delta}_m+\cdots+\bar{\delta}_1$ was small enough to cap off with a single 2–cell satisfying the desired mesh bound.

Here we argue additionally that very small parts can be capped off. Recall from Section 7.3 that the non-central part $\gamma|_P$ of γ at some coset of H is called "very small" when its length is less than J, where J is some pre-specified constant, independent of γ. The setup is similar to the case described following (8.1.3): the central escape of γ from the coset has trace subdivided into at most $m=2(\Lambda+1)$–many subsegments, and there are given geodesics δ_i with the same endpoints as the subsegments.

$$\boxed{\text{Assume } M\geq (C(2(\Lambda+1))^{1-1/\alpha}+1)J.} \tag{8.4.1}$$

Since $\gamma|_P$ has the same endpoints as the central escape and length less than J, by Theorem 3.2.9 the exponent of the central escape is less than J^α. Suppose that the exponent of δ_i is e_i. Then $|\sum_i e_i|<J^\alpha$. By Theorem 3.2.9, $|\delta_i|<C|e_i|^{1/\alpha}$. By reverse Hölder, $\sum_{i=1}^m |e_i|^{1/\alpha}\leq m^{1-1/\alpha}|\sum_{i=1}^m e_i|^{1/\alpha}$. Therefore, the length of $\gamma|_P+\bar{\delta}_m+\cdots+\bar{\delta}_1$ is less than:

$$(Cm^{1-1/\alpha}+1)J\leq (C(2(\Lambda+1))^{1-1/\alpha}+1)J\leq M \tag{8.4.2}$$

Thus, we can cap off a very small part $\gamma|_P$ of γ with a single 2–cell with boundary $\gamma|_P+\bar{\delta}_m+\cdots+\bar{\delta}_1$, whose length is at most M.

Inductive step: enfilades.

$$\boxed{\text{Define } M_1:=2C+1+C\cdot 2^{2+1/\alpha} \text{ and } M_2:=C.} \tag{8.4.3}$$

$$\boxed{\text{Assume } R\geq 2M_1/\lambda \text{ and } \Lambda\geq (2M_2/\lambda)^\alpha.} \tag{8.4.4}$$

Suppose we have an escape $\gamma|_P$ in the n–th level, so that by (8.1.1) the central side has been subdivided into at most $2(\Lambda+1)$–many geodesic segments of exponent at most $|\gamma|^\alpha E(3/L)^n$, where E is the constant of Lemma 8.3.1, which depends on R and Λ, but not on γ. Suppose this exponent bound exceeds that of (8.1.3), so that the escape is not small enough to cap off. This means:

$$|\gamma|^\alpha E(3/L)^n > L(|\gamma|/R)^\alpha \implies \frac{1}{R^\alpha}<\frac{3^nE}{L^{n+1}} \tag{8.4.5}$$

$$\boxed{\text{Assume } J \text{ and } K \text{ satisfy Proposition 7.3.5 with } R_{7.3.5}=3R.} \tag{8.4.6}$$

Apply Proposition 7.3.5 with $R_{7.3.5}=3R$. Then the distance between the endpoints of the escape and the corresponding endpoints of the end of the enfilade is at most $3|\gamma|_P|/R_{7.3.5}=|\gamma|_P|/R\leq|\gamma|/2R$. We claim that we can fill the enfilade with the same argument as Lemma 8.2.4, treating the enfilade as a $(|\gamma|/(2R))$–approximate bigon. Specifically, the point in that proof where we used that the two sides of the bigon were in the same coset of $\langle a,x,y\rangle$ was to say that we could translate δ_0 along the bottom side and obtain "parallel" copies, in the sense that $g^a.\delta_0$ and $g^b.\delta_0$ are both paths from the bottom side to the top side and their endpoint at the bottom and top both differ by g raised to the power $b-a$. By Lemma 7.3.3, exactly the same thing is true for enfilades, except that we possibly have different g's from the set $\{a, x, y\}$ on the two sides. As our length versus exponent estimates are uniform for $\{a, x, y\}$, this does not change the rest of the argument.

Apply that argument with $\Lambda_{8.2.4} := 2(\Lambda+1)$, $E_{8.2.4} := |\gamma|^\alpha E(3/L)^n$, and $D_{8.2.4} := |\gamma|/(2R)$, with $M_{i,8.2.4}$ denoting the constant M_i in the conclusion of Lemma 8.2.4. This yields a subdivision of the outgoing side into at most $2(\Lambda+1)$–many subsegments of exponent at most $E_{8.2.4} + LD_{8.2.4}^\alpha$ and a filling diagram of area $\Lambda_{8.2.4}$ and mesh at most:

$$\begin{aligned}
&M_{0,8.2.4} + M_{1,8.2.4}D_{8.2.4} + M_{2,8.2.4}E_{8.2.4}^{1/\alpha} \\
&\quad = 0 + 2(2C+1)D_{8.2.4} + 2CE_{8.2.4}^{1/\alpha} \\
&\quad = (2C+1)|\gamma|/R + 2C|\gamma|(E(3/L)^n)^{1/\alpha} \\
&\quad = (2C+1)|\gamma|/R + 2CE^{1/\alpha}\,(3/L)^{n/\alpha}\cdot|\gamma| \\
&\quad = (2C+1)|\gamma|/R + 2C\left(\frac{1}{L\Lambda}+\frac{2L}{R^\alpha}\right)^{1/\alpha}\cdot(3/L)^{n/\alpha}\cdot|\gamma| && \text{definition of } E \\
&\quad < (2C+1)|\gamma|/R + 2C\left(\frac{1}{L\Lambda}+\frac{2L}{R^\alpha}\right)^{1/\alpha}\cdot|\gamma| && \text{because } L>3 \\
&\quad \le (2C+1)|\gamma|/R + 2C\left(\frac{1}{2\Lambda^{1/\alpha}}+\frac{2^{1+1/\alpha}}{R}\right)\cdot|\gamma| && \text{reverse Hölder} \\
&\quad = (2C+1+C\cdot 2^{2+1/\alpha})|\gamma|/R + C|\gamma|/\Lambda^{1/\alpha} \\
&\quad = M_1|\gamma|/R + M_2|\gamma|/\Lambda^{1/\alpha} && \text{definition of } M_i
\end{aligned}$$

Since $R \ge 2M_1/\lambda$ and $\Lambda \ge (2M_2/\lambda)^\alpha$, the mesh is at most $\lambda|\gamma|$.

Consider the ratio of outgoing to incoming exponent bounds:

$$\begin{aligned}
\frac{E_{8.2.4}+LD_{8.2.4}^\alpha}{E_{8.2.4}} &= 1 + \frac{L(|\gamma|/(2R))^\alpha}{|\gamma|^\alpha E(3/L)^n} \\
&= 1 + \frac{L^{n+1}}{2^\alpha 3^n E R^\alpha} \\
&= 1 + \frac{L^n}{3^n E R^\alpha} \\
&< 1 + \frac{L^n}{3^n E}\cdot\frac{3^n E}{L^{n+1}} && \text{by (8.4.5)} \\
&\le 1 + \frac{1}{L} = \frac{L+1}{L}
\end{aligned}$$

Recall that for the induction we are aiming for an exponent ratio of $3/L$, and here we have only shown for enfilades that it is not too much larger than 1. The branching parts compensate.

Inductive step: branching parts.

$$\boxed{\text{Let } M_0 := 4C,\ M_1 := C\cdot 2^{3+1/\alpha} + 6C + 2, \text{ and let } M_2 := 2C.} \tag{8.4.7}$$

Assume (8.4.4) and (8.4.6) are satisfied, and furthermore:

$$\boxed{\text{Assume } R \geq 2M_1/\lambda \text{ and } \Lambda \geq (2M_2/\lambda)^\alpha \text{ and } J \geq 2R \text{ and } M \geq M_0.} \tag{8.4.8}$$

Let E be the constant of Lemma 8.3.1, which depends on R and Λ.

Suppose now that we have reached a branching part of γ at the end of an enfilade as in the previous subsection. Then by the induction hypothesis (8.1.1) and the result of the previous subsection, the trace of the central escape is subdivided into at most $2(\Lambda+1)$–many subsegments of exponent at most $\frac{L+1}{L}|\gamma|^\alpha E(3/L)^n$. Again, we assume that the branching part is not small enough to cap off yet, so that (8.1.3) fails and we have:

$$\frac{L+1}{L}|\gamma|^\alpha E(3/L)^n > L(|\gamma|/R)^\alpha \implies \frac{1}{R^\alpha} < \frac{3^n E(L+1)}{L^{n+2}} \tag{8.4.9}$$

The traces of the central and two long non-central escapes form an approximate triangle, so we apply Lemma 8.2.5 with $\Lambda_{8.2.5} := 2(\Lambda+1)$, $E_{8.2.5} := \frac{L+1}{L}|\gamma|^\alpha E(3/L)^n$, and $D_{8.2.5} := |\gamma|/R$. This yields subdivisions of the other two sides into at most $2(\Lambda+1)$–many subsegments of exponent at most $1 + E_{8.2.5}/L + D_{8.2.5}^\alpha$ and a filling diagram of area quadratic in Λ and mesh at most:

$$\begin{aligned}
&M_{2,8.2.5}E_{8.2.5}^{1/\alpha} + M_{1,8.2.5}D_{8.2.5} + M_{0,8.2.5} \\
&\quad = 2CE_{8.2.5}^{1/\alpha} + (6C+2)D_{8.2.5} + 4C \\
&\quad = 2C\left(\frac{L+1}{L}|\gamma|^\alpha E(3/L)^n\right)^{1/\alpha} + (6C+2)|\gamma|/R + 4C \\
&\quad < 4C|\gamma|E^{1/\alpha} + (6C+2)|\gamma|/R + 4C && \text{because } L \geq 6 > 3 \\
&\quad = 4C|\gamma| \cdot \left(\frac{1}{L\Lambda} + \frac{2L}{R^\alpha}\right)^{1/\alpha} + (6C+2)|\gamma|/R + 4C && \text{definition of } E \\
&\quad \leq 4C|\gamma| \cdot \left(\frac{1}{2\Lambda^{1/\alpha}} + \frac{2^{1+1/\alpha}}{R}\right) + (6C+2)|\gamma|/R + 4C && \text{reverse Hölder} \\
&\quad = (C \cdot 2^{3+1/\alpha} + 6C + 2)|\gamma|/R + 2C|\gamma|/\Lambda^{1/\alpha} + 4C \\
&\quad = M_0 + M_1|\gamma|/R + M_2|\gamma|/\Lambda^{1/\alpha} && \text{definition of } M_i
\end{aligned}$$

Since $M \geq M_0$, $R \geq 2M_1/\lambda$, and $\Lambda \geq (2M_2/\lambda)^\alpha$, the mesh is less than $\lambda|\gamma| + M$.

Since $|\gamma| > J \geq 2R$, the ratio of outgoing to incoming exponents is at most:

$$\begin{aligned}
\frac{1 + E_{8.2.5}/L + D_{8.2.5}^\alpha}{E_{8.2.5}} &= \frac{1}{L} + \frac{L}{L+1} \cdot \frac{L^n}{3^n E|\gamma|^\alpha} + \frac{L}{L+1} \cdot \frac{L^n}{3^n E R^\alpha} \\
&= \frac{1}{L} + \frac{L}{L+1} \cdot \frac{L^n}{3^n E}\left(\frac{R^\alpha}{|\gamma|^\alpha} + 1\right)\frac{1}{R^\alpha} \\
&\leq \frac{1}{L} + \frac{L}{L+1} \cdot \frac{L^n}{3^n E} \cdot \frac{5}{4} \cdot \frac{1}{R^\alpha} && \text{Since } \alpha > 2 \text{ and } |\gamma| \geq 2R. \\
&\leq \frac{1}{L} + \frac{L}{L+1} \cdot \frac{L^n}{3^n E} \cdot \frac{5}{4} \cdot \frac{3^n E(L+1)}{L^{n+2}} && \text{by (8.4.9)}
\end{aligned}$$

$$= \frac{9}{4L}$$

This means that if we take the ratio of the exponent bound when entering the enfilade to the bound when exiting through one of the long escapes of the branching part at the end of the enfilade, then we get $\frac{L+1}{L} \cdot \frac{9}{4L}$. Since we have $L > 3$, it follows that $\frac{L+1}{L} \cdot \frac{9}{4L} < \frac{3}{L}$, so this confirms (8.1.1).

9. Proof of the main theorem and closing remarks.

Theorem 9.0.1. *For all even $L \geq 6$, every asymptotic cone of G_L is simply connected.*

Proof. For $i \in \{1, 2\}$ let $M_i := \max\{M_{i,8.3.1}, M_{i,8.4.3}, M_{i,8.4.7}\}$. These depend only on C.

Pick any $\lambda \in (0, 1)$. Pick any $\Lambda > (2M_2/\lambda)^\alpha$. Pick any $R > \max\big\{3, 2M_1\lambda, 12C(\Lambda + 1)/\lambda, \big(\frac{L^2\Lambda}{L-1}\big)^{1/\alpha}\big\}$. Pick J large enough and $1 < K < 2$ close enough to 1 to satisfy Corollary 7.2.4 and Lemma 8.3.1 with respect to R and Proposition 7.3.5 with respect to $3R$. Assume further that $J \geq 2R$. Define $M = M_0 := \max\{4C, (C(2(\Lambda+1))^{1-1/\alpha} + 1)J\}$.

These choices simultaneously satisfy Lemma 8.3.1 and the assumptions (8.4.1), (8.4.3), (8.4.4), (8.4.6), (8.4.7), and (8.4.8).

Let $\mathcal{C}$ be the area bound given by Lemma 8.3.1, which is a quadratic function of Λ. Let $\mathcal{E} = \Lambda_{8.2.4} = 2(\Lambda + 1)$ be the area bound for enfilades. Let $\mathcal{B}$ be the area bound for branching parts, which is quadratic in Λ. Let A be the area bound of (8.1.5) with respect to $\mathcal{C}$, $\mathcal{E}$, and $\mathcal{B}$.

If γ is a K–biLipschitz loop of length at most J we fill it by a single 2–cell with mesh $J < M$.

If γ is a K–biLipschitz loop of length greater than J then we apply the inductive argument of Section 8 to get a filling diagram of γ with area at most A and mesh at most the maximum of the meshes for the central part, very small parts, enfilades, and branching parts. We have chosen M_0, M_1, M_2, R, and Λ so that this is at most $\lambda|\gamma| + M$.

We conclude that for this choice of $K > 1$, every K–biLipschitz loop γ can be filled by a diagram of area at most A and mesh at most $\lambda|\gamma| + M$, with A, λ, and M independent of γ. Now apply Corollary 6.0.3 and Theorem 2.3.2 to conclude that every asymptotic cone of G_L is simply connected. □

We close with a list of open questions:

1. Is G_L a strongly shortcut group?
2. If every asymptotic cone of a group is simply connected, is the group strongly shortcut?
3. Is the strong shortcut property for Cayley graphs of groups invariant under change of generating set?
4. Is the strong shortcut property for groups invariant under quasi-isometry?
5. Can a group of polynomial growth have an asymptotic cone containing an isometrically embedded circle?
6. Can a group with quadratic Dehn function have an asymptotic cone containing an isometrically embedded circle?
7. Are all asymptotic cones of all of the Brady-Bridson snowflake groups $G_{p,q}$ of (3.0.2) simply connected, or is it important that we have taken $q = 1$?

Note that, by Theorem 9.0.1 and Corollary 4.0.2,

- if (1) has a negative answer then (2) has a negative answer and
- if (1) has a positive answer then (3) has a negative answer.

Thus (2) and (3) cannot both have positive answers.

References

[1] G. N. Arzhantseva, C. H. Cashen, and J. Tao, *Growth tight actions*, Pacific J. Math. **278** (2015), no. 1, 1–49.

[2] S. P. Avann, *Metric ternary distributive semi-lattices*, Proc. Amer. Math. Soc. **12** (1961), no. 3, 407–414.

[3] H.-J. Bandelt, *Hereditary modular graphs*, Combinatorica **8** (1988), no. 2, 149–157.

[4] J. Behrstock, M. Hagen, and A. Sisto, *Hierarchically hyperbolic spaces II: Combination theorems and the distance formula*, Pacific J. Math. **299** (2019), no. 2, 257–338.

[5] J. Behrstock, M. F. Hagen, and A. Sisto, *Hierarchically hyperbolic spaces, I: Curve complexes for cubical groups*, Geom. Topol. **21** (2017), no. 3, 1731–1804.

[6] J. Behrstock, B. Kleiner, Y. Minsky, and L. Mosher, *Geometry and rigidity of mapping class groups*, Geom. Topol. **16** (2012), no. 2, 781–888.

[7] J. A. Behrstock, *Asymptotic geometry of the mapping class group and Teichmüller space*, Geom. Topol. **10** (2006), 1523–1578.

[8] J. A. Behrstock and Y. N. Minsky, *Dimension and rank for mapping class groups*, Ann. of Math. (2) **167** (2008), no. 3, 1055–1077.

[9] N. Brady and M. R. Bridson, *There is only one gap in the isoperimetric spectrum*, Geom. Funct. Anal. **10** (2000), no. 5, 1053–1070.

[10] N. Brady, T. Riley, and H. Short, *The geometry of the word problem for finitely generated groups*, Advanced Courses in Mathematics CRM Barcelona, Birkhäuser, 2007.

[11] M. R. Bridson, *Asymptotic cones and polynomial isoperimetric inequalities*, Topology **38** (1999), no. 3, 543–554.

[12] M. R. Bridson and A. Haefliger, *Metric spaces of non-positive curvature*, Grundlehren der Mathematischen Wissenschaften [Fundamental Principles of Mathematical Sciences], vol. 319, Springer-Verlag, Berlin, 1999.

[13] C. H. Cashen, *Quasi-isometries between tubular groups*, Groups Geom. Dyn. **4** (2010), no. 3, 473–516.

[14] J. Chalopin, V. Chepoi, A. Genevois, H. Hirai, and D. Osajda, *Helly groups*, preprint (2020), `arXiv:2002.06895`.

[15] V. Chepoi, *Graphs of some* CAT(0) *complexes*, Adv. in Appl. Math. **24** (2000), no. 2, 125–179.

[16] C. Druţu and M. Sapir, *Tree-graded spaces and asymptotic cones of groups*, Topology **44** (2005), no. 5, 959–1058, With an appendix by Denis Osin and Mark Sapir.

[17] C. Druţu, *Quasi-isometry invariants and asymptotic cones*, Internat. J. Algebra Comput. **12** (2002), no. 01n02, 99–135.

[18] M. Gromov, *Hyperbolic groups*, Essays in group theory, Math. Sci. Res. Inst. Publ., vol. 8, Springer, New York, 1987, pp. 75–263.

[19] M. Gromov, *Asymptotic invariants of infinite groups*, Geometric group theory, Vol. 2 (Sussex, 1991), London Math. Soc. Lecture Note Ser., vol. 182, Cambridge Univ. Press, Cambridge, 1993, pp. 1–295.

[20] M. Gromov, *Groups of polynomial growth and expanding maps*, Publ. Math. Inst. Hautes Études Sci. **53** (1981), 53–78, with an appendix by Jacques Tits.

[21] T. Haettel, N. Hoda, and H. Petyt, *Coarse injectivity, hierarchical hyperbolicity and semihyperbolicity*, Geom. Topol. **27** (2023), no. 4, 1587–1633.

[22] F. Haglund, *Complexes simpliciaux hyperboliques de grande dimension*, Preprint (2003).

[23] N. Hoda, *Strongly shortcut spaces*, Algebr. Geom. Topol., to appear.

[24] N. Hoda, *Quadric complexes*, Michigan Math. J. **69** (2020), no. 2, 241–271.

[25] N. Hoda, *Shortcut graphs and groups*, Trans. Amer. Math. Soc. **375** (2022), no. 4, 2417–2458.
[26] N. Hoda and P. Przytycki, *The Heisenberg group is strongly shortcut*, In progress.
[27] T. Januszkiewicz and J. Świątkowski, *Simplicial nonpositive curvature*, Publ. Math. Inst. Hautes Études Sci. **104** (2006), no. 1, 1–85.
[28] A. Kar, *Asymptotically* CAT(0) *groups*, Publ. Mat. **55** (2011), no. 1, 67–91.
[29] C. Kent, *Asymptotic cones of HNN extensions and amalgamated products*, Algebr. Geom. Topol. **14** (2014), no. 1, 551–595.
[30] H. A. Masur and Y. N. Minsky, *Geometry of the complex of curves. II. Hierarchical structure*, Geom. Funct. Anal. **10** (2000), no. 4, 902–974.
[31] H. A. Masur and Y. N. Minsky, *Geometry of the complex of curves. I. Hyperbolicity*, Invent. Math. **138** (1999), no. 1, 103–149.
[32] L. Nebeský, *Median graphs*, Comment. Math. Univ. Carolinae **12** (1971), no. 2, 317–325.
[33] G. A. Niblo and L. D. Reeves, *Coxeter groups act on* CAT(0) *cube complexes*, J. Group Theory **6** (2003), no. 3, 399–413.
[34] A. Y. Ol'shanskii and M. V. Sapir, *Groups with non-simply connected asymptotic cones*, Topological and asymptotic aspects of group theory, Contemp. Math., vol. 394, Amer. Math. Soc., Providence, RI, 2006, pp. 203–208.
[35] D. Osajda and T. Prytuł a, *Classifying spaces for families of subgroups for systolic groups*, Groups Geom. Dyn. **12** (2018), no. 3, 1005–1060.
[36] P. Pansu, *Croissance des boules et des géodésiques fermées dans les nilvariétés*, Ergodic Theory Dynam. Systems **3** (1983), no. 3, 415–445.
[37] P. Papasoglu, *On the asymptotic cone of groups satisfying a quadratic isoperimetric inequality*, J. of Diff. Geom. **44** (1996), 789–806.
[38] T. R. Riley, *Higher connectedness of asymptotic cones*, Topology **42** (2003), no. 6, 1289–1352.
[39] M. V. Sapir, J.-C. Birget, and E. Rips, *Isoperimetric and isodiametric functions of groups*, Ann. of Math. (2) (2002), 345–466.
[40] V. P. Soltan and V. D. Chepoi, *Conditions for invariance of set diameters under d-convexification in a graph*, Kibernetika (Kiev) **19** (1983), no. 6, 14–18.
[41] L. Van den Dries and A. J. Wilkie, *Gromov's theorem on groups of polynomial growth and elementary logic*, J. Algebra **89** (1984), no. 2, 349–374.
[42] D. T. Wise, *Sixtolic complexes and their fundamental groups*, Preprint (2003).

Faculty of Mathematics, University of Vienna, Oskar-Morgenstern-Platz 1, 1090 Vienna, Austria, iD 0000-0002-6340-469X
Email address: `christopher.cashen@univie.ac.at`

DMA, École normale supérieure, Université PSL, CNRS, 75005 Paris, France
Email address: `nima.hoda@mail.mcgill.ca`

Mathematical Institute, University of Oxford, Andrew Wiles Building, Radcliffe Observatory Quarter (550), Woodstock Road, Oxford, OX2 6GG
Email address: `daniel.woodhouse@mail.mcgill.ca`